Synthesis of Hydrophobically Modified Polyacrylamide in Inverse Miniemulsion

DISSERTATION

zur Erlangung des
Doktorgrades Dr. rer. nat.
der Fakultät für Naturwissenschaften



der Universität Ulm

vorgelegt von
Elena Kobitskaya
aus Moskau, Russland

Ulm, 2008

Amtierender Dekan : Prof. Dr. Klaus-Dieter Spindler
1. Gutachter : Prof. Dr. Alexei Khokhlov
2. Gutachter : Prof. Dr. Katharina Landfester
Tag der Promotion : 31.10.2008

Dedicated to my ever loving mother and husband...

CONTENTS

LIST OF ABBREVIATIONS.....vi

LIST OF TABLES.....viii

LIST OF FIGURES.....ix

1. INTRODUCTION 1

2. THEORETICAL SECTION..... 4

2.1. Synthesis, Characterization and Application of Hydrophobically Modified Polyacrylamide 4
2.2. Miniemulsion Polymerization..... 11
2.3. Redox Systems based on Cerium (IV) Ion for Polymerization Initiation ... 20

3. RESULTS AND DISCUSSION 27

3.1. Colloidal Properties of a Reaction Medium 27
3.2. Free-radical Polymerization and Copolymerization of Acrylamide Initiated by Azobisisobutyronitrile 30
3.2.1. Free-radical Polymerization of Acrylamide.....30
3.2.2. Free-radical Copolymerization of Acrylamide with Styrene 33
3.2.3. Free-radical Copolymerization of Acrylamide with Laurylmethacrylate 34
3.3. Free-radical Polymerization and Copolymerization of Vinyl Monomers Initiated by Surface-Activ Redox System based on Ce (IV) Salt 38
3.3.1. Free-radical Polymerization of Acrylamide.....39
3.3.2. Free-radical Polymerization of Acrylic Acid 46
3.3.3. Free-radical Copolymerization of Acrylamide with Styrene 46
3.3.4. Free-radical Copolymerization of Acrylamide with Laurylmethacrylate 48
3.4. Assotiative and Rheological Polymer Properties..... 50

4. EXPERIMENTAL PART 60

4.1. Reagents and Materials 60
4.2. Synthetic Methods 60
4.2.1. Polymerization and Copolymerization of Acrylamide Initiated by Azobisisobutyronitrile.....60
4.2.2. Polymerization and Copolymerization of Vinyl Monomers Initiated by Surface-Active Redox System based on Ce (IV) Salt 61
4.2.3. Synthesis of Cross-linked Polyacrylic Acid Initiated by Surface-Active Redox System based on Ce (IV) Salt 61
4.2.4. Synthesis of Cross-linked Polymeric Latex 62
4.2.5. Polymerization of Lauryl methacrylate.....62
4.2.6. Polymer Purification from Emulsifier 62
4.2.7. Polymer Purification from Ceric Salts 62
4.3. Methods of Polymer Characterization..... 63
4.3.1. Static and Dynamic Light Scattering.....63
4.3.2. Gel Permeation Chromatography (GPC) 66
4.3.3. Fluorescent Spectroscopy.....67
4.3.4. Other Physicochemical Metods.....69

CONCLUSION 72

ZUSAMMENFASSUNG 74

REFERENCES 77

ERKLÄRUNG I

CURRICULUM VITAE II

ACKNOWLEDGEMENTS VI

LIST OF ABBREVIATIONS

AIBN	Azobisisobutyronitrile
ATMP	Amino tri(methylene phosphonic acid)
BAAm	N,N′-methylenebis(acrylamide)
CAC	Critical aggregation concentration
CAN	Ceric ammonium nitrate
CMC	Critical micellar concentration
DLS	Dynamic light scattering
GPC	Gel permeation chromatography
HLB	Hydrophilic-lipophilic balance
HM	Hydrophobically modified
IR	Infra-Red
LMA	Lauryl methacrylate
MMA	Methyl methacrylate
MMD	Molecular mass destribution
MPP	Monomer-swollen polymer particle
NMR	Nuclear magnetic resonance
O/W	Oil-in-water
PAAm	Polyacrylamide
PEO	Polyethylene oxide
PLMA	Polylaurylmethacrylate
PMMA	Polymethylmethacrylate
RPW	Relative peak width
SDS	Sodium dodecylsulfate
SLS	Static light scattering
TEM	Transmission electron microscopy
THF	Tetrahydrofuran
TMS	Tetramethyl-silane

Γ_m	Surface excess concentration
η	Effective viscosity
$[\eta]$	Intrinsic viscosity
λ	Wavelength
ν	Kinematic viscosity
Π_{osm}	Osmotic pressure
σ_{12}	Interface energy
τ	Shear stress

a_s	Surface area per surfactant molecule
c_{AAm}	Acrylamide concentratrion
c^*	Overlap concentration
c_{em}	Emulsifier concentratrion
d	Diameter
D	Rate of shear strain
dn/dc	Refractive index increment
E_a	Effective activation energy of viscous flow
I_1/I_3	Polarity parametr
k	Ostwald – de Waele coefficient
$k_Б$	Boltzmann constant
M	Molar mass
M_n	Number-average molecular mass
M_w	Mass-average molecular mass

M_w/M_n	Polydispercity
$\bar{n}$	Number of active radicals per particle
n	Flow index
$p_{Laplace}$	Laplace pressure
q	Scattering wave vector
R_g	Radius of gyration
R_h	Hydrodynamic radius
R_p	Rate of polymerization
T	Temperature
t	Time
T_b	Boiling-point
V_{all}	Total volume of droplets

LIST OF TABLES

Tab. 1. HLB scale

Tab. 2. The colloidal properties of emulsifier Span 60 (T = 25°C)

Tab. 3. Interfacial tension σ_{12} at the water/oil interface

Tab. 4. Yield of polyacrylamide and its M_w in relation to the concentrations of initiator c_{AIBN} and emulsifier c_{em} in oil phase

Tab. 5. Copolymerization of acrylamide and LMA in miniemulsions

Tab. 6. The results of polymerization of acrylamide in inverse miniemulsions with initiation by system CAN - Span 60

Tab. 7. Synthesis conditions and sizes of cross-linked latex based on acrylamide in inverse miniemulsion with initiation by system CAN – Span 60 (c_{em} = 1.7 – 2.2 wt.%, W/O =1/6)

Tab. 8. The results of copolymerization of acrylamide with styrene in inverse miniemulsions with CAN - Span initiation system, c_{em} = 1.7 – 2.2 wt. %, W/O = 1/6

LIST OF FIGURES

Fig. 1. Schematic illustration of the structure of (***a***) telechelic and (***b***) comb like HM-polymers. The hydrophilic units are shown with red and hydrophobic with green.

Fig. 2. Polymer concentration intervals: dilute regime ($c<c^*$), semidilute regime ($c\sim c^*$) and concentrated regime ($c>c^*$).

Fig. 3. Schematic illustration of the HM-polymer solution viscosity as a function of polymer concentration. Red line – unmodified polymer, green – HM-polymer. Explanation of the drawn behavior is given in the text.

Fig. 4. Schematic illustration of the influence of surfactant concentration on the viscosity of HM-polymer solution. Explanation is given in the text.

Fig. 5. Schematic representation of aggregative stability as a function of droplet size for the three types of emulsions [51].

Fig. 6. Schematic representation of (***a***) direct and (***b***) inverse emulsion.

Fig. 7. The scheme of inverse miniemulsion polymerization.

Fig. 8. (***a***) – Typical calorimetric curve of a direct miniemulsion polymerization. The synthesis conditions: 20% of styrene in water, 1.2% SDS (relative to styrene), and potassium persulfate as initiator [87].

(***b***) – Conversion of monomer into polymer and rate of polymerization *vs* time for a styrene *ab initio* emulsion polymerization system [50].

Fig. 9. Scheme of primary free radicals formation by interaction of (***a***) CAN – nitrilotriacetic acid and of (***b***) CAN – amino tri(methylene phosphonic acid) (ATMP).

Fig. 10. Dependence of the hydrodynamic radius (R_h) of (***1***) droplets and (***2***) latexes on the angle of scattered light. Conditions of synthesis: W/O = 1/7, c_{AAm} = 7.0 mol/l, c_{LMA} = 1.1 $\times 10^{-2}$ mol/l, c_{AIBN} = 3.7×10^{-4} mol/l and c_{em} = 3.3 wt. % (in oil).

Fig. 11. Dependence of polymer yield on reaction time at homopolymerization of acrylamide (Tab. 4, sample PAAm-4_{AIBN}).

Fig. 12. Dependence of products yield on reaction time at copolymerization of acrylamide with styrene.

Fig. 13. Dependence of copolymer yield on reaction time at copolymerization of acrylamide with LMA at LMA concentration of 10 mol. % in the initial reaction mixture (Tab. 5, sample HMPAAm-8_{AIBN}).

Fig. 14. The IR spectra of the samples PAAm-2_{AIBN} (Tab. 4), PLMA and copolymer HMPAAm-9_{AIBN} (Tab. 5).

Fig. 15. Dependence of PLMA yield on reaction time at the presents of miniemulsion (Tab. 5, sample PLMA).

Fig. 16. Scheme of the miniemulsion copolymerization with initiation by AIBN at both phases and on the interfacial boundary. The hydrophilic monomer shows with red, and hydrophobic with green color.

Fig. 17. Distributions of scattered light over hydrodynamic radii (R_h) of scattering particles for (***1***) miniemulsion and (***2***) latex. The observation angle is 90°. Sample PAAm-11_{CAN} (Tab. 6).

Fig. 18. Dependence of molecular mass on concentration of Ce(IV) in the system. Conditions of synthesis: W/O=1/6, c_{em}=1.7÷2.2 wt.%, T=25°C, (●) – c_{AAm} = 3.5 mol/l, (▲) – c_{AAm} = 4.4 mol/l and (○) – c_{AAm} = 7.0 mol/l. The figures are designated the numbers of samples from Tab. 6.

Fig. 19. TEM images of chemically crosslinked nanoparticles in (***a***, ***b***, ***c***) cyclohexane and their dispersion in (***d***) water. Distributions over hydrodynamic radii (R_h) of scattering particles in (***e***, ***1***) cyclohexane and (***e***, ***2***) water. Observation angle 90°. Samples: ***a*** – PAAm-14_{CAN}, ***b*** – PAAm-16_{CAN}, ***c***, ***d***, ***e*** – PAAm-17_{CAN} (Tab. 7).

Fig. 20. Distributions of scattered light over hydrodynamic radii (R_h) of scattering particles of latex in (***1***) cyclohexane and (***2***) water. Observation angle 90°.

Fig. 21. The IR spectra of the samples PAAm-2_{AIBN} (Tab. 4), PLMA and copolymer *acrylamide–LMA* prepared with initiation by CAN – Span 60.

Fig. 22. Hydrodynamic radius (R_h) distributions of crosslinked latex particles based on copolymer *acrylamide–LMA* in (***1***) cyclohexane and (***2***) water. Observation angle 90°.

Fig. 23. TEM image of chemically crosslinked *acrylamide–LMA* copolymer nanoparticles in cyclohexane.

Fig. 24. Scheme of the miniemulsion copolymerization with initiation at the interfacial boundary by surface-active system based on Ce(IV).

Fig. 25. Concentration dependences of pyrene polarity parameter I_1/I_3 in aqueous solutions of polymers (***a***) HMPAAm-6_{AIBN} and (***b***) PAAm-2_{CAN}. ● – initial polymer, ○ – purified polymer.

Fig. 26. Concentration dependences of pyrene polarity parameter I_1/I_3 in aqueous solutions of HM polyacrylamide with various content of LMA in the initial reaction mixture: (curve 1, sample HMPAAm-6_{AIBN}) 2 mol. % and (curve 2, sample HMPAAm-7_{AIBN}) 5 mol. %.

Fig. 27. Concentration dependences of pyrene polarity parameter I_1/I_3 in aqueous solutions of HM polyacrylamide: (○) PAAm-9_{CAN}, (▲) PAAm-2_{CAN} and (●) PAAm-10_{CAN}.

Fig. 28. Intensity normalized spectra of decay times for (○) high- and (●) low-molecular weight fractions of copolymer *acrylamide–styrene*, prepared with AIBN. The observation angle is 90°. c = 1 mg/ml.

Fig. 29. Scattered light intensity distribution with respect to the apparent size of scattering particles in the aqueous solution of copolymers (***1***) HMPAAm-6_{AIBN} and (***2***) HMPAAm-7_{AIBN}. The concentration is 0.5 mg/ml, and the observation angle is 60°.

Fig. 30. Zimm plots for (***a***) PAAm-2_{AIBN} and (***b***) HMPAAm-6_{AIBN} in water.

Fig. 31. Zimm plots for (***a***) HMPAAm-1_{AIBN} and (***b***) HMPAAm-2_{AIBN} in formamide.

Fig. 32. Scattered light intensity distribution with respect to the apparent size of scattering particles for (○) high- and (●) low-molecular weight fractions of copolymer PAAm-9_{CAN}. The concentration is 1 mg/ml, and the observation angle is 90°.

Fig. 33. Zimm plot for PAAm-2_{CAN} in water.

Fig. 34. Concentration dependence of the kinematic viscosity ν for the aqueous solution of (***1***) PAAm-2_{AIBN} and (***2***) HMPAAm-6_{AIBN}.

Fig. 35. The kinematic viscosity ν of 0.5% aqueous solution of HM polyacrylamide *vs* the content of LMA in the reaction mixture. The synthesis conditions are as follows: c_{AIBN} = 4.7×10^{-3} mol/l и c_{em} = 3.3 wt. % (in the oil phase) (Tab. 4 and Tab. 5).

Fig. 36. Flow curves τ(*D*) (***a***) and dependende of effective viscosity η on shear rate *D* (***b***) of 2% aqueous solutions of (***1***) PAAm-2_{AIBN} and (***2***) copolymer PAAm-5_{AIBN}, T = 20°C.

Fig. 37. The dependence of Ostwald – de Waele coefficient on temperature for (***1***) PAAm-2_{AIBN} and (***2***) HMPAAm-5_{AIBN}.

Fig. 38. The dependence of ln η on 1/T for 2% aqueous solutions of (***1***) PAAm-2_{AIBN} and (***2***) copolymer PAAm-5_{AIBN} for determination of E_a at τ = 20 Pa.

Fig. 39. The dependence of dynamic viscosity η on (***a***) reduced concentration c/c^* and (***b***) concentration *c* for aqueous solutions of copolymer *acrylamide-LMA* prepared by (***1***) miniemulsion technique (M_w = 2.17×10^6) and by (***2***) micellar polymerization (M_w = 0.62×10^6) and (***3***) homogeneous polymerization (M_w = 1.96×10^6).

Fig. 40. Schematic static Zimm plot.

Fig. 41. Fluorescence spectrum of pyrene in water. Using pyrene properties to study hydrophobic interaction.

Fig. 42. ^{1}H NMR spectrum of PLMA in deuterated chloroform using TMS as internal standard.

Fig. 43. ^{1}H NMR spectrum of copolymer *acrylamide-styrene* in deuterated water.

1. INTRODUCTION

One of the main trends in polymer science is the search of new synthetic methods for the design of polymer materials with particular properties. Modification of well-known polymers, that permit to impart on them new qualitative characteristics, takes the noticeable place in this research. Hydrophobically modified (**HM**) water-soluble polymers based on acrylamide are among the main classes of associating amphiphilic polymers. Incorporation of a small amount of hydrophobic units into a hydrophilic polymer backbone results in the formation of systems with unique rheological properties. Due to hydrophobic interactions, these polymers can associate in aqueous solutions with a formation of hydrophobic microdomains. This results in a sharp increase in viscosity above a certain polymer concentration [1, 2]. These systems are very promising as aqueous thickeners in different areas of industry [2, 3].

At present, micellar polymerization is the main synthetic method for preparation of HM polyacrylamides (**HM PAAm**) [4–6]. The disadvantage of this method is a restricted initial concentration of the reaction mixture associated with the process of gelation during polymerization. This can be overcome in inverse emulsions, where the concentration of monomers in the reaction system is increased [7]. Nowdays, one of the highly promising types of emulsion polymerization is miniemulsion polymerization [8, 9]. Compared to microemulsions [10], the miniemulsion polymerization is characterized by a more efficient use of emulsifier, and in comparison with conventional emulsion polymerization [11], it gives more stable and homogeneous latexes. The idea of miniemulsion polymerization is to initiate the polymerization in each of the small droplets stabilized against a coalescence (with addition of emulsifier) and against an Ostwald ripening (with the addition of osmotic pressure agent). This method allows one to form a distinct interfacial boundary between water and oil phases that creates favorable conditions for the polymerization near the interface. In addition, the choice of appropriate initiator, concentrating on the interfacial boundary and initiating the polymerization near this boundary, will increase the probability of the copolymerization of monomers with strongly different degrees of hydrophilicity.

In this thesis, the method of inverse miniemulsion has been adopted for the synthesis of HM polyacrylamides by free radical copolymerization. An influence of different conditions, such as temperature, duration of reaction, concentration of monomers, emulsifier and initiators, and phase ratio, on aggregative stability of emulsions and latexes and molecular-mass characteristics of resulted polymers was studied. It was shown that HM polyacrylamides with good thickening properties can be produced.

First, in order to optimize synthesis conditions, free-radical miniemulsion polymerization of acrylamide initiated by a well-known oil-soluble initiator azobisisobutyronitrile (**AIBN**) was carried out. Then, the possibility of copolymerization of comonomers with different hydrophilicities on *acrylamide – styrene* and *acrylamide – lauryl methacrylate* (**LMA**) model pairs was shown. As a result of this research, high-molecular weight water-soluble HM polyacrylamides with hydrophobic LMA units were obtained by inverse miniemulsion technique. Associative and rheological properties of their aqueous solutions were studied. It was shown that solutions of these polymers possess an increased viscosity in comparison with solutions of corresponding polyacrylamides. Moreover, the rheological behavior of miniemulsion HM polyacrylamides was compared with micellar and solution HM polyacrylamides. It was found that HM polymers obtained by miniemulsion and micellar techniques have similar thickening properties.

In this study, along with the well-known initiator AIBN, a new surface-active initiating system based on tetravalent cerium was proposed and investigated. It is known that free-radicals, formed under the treatment of 1,2-diol containing substances with ceric ions, are used in grafting acrylamide, acrylonitrile, acrylates and other vinyl monomers onto cellulose [12, 13], sodium alginate [14], starch [15], and dextran [16]. One commercially available emulsifier for inverse emulsions is sorbitan monostearate (Span 60), which contains a 1,2-diol fragment. It was of interest therefore to use the Ce(IV) – Span 60 redox system for miniemulsion polymerization of water-soluble vinyl monomers, in practicular acrylamide. The proposed polymerization method resulted in the increased stability of water-in-oil emulsions and latexes at lower amount of emulsifier as compared with initiating by conventional oil-soluble AIBN inintiator.

Water-soluble monochelic HM polyacrylamides containing the residual of stearic acid as hydrophobic end-group have been synthesized with ceric ammonium nitrate (**CAN**) – Span 60 redox system. It has been shown that these polymers are able to associate in aqueous solutions. Then acrylamide was copolymerized with hydrophobic monomers – styrene and LMA. It was stated that this surface-active redox

system initiates polymerization at the interfacial boundary in contrast to the oil-soluble initiator. At the same time, this redox system does not initiate the polymerization in oil phase that provides the absence of hydrophobic homopolymer in the reaction products.

Finally, the possibility of synthesis of chemically cross-linked nanoparticles based on polyacrylamide and polyacrylic acid by miniemulsion technique with CAN – Span 60 initiating pair was shown. The resulting nanoparticles were easily dispersed in both hydrophobic and hydrophilic media. From a practical point of view, these nanoparticles could be used after an appropriate modification in bio-sensing and diagnostic systems.

2. THEORETICAL SECTION

2.1. Synthesis, Characterization and Application of Hydrophobically Modified Polyacrylamide

Hydrophobic interactions were first discovered while studying the conformations of proteins and have been found to be an important factor in the stabilization of their tertiary fold. In such systems the grouping of the non-polar side chains of amino acids in polar medium was revealed [17]. The unique solution behavior of these hydrophobically modified water-soluble polymers has led to the synthesis and characterization of synthetic analogs with specific properties.

Hydrophobically modified (**HM**) polymers are polymers with a small amount (from several tenths of a molar percent to several percents) of hydrophobic groups chemically attached to a hydrophilic polymer backbone. Depending on how the hydrophobic groups are situated in the molecule, HM-polymers can be divided into two categories. The first has the hydrophobic groups attached at the ends of the polymer backbone and they are referred to as hydrophobically end-capped polymers or telechelic (**Fig.1*a***). The examples of that category are HM ethoxylated urethanes [18, 19], HM poly(ethylene oxides) (**HM PEO**) [20], and HM poly(N-isopropylacrylamides) [21]. The polymer carrying only one endgroup is named as monochelic. The second category has the hydrophobic groups distributed statistically or as blocks in the polymer backbone. These are called comb like HM-polymers (**Fig.1*b***), i.e. HM cellulose

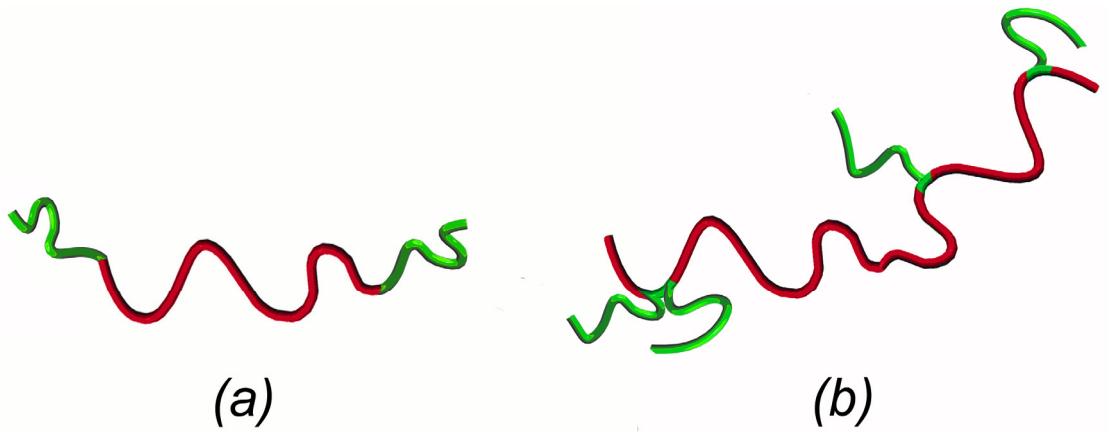


Fig. 1. Schematic illustration of the structure of (***a***) telechelic and (***b***) comb like HM-polymers The hydrophilic units are shown with red and hydrophobic with green.

derivatives [22] and HM poly(acrylamides) [23].

The unique properties of HM-polymers are their ability for hydrophobic association. Above a certain polymer concentration, the hydrophobic moieties associate, this in turn induces a strong increase in viscosity [1, 2]. These systems are very promising as aqueous thickeners in paints, cosmetics, latex coatings, etc. [2, 3]. Due to the biocompatibility of many of the HM-polymers they are useful in the biomedicine and pharmaceutical industries [24]. HM polyacrylamides are among the most interesting of the HM-polymers, since they are very attractive as mobility control agents in enhanced oil recovery [25–27]. It is supposed that HM polyacrylamides can overcome the disadvantages of superhighmolecular analogs (namely, polyacrylamides or partly hydrolyzed polyacrylamides) as high sensitivity to mechanical degradation, a presence of electrolyte and high temperature.

Synthesis of HM polyacrylamides

HM polyacrylamides can be obtained either by chemical modification of a preformed polymer or by free radical copolymerization of the appropriate monomers. Synthesis of HM polyacrylamide by chemical modification is described in Ref. [28]. This method allows one to prepare polymers with the given amount of hydrophobic groups at the given molecular mass of polymer, since polyacrylamide is used as initial material.

One major difficulty in the synthesis of HM polyacrylamides originates from the insolubility of the hydrophobic comonomer in water. Simply dispersing this insoluble monomer as fine particles in the aqueous medium of acrylamide (heterogeneous polymerization) is not a satisfactory process. To overcome this problem, the polymerization was carried out in an organic solvent or a water-based solvent mixture in which both monomers are soluble. However, only a few examples of such solvents are reported (formalin, morpholine) [29]. The use of these solvents is undesirable from an ecological point of view.

At present, HM polyacrylamides are synthesized, as a rule, via micellar polymerization. This approach is rather attractive since it allows one to prepare copolymers with microblocky distribution of hydrophobic units along the chains and makes it possible to control the length of blocks [4–6]. The main drawback of this method consists of several limitations with respect to the initial concentration of the reaction mixture associated with the gelation in the course of polymerization.

As compared to the above-described methods, the polymerization in inverse emulsions allows one to improve the economic efficiency due to an increase in the concentration of the monomers in the reaction system. This method of synthesis of HM polyacrylamides was described in a patent [30]. It was shown that polymerization

affords associating polymers when oil-soluble initiators were employed. The use of water-soluble initiators led to the formation of polymers lacking thickening properties.

In recent years, mini- and microemulsion polymerization processes have found wide use [8, 10]. The formation of a distinct interfacial boundary between water and oil phases creates favorable conditions for the occurrence of polymerization near the interface. Therefore, the copolymerization of monomers with strongly different hydrophilicities becomes more probable. In detail, the synthesis of HM polyacrylamides will be shown in section 2.2.

Properties of HM polyacrylamides

The main regularities of the behavior of macromolecules in solution are summarized in **Fig. 2** [31, 32]. As the concentration of a polymer solution grows, it passes through three characteristic regimes: 1) the dilute solution, in which individual coils do not overlap, 2) the semi-dilute solution in which coils are strongly overlapped but the volume fraction of the polymer in the solution is small (such an intermediate regime is intrinsic for polymers), and 3) the concentrated solution in which the volume fraction of the polymer is on the order of unity.

In the dilute regime, the mean centrum to centrum distance between the polymer coils is larger than the mean radius of a single polymer coil denoted as the radius of gyration, R_g. The individual polymer chains move independently of each other in the solution.

In the semidilute regime, R_g is larger than the mean distance between the coils. The polymeric chains of different macromolecules begin to entangle with a formation of a transient polymer network. During the formation of the network the mechanism of mass transfer changes from translational motion in the dilute regime to reptation-type motion in the semidilute regime. The concentration of a macromolecular solution, at

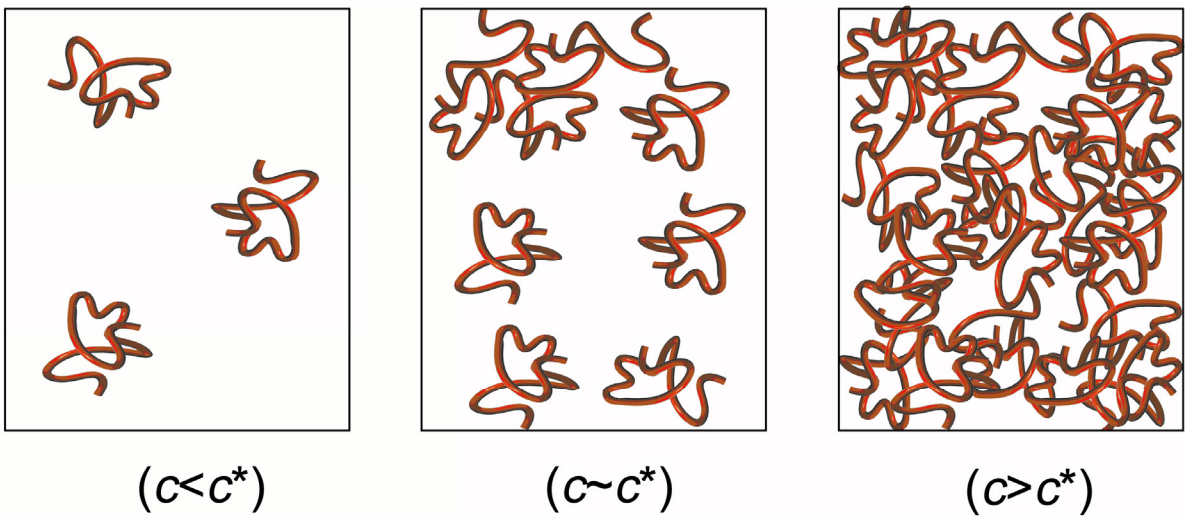


Fig. 2. Polymer concentration intervals: dilute regime ($c<c^*$), semidilute regime ($c\sim c^*$) and concentrated regime ($c>c^*$).

which the overall concentration equals the segment concentration in one swollen coil, is called the overlap concentration, c^*. c^* is the lowest concentration, at which individual coils start overlapping, thus defining the lower limit of the semidilute regime. The result of the formation of the polymer network is a drastic increase in the viscosity of the polymer solution. The overlap concentration can roughly be estimated as the reciprocal of the intrinsic viscosity, $c^* \approx 1/[\eta]$ [33]. The chemical structure of the polymer is very important for the coil size and thereby for the behavior of the polymer in solution. The flexible chains more easily form compact coils than stiff-chains. An increase in molecular mass results in a larger coil and more chain entanglements, which can be seen as increase in viscosity. For solutions of charged polymers "polyelectrolyte effect" is characteristic [34]. If the solution is free of added electrolytes the polymer coil expands and a reduced viscosity increases as the polymer concentration decreases. Dilution of the solution results in increased volume where counterions are distributed. Therefore the screening of fixed charges of polyions is decreased, their mutual repulsion is increased, and the polyions swell. The repulsion between the ionic groups makes the polymer backbone of a polyelectrolyte stiff. One can decrease or completely remove polyelectrolyte effect by introducing low molecular weight electrolytes into the solution. In the presence of added electrolytes, the polyelectrolytes behave like non-ionic polymers and chain expansion is not observed.

In the concentrated region the system consists of highly entangled polymer chains. The behavior of the polymer molecules is more similar to that of a polymer melt, than to the behavior in the polymer network in the semidilute solution [31, 32].

As was mentioned above, the hallmark property of HM-polymers is their ability to have hydrophobic association in aqueous solutions with a formation of microdomains. Just due to hydrophobic interactions, a sharp rise in viscosity of telechelic and comb like polymers and a formation of reversible physical gel below c^* is observed.

Although no bond actually exits, the terms "hydrophobic bond" or "hydrophobic interaction" have received wide acceptance in literature. There are several points of view in thermodynamics of hydrophobic association process. But all of them have lead to that the main contribution in the changing of free energy is brought with the change in entropy and not with the change in enthalpy, which is accordingly small. According to the "iceberg" theory, when non-polar groups are introduced into a polar medium such as water, the water molecules' hydrogen bond around the hydrophobic group creating what have been called "iceberg" [35]. These icebergs are quasi-crystalline structures in which there is less randomness and slightly better hydrogen

bonding than in ordinary liquid water at the same temperature. The ordering of water molecules around a hydrophobic group results in an energetically unfavorable decrease in entropy. If a sufficient number of non-polar groups are present, micellar structures will spontaneously form as the hydrophobic molecules are expelled from the solvent creating a more favorable entropic environment and an increase in free energy. The addition of external electrolytes promotes hydrophobic associations by increasing the polarity of the medium [36]. According to Ref. [37] entropic contribution is also the main driving force of this process and arises due to the decrease in number of rotational degrees of freedom in strong oriented layers of water molecules adjoined with hydrophobic groups.

A hydrophobic group on one polymer molecule can either take part of an intra-molecular association, i.e. it interacts with another hydrophobic group on the same polymer chain (**Fig. 3, I**), or interacts with a hydrophobic group on another polymer molecule (inter-molecular association) (**Fig. 3, II**). At low solution concentrations the probability of interaction between different HM-polymer molecules is small. Intra-aggregation is predominant which results in a reduced coil size [38]. Therefore, the intrinsic viscosity of HM-polymers is often lower than that of the unmodified analogue of the same polymer. There is no sufficient polymer in solution to form physical gel in whole volume at low polymer concentrations, and there exsist macromolecules aggregates and clusters (size from 100 nm to several microns) in the solution. Further increasing of solution concentration results in aggregation of clusters and formation of continuous network in the whole volume (**Fig. 3, II**). The onset concentration of inter-molecular association is often well below the overlap concentration, c^*, of the corresponding unmodified polymer with the same molecular weight [6, 39, 40].

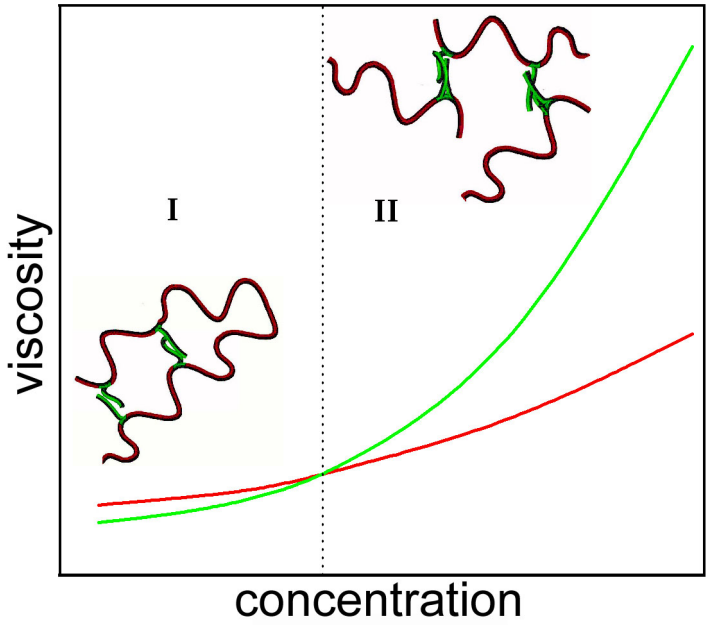


Fig. 3. Schematic illustration of the HM-polymer solution viscosity as a function of polymer concentration. Red line – unmodified polymer, green – HM-polymer. Explanation of the drawn behavior is given in the text.

The main factors influencing the strength of the hydrophobic interactions between polymer chains are:

1. the chemical nature of the hydrophobic groups,
2. the relative content of hydrophobic groups,
3. the distribution of the hydrophobic groups along the polymer backbone.

Longer hydrophobic groups give an increased efficiency of hydrophobic interactions, an increased residence time of a hydrophobic group within the micelle and also increased lifetime and durability of the aggregates of hydrophobic groups. It was shown by Rogovina et al [5] that the aqueous solution of polyacrylamide with dodecyl side group possesses the higher viscosity that the solution of polyacrylamide with nonyl hydrophobic groups at same system concentration.

The influence of the relative content of hydrophobic groups on the solution viscosity can be divided into three different regions. At low content of hydrophobic groups there is a positive correlation between the content and system viscosity. This can be explained by an increased number of inter-connection points. Further increasing in the content of hydrophobic groups can result in a drop in viscosity, which is connected with the transition of inter-molecular associations into intra-molecular associations and gradual disruption of the polymer network [40]. The strengthening of hydrophobic interactions can result in macrosegregation of system into two phases [41]. Such behavior often observes in dilute solution of HM polyacrylamides [39, 42].

Depending on the synthetic method, one can obtain a number of different distributions of the hydrophobic groups along the backbone. The modification and solution polymerization result in statistic distribution, and micellar polymerization gives microblock distribution [28, 29, 43]. Many authors [4, 40, 42] show that the increase in the length of hydrophobic block strengthens the efficiency of hydrophobic interactions. Therefore the viscosity rises and critical aggregation concentration (**CAC**) drops at equal content of hydrophobic groups.

The characteristic feature of HM polyacrylamide gel is thixotropy – the property of a material, which enables it to rapid restore of the structure (and modulus of elasticity and viscosity corresponding to initial structure) after disruption. Such behavior can be explained with the presence of previously formed aggregates [5].

One of the advantages of emulsion polymerization is the possibility to obtain a stable latex, which can be used as is without further precipitation of the polymer. Therefore it is important to know how the emulsifier molecules influence the hydrophobic interaction.

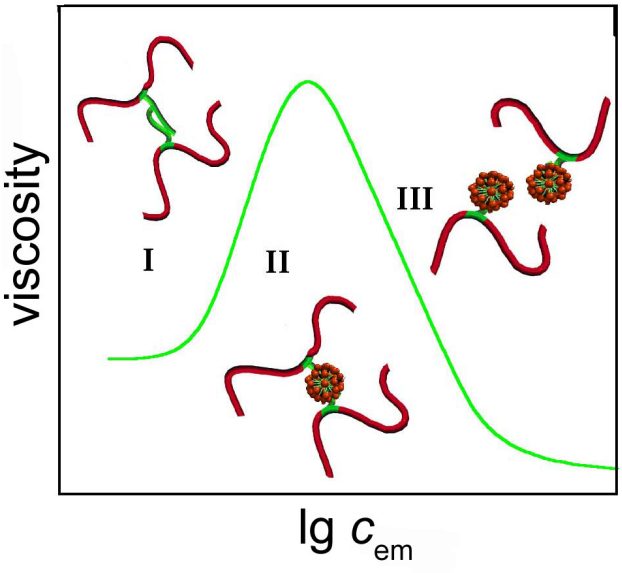


Fig. 4. Schematic illustration of the influence of surfactant concentration on the viscosity of HM-polymer solution. Explanation is given in the text.

As can see in **Fig. 4** in semidilute regime the viscosity HM-polymer solution passes via a pronounced maximum when the surfactant concentration is gradually increased [44, 45]. At low surfactant concentrations (**Fig. 4, II**), below the critical micellar concentration (**CMC**), the surfactant molecules are incorporated in the existing micelles from the HM-polymer. Such merging reduces the water hydrocarbon contact that increases the activation energy for the escape of a hydrophobic group from the micelle thereby increasing the residence time of the hydrophobic groups within the micelles and the efficiency of hydrophobic interactions. In addition to the aforementioned interaction, at some emulsifier concentrations the viscosity reaches its maximum. Further increases in the emulsifier concentration (**Fig. 4, II**) result in an increased ratio between micelles and hydrophobic groups in the polymer. In this process the decreased viscosity is a consequence of the physical network losing some of its connectivity. In a limiting case where the number of micelles exceeds the number of polymer hydrophobic groups in the system, there is only one polymer hydrophobic group in each micelle. At this stage the viscosity is independent of the surfactant concentration and has a constant value. Normally nonionic polymers interact more strongly with anionic surfactants than with non-ionic or cationic surfactants. In Ref. [46], it was found that anionic surfactants give the most pronounced viscosity increase and also the largest reduction of the viscosity at excess surfactant.

Problem statement

On the base of all above-mentioned one can conclude that the search of new synthetic methods for preparation of HM polyacrylamides is the actual task. This work is the development of systematic study of HM polyacrylamides carried out in A.N. Nesmeyanov Institute of Organoelement Compounds RAS and in Institute of Polymer Science, Ulm University.

2.2. Miniemulsion Polymerization

Emulsion polymerization is one of the widely used industrial processes for polymerization of unsaturated monomers in heterogeneous conditions, which results in formation of polymer dispersion [47]. The main advantage of emulsion polymerization in comparison with bulk and solution polymerization is low viscosity of the reaction medium, which provides an effective heat sink and the possibility to obtain a linear polymer. At equal polymer content in solution and in emulsion the viscosity of the latter is lower and the resulting latex can contain a polymer of about 30% and higher in density. Emulsion polymerization is well suited for the preparation of high-molecular weight polymers at rapid reaction rates due to high local monomer concentration within the particles. Add to the fact that free radicals grow in separate particles that prevent their mutual termination. The above-mentioned concerns for polymerization as in direct (type oil-in-water, O/W) so as in inverse (type water-in-oil, W/O) emulsions.

Types of emulsions

According to the droplet size and aggregative stability the emulsions are typically divided into three types: macroemulsions (conventional), miniemulsions and microemulsions (**Fig. 5**) [7, 48].

Macroemulsions have the largest droplet size (1-100 μm) and the lowest stability. It is necessary to subject this system to constant vigorous stirring for synthesis. Therefore the coalescing droplets are broken and the system is not separated into two phases. In the initial stage, monomer droplets are stabilized with emulsifier and emulsifier micelles are present in the emulsion. Nucleation (or

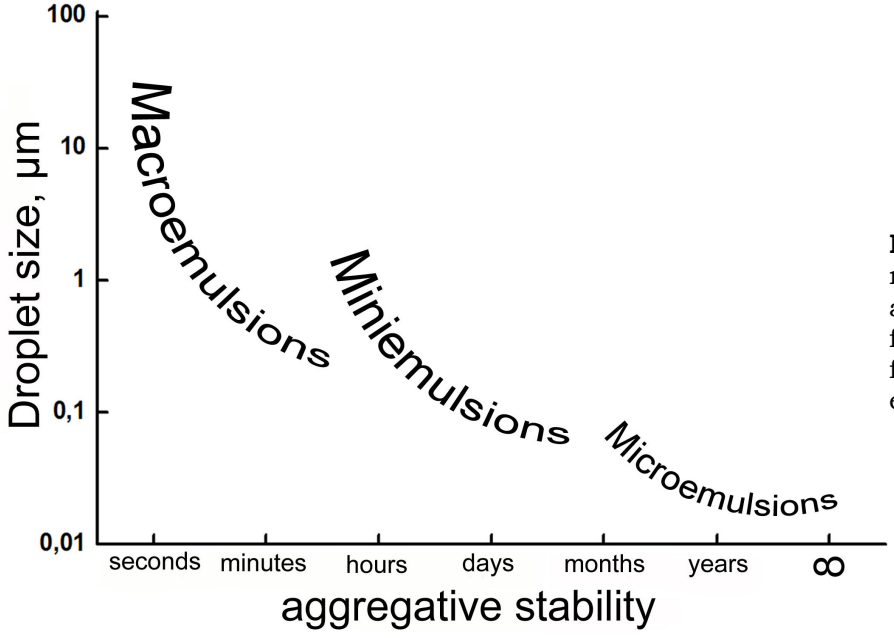


Fig. 5. Schematic representation of aggregative stability as a function of droplet size for the three types of emulsions [49].

formation of monomer-swollen polymer particles, **MPP**) can proceed by three major mechanisms: micellar, homogeneous and droplet nucleation [50]. In micellar nucleation, initiator radicals generated in the continuous phase enter the monomer-swollen surfactant micelles as single radicals or oligoradicals and initiate polymerization to form MPP, which then grow via propagation reactions. Unentered micelles give their surfactant and monomer molecules to the growing particles. At homogeneous nucleation, radicals generated in the continuous phase propagate by adding monomer units to form oligomers until they reach the limit of their solubility in continuous phase and precipitate out of solution. The precipitated oligoradicals form primary particles, which adsorb surfactant, bringing their stabilization, and absorb monomer, allowing further propagation and growth. At droplet nucleation, radicals generated in the continuous phase enter the monomer droplets as single radicals or oligoradicals and propagate to form particles.

Another type of emulsion is microemulsions, which is thermodynamically stable and has the smallest droplet size (10 – 100 nm). The interfacial tension and surface energy in these emulsions is roughly zero. However it is necessary to add a relatively large amount of emulsifier in order to obtain a stable microemulsion. Formation of MPP proceeds mainly by droplet nucleation [10].

The intermediate type of emulsion is miniemulsion. The main specific feature of miniemulsion polymerization, compared to the traditional emulsion polymerization, is the use of an osmotic agent along with a surfactant. This agent suppresses the Ostwald ripening of droplets, that is, the passage of the monomer from small into large droplets and the disappearance of former. The distinguishing feature of miniemulsion is the absence of free surfactant micelles in the system; therefore, the mechanism of chain nucleation in droplets prevails. In contrast to microemulsions, miniemulsions are thermodynamically unstable and possess only kinetic stability, which makes it essential to apply strong shear stresses for creation of miniemulsions [8, 9]. Details of the miniemulsion polymerization will be described below.

Inverse emulsion polymerization

In 1962, Vanderhoff *et al.* were the first to polymerize vinyl monomers in inverse emulsions using a water/o-xylene system [51]. In spite of the wide use of this polymerization in inverse emulsions for industrial production of polyacrylamide, the method is not investigated as well as polymerization in direct emulsions. There are several groups studying this technique systematicaly: F. Candau [52, 53], K. Landfester [54], D.J. Hunkeler [55], I. Capek [56], and V. Gromov [57]. Among different water-soluble monomers, acrylamides and its derivatives are commonly synthesized with this method.

Tab. 1. HLB scale

Solubility of surfactant	HLB		Application
Not disperse	0		
	2		
	4		water-in-oil
Poorly disperse	6		emulsifier
Turbid unstable dispersion	8		wetting agent
Turbid stable dispersion	10		
Translusent or transparent solution	12		
Transparent solution	14	detergent	oil-in-water
	16		emulsifier
	18	solubilizer	

In W/O polymerization, a hydrophilic monomer (usually as aqueous solution) is dispersed in a continuous organic phase using emulsifiers with the values of hydrophyl-lipophile balance (**HLB**) lying in the range 4–6 [52]. The HLB numbers were proposed by Griffin for a quantitative estimation of emulsifier efficiency. According to him, numbers are assigned on a one-dimensional scale of surfactant action, as given in **Tab. 1**; note the correlation with their solubility in water. Each surfactant is then rated according to this scale from 0 to 20 [58].

Usually aliphatic rarely aromatic hydrocarbons are used as a continuous medium. The free-radical polymerization is carried out with oil- (AIBN, benzoyl peroxide) or water-soluble (potassium persulfate) initiators, and redox systems (cumene hydroperoxide/thionyl chloride). Typically, by compairing oil- and water-soluble initiators, the reaction rate is higher [59] but emulsion stability and molecular mass of polymer are lower [60] in the latter case. Nonionic oil-soluble emulsifiers such as fatty acid esters of sorbitan (Span) and polyoxyethylene derivatives (Tween) are served as the stabilizers of inverse emulsion. For creating more stable emulsions the mixtures of emulsifier with low (~4) and high (~10-15) HLB are usually used. In this case strong mixed adsorption layers with dense packing of emulsifier molecules on the droplets surface are formed.

At first glance, inverse polymerization can be considered as a replica of the direct emulsion polymerization in which the water is replaced by the oil and the hydrophobic monomer by the aqueous solution of hydrophilic monomer. In fact, this is incorrect. First of all, it concerns the mechanism and kinetics of the polymerization.

Also, the emulsifier and the nature of oil phase play an enormous role on the polymerization rate and molecular mass. Recently, a number of concepts were proposed for the mechanism of inverse emulsion polymerization differing by the type of nucleation. In reviews of Cando [52] and Sochilina [61] the well-known studies in this field were summarized and analyzed, including the problems of realization of inverse emulsion polymerization, stability of emulsions and latexes in organic medium, kinetic and mechanisms were stated. It was proposed that the monomer droplets of inverse emulsion are the locus of nucleation. Such conclusion was made on the basis of dispersed composition of monomer emulsions and polymer dispersions.

The specific feature of inverse emulsions is their considerable aggregative instability compared with direct emulsions. In the latter, the continuous phase is exclusively water, and particles are stabilized by electrostatic forces and/or steric effects. In the former, an aromatic or aliphatic continuous phase is commonly used and the stabilization is steric in origin. And it is important to note that the energy of interaction between water droplets in nonpolar media is considerably higher than the energy of their thermal motion. A comparison of the direct and inverse emulsion is schematically drawn in **Fig. 6**.

Low stability of emulsions in such systems causes the formation of polymer particles with broad size distribution. Moreover, large amount of coagulum is often formed during polymerization. Incorporation of polar monomers into the aqueous phase leads to a decrease of emulsion stability due to emulsifier desorption from the W/O interface. The usage of a large amount of stabilizers (more than 10% relative to total weight of emulsion) is undesirable because it results in decreasing of polymerization rate and complicates the processing of polymer product.

Miniemulsion polymerization

Ugelstad *et al.* [62] was the first, who applied the miniemulsion polymerization.

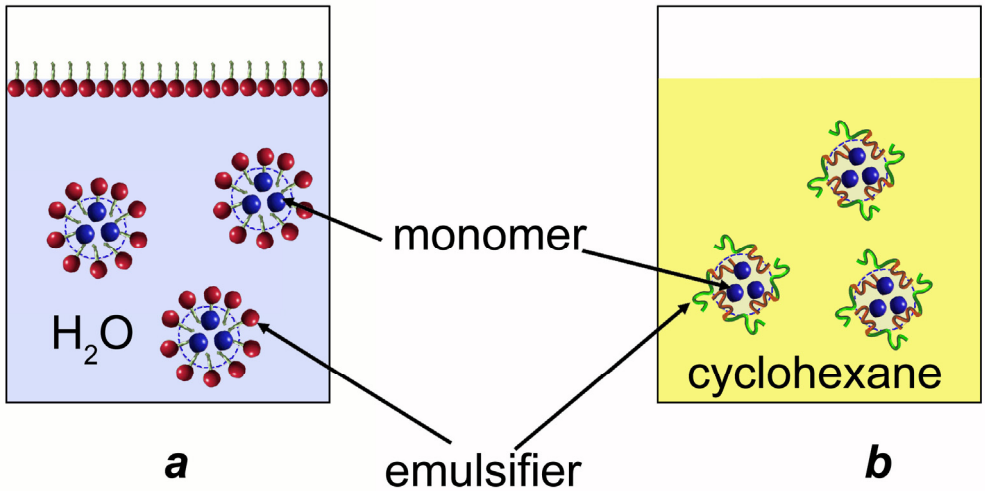


Fig. 6. Schematic representation of (***a***) direct and (***b***) inverse emulsion.

In this work, polymerization of styrene was carried out in emulsion droplets (with sizes of less than 0.7 μm) with sodium dodecylsulfate (**SDS**) as a surfactant and cetyl alcohol as a hydrophobe. The term "miniemulsion" itself was introduced later by Chou *et al.* [63]. At the present time, there are several studies devoted to free-radical polymerization of different hydrophobic (for example, styrene [64], butyl acrylate [65], methyl methacrylate (**MMA**) [66]) and hydrophilic monomers (acrylamide, acrylic acid [67]). This method is applicable for copolymerization of different monomers [68–71], creating polymer-polymer hybrids [72], formation of capsules [73], encapsulation of pigments [74, 75], etc. Beside the free-radical polymerization, anionic polymerization [76], polyaddition and polycondencation [77–79] can be perfomed in miniemulsified systems.

The principle of miniemulsion polymerization consists of the following [80]: The initial mixture of two phases, one of which contains a monomer and an osmotic pressure agent and another one – an emulsifier, subjected to high mechanical agitation. Stabilization of emulsions against coalescence is obtained by the addition of surfactants. The additional level of stabilization is reached due to an osmotic pressure agent. Because of polydispersity of droplet sizes interdroplet mass transfer (Ostwald ripening) arises; small droplets disappear, increasing the average droplet size. This phenomenon is connected with well-known dependence of Laplace pressure ($p_{Laplace}$) inside the original miniemulsion droplet on their size [80]:

$$p_{Laplace} = \frac{2\sigma_{12}}{r}, \qquad (2.2.1)$$

Where r is the droplet radius and σ_{12} is the interface energy on the boundary between droplet and continuous phase. The addition of the third component (osmotic agent), which is practically insoluble in the continuous phase, constructs an osmotic pressure [80]:

$$\Pi_{osm} = \frac{R_{gas}Tc}{M}, \qquad (2.2.2)$$

Where R_{gas} is the gas constant, T is the absolute temperature, c is the concentration of reagents, M is the molar mass. This pressure counterbalances the Laplace pressure in droplets. Therefore, the reversible transition of the monomer to the continuous phase and backwards takes place; as a result, a certain size distribution of droplets is formed but their amount remains unchanged [81].

For homogenization of small volumes, an ultrasonifier is commonly used, for large volumes, rotor-stator systems, microfluidizers and high-pressure homogenizers are substituted [9]. In the case of ultrasound, the possible mechanism of droplet

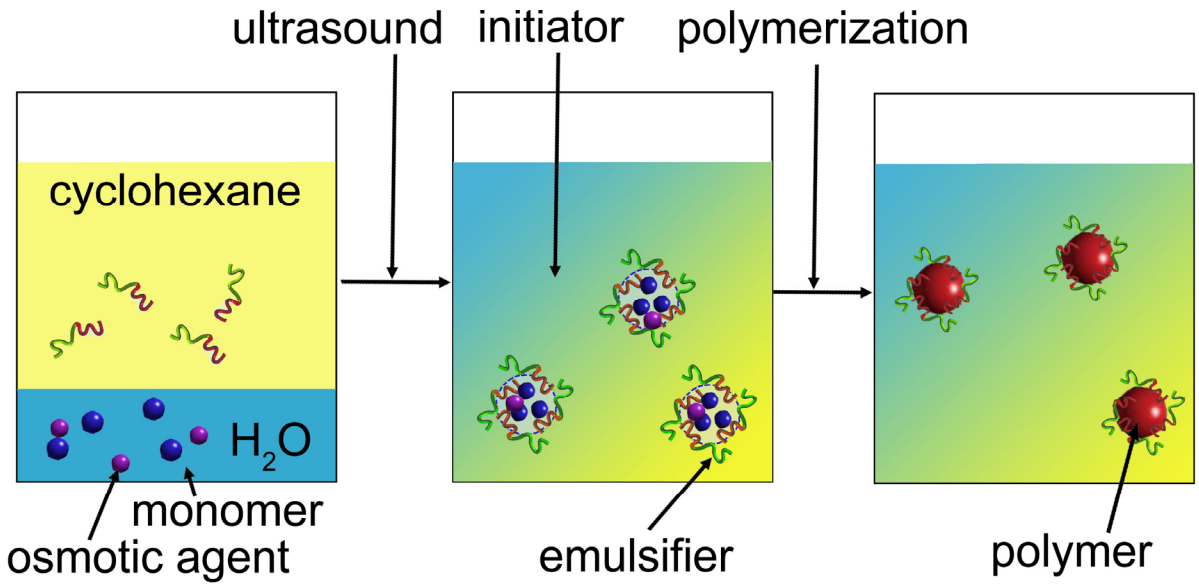


Fig. 7. The scheme of inverse miniemulsion polymerization.

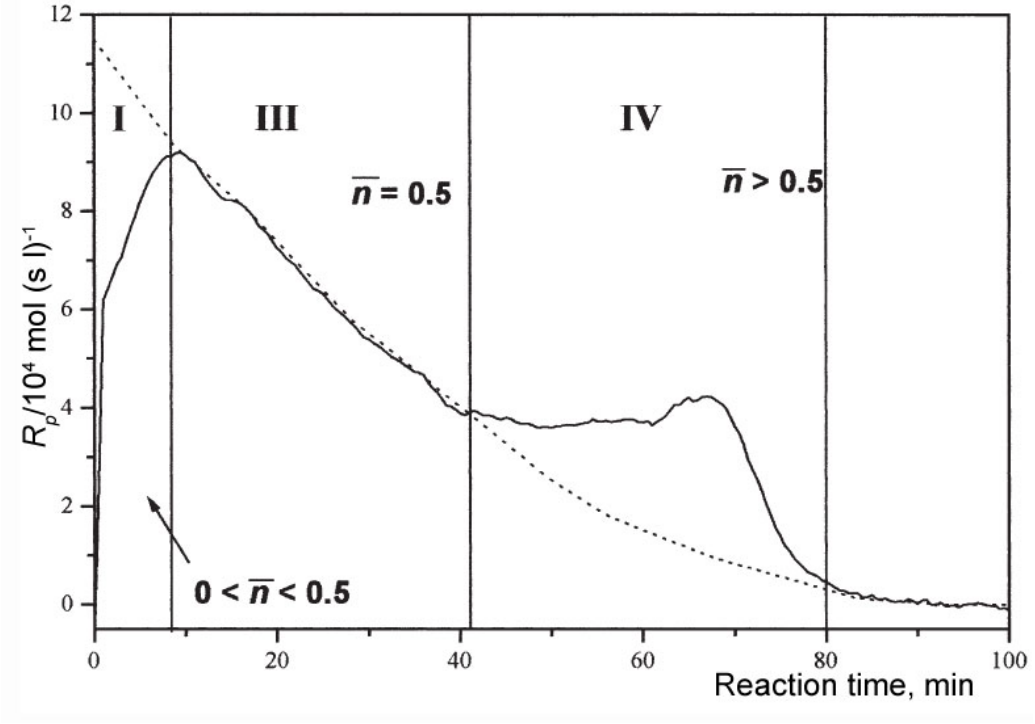
disruption can be cavitation. The shock waves produced on the total collapse of the bubbles cause the break up of the surrounding monomer droplets [82, 83].

During polymerization the emulsion is in dynamic equilibrium because of a fusion and fission of the droplets. Steady-state dispersed miniemulsions are stable against diffusional degradation, but critically stabilized with respect to colloidal stability. Thus, one can say about kinetic stability of emulsion and consider the emulsion droplets as nanoreactors with droplet nucleation only [84]. The scheme of inverse miniemulsion polymerization is represented in **Fig. 7**.

In **Fig. 8*a***, a typical calorimetric curve of polymerization in direct miniemulsion is presented [85]. In this case the polymerization of styrene with initiation from the water phase was carried out. The droplet size was 100 nm. For comparison, a classical curve of reaction rate for conventional emulsion polymerization is shown (**Fig. 8*b***). Three different intervals can be identified in miniemulsion curve: intervals I and III, which are also typical for classical emulsion polymerization [48], and an interval IV describing a gel effect. There is not an interval II of constant reaction rate similarly to polymerization in microemulsions. This means that the diffusion of monomer is not a rate-determining step.

Particle nucleation takes place during the interval I. Rising branch of the curve describes the process of reaching an equilibrium radical concentration within every droplet formed during emulsification. Here, the number of active radicals per particle, $\bar{n}$, slowly increases to ~0.5. In the course of nucleation, the polymerization in each miniemulsion droplet starts asynchronously. Thus, every miniemulsion droplet can be perceived as a separate nanoreactor in which the evolution of conversion begins independently. After reaching $\bar{n} \approx 0.5$, the rate curve goes down following exponential

kinetics (interval III in emulsion polymerization). According to the droplet nucleation mechanism, only monomer in the droplet is available for polymerization. Therefore, in miniemulsion polymerization interval II, where the constant reaction rate is



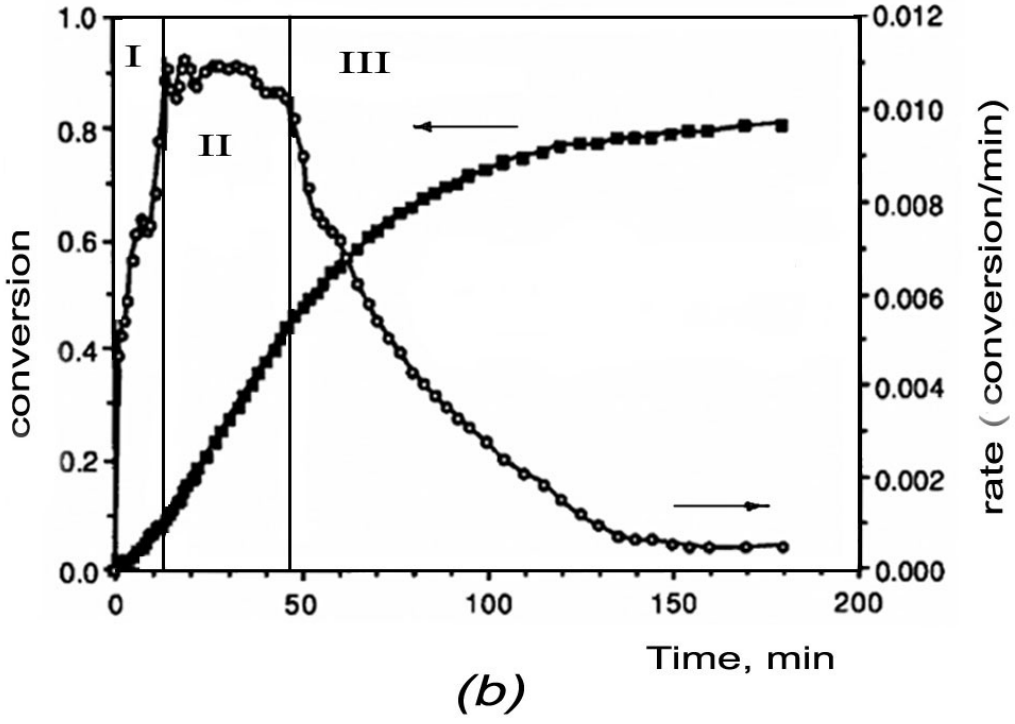


Fig. 8. (***a***) – Typical calorimetric curve of a direct miniemulsion polymerization. The synthesis conditions: 20% of styrene in water, 1.2% SDS (relative to styrene), and potassium persulfate as initiator [85].
(***b***) – Conversion of monomer into polymer and rate of polymerization *vs* time for a styrene *ab initio* emulsion polymerization system [48].

maintained by migration of monomer from monomer droplets through continuous phase into MPP, is absent. In interval III, the reaction rate decreases due to consumption of the monomer. During interval III, n is quite accurately kept at 0.5. Due to the viscosity increasing inside the particles there is a gel effect in interval IV (peak on the curve). High viscosity of the system makes the radical meeting difficult and, thus, the rate of termination reaction decreases. So, in this interval several macroradicals can be present in one MPP ($\bar{n}$ >0.5).

In Ref. [67], the inverse miniemulsion polymerization of hydroxyethyl methacrylate, acrylamide, and acrylic acid were studied. Stable narrow-distributed latexes within the size range 50 nm to 200 nm were obtained using the nonionic amphiphilic block copolymer (poly(ethylene-co-butelene)-b-poly(ethylene oxide), KLE3729) as the emulsifier. Depending on the system, the surfactant loads can be as low as 1.5 wt. % per monomer. For example, 1.8 wt. % of surfactant with respect to aqueous phase was enough to create stable miniemulsion and latex in polymerization of acrylamide. Thus, miniemulsion polymerization requires a smaller amount of emulsifier than microemulsion [10], and also it gives more stable and homogeneous latexes in comparison with conventional emulsion [11].

Formation of a distinct interfacial boundary between water and oil phases creates favorable conditions for the occurrence of polymerization near the interface. Therefore, the copolymerization of monomers with strongly different hydrophilicities becomes more probable.

In the case of homogeneous polymerization the composition of copolymer can be predicted with the copolymerization equation, which depends on the relative reactivities of monomers reacting with themselves or with the comonomer [86]. In most cases of free-radical copolymerization, the relative reactivities of monomers do not depend on the type of reaction medium [7]. Wu and Schork [70] have studied mini- and macroemulsion copolymerization of different comonomer pairs with large differences in reactivity ratios and water solubility (vinyl acetate/butyl acrylate, vinyl acetate/dioctyl maleate, and vinyl acetate/N-methylol acrylamide). It was found that the miniemulsion system follows more closely the integrated Mayo-Lewis equations than the comparable emulsion system. This points to the stronger influence of mass transfer on copolymerization. In the case of miniemulsion, the system consists of “nanoreactors” in each of which the polymerization goes as in bulk. In conventional emulsion copolymerization, the mass transfer from monomer droplets into MPP has a larger influence on copolymer composition, and ratio of monomers in MPP highly differs from the initial comonomer feed.

The possibility of amphilphilic polymer synthesis from comonomers located in different phases both by direct and inverse miniemulsions was first shown by Willert and Landfester [54] for the case of acrylamide and styrene (or MMA). It was found that the locus of initiation has a large influence on the copolymer composition. In acrylamide–styrene system, the copolymer practically lacking the admixtures of homopolymers (3 wt. % polyacrylamide and 1 wt. % polystyrene) was prepared in inverse miniemulsion with the use of a surface-active initiator (azo-di(poly(ethylene glycol)isobutyrate), PEGA200). In the case of the acrylamide–MMA system, a good yield of the copolymer relative to those of homopolymers (9 wt. % polyacrylamide and 13 wt. % PMMA) was achieved with the initiator soluble in the oil phase.

The classical copolymer equation cannot predict properly the copolymer composition, because the reaction medium and the place of inintiation affect on copolymer composition. Therefore, Kuchanov and Khokhlov [87] elaborated a theoretical model of heterogeneous copolymerization with the initiation occurring at minidroplet surface. That can be realized with a surface active initiator poorly soluble in both phases. Such processes lead to the formation of multiblock copolymers with hydrophilic and hydrophobic monomeric units. The model deals with the parameters such as concentrations of monomers, initiation rates in both phases close to their boundary, and rate constants of the elementary chain propagation and termination reactions under the homopolymerization of these monomers. In fact, the propagation of a polymer chain in the vicinity of the interphase boundary is controlled along with the stoichiometric and kinetic factors. Under the interphase copolymerization, thermodynamic factors also play an important role among the kinetic factors. These factors are characterized in the proposed kinetic model by parameters k_1 and k_2, where $k_\alpha=\exp(-\Delta F_{\alpha\beta}/k_Б T)$ is predetermined by the loss of the free energy ΔF_α of an α-th type macroradical under the transition of its terminal unit through the interface from phase α to phase β. It is supposed that the parameter k_a coincides with molar solubility of α-monomer in phase β.

Problem statement

The represented review evidences that the polymerization in inverse miniemulsions is an attractive alternative to micellar polymerization used for HM polyacrylamide synthesis from the standpoint of an efficient usage of surfactant. There is a large interfacial boundary between water and oil phases in miniemulsion, which creates favorable conditions for the polymerization near the interface. This system has a high aggregative stability of miniemulsion droplets and resulted latexes. The copolymer composition can be controlled by the type of initiator. In particular, the usage of surface-active initiator is expected to result in microblock structure.

2.3. Redox Systems based on Cerium (IV) Ion for Polymerization Initiation

Free radicals, for the purpose of initiating polymerization, can be obtained with two different methods [7]: (i) by homolytic decomposition of covalent bonds – spontaneously or as a result of thermolysis or photolysis, and (ii) by electron transfer from ions or atoms containing unpaired electrons followed by bond dissociation in the acceptor molecule as a result of chemical or electrochemical redox reaction. Effective initiators of free radical polymerization are various redox systems, where free radicals are produced during bimolecular and increasingly complicated reactions between oxidizing and reducing agents. Such reactions are characterized by very short induction period (almost negligible) and low activation energy of about 40 – 80 kJ/mol (for comparison, bond dissociation energy for most practical thermal initiators is in the range of 125–160 kJ/mol), that allows one to carry out polymerization with high rates at low temperatures [88]. When a metal ion is applied as an oxidant in a redox system, single free-radical forms. As a concequence, probability of primary radical recombination becomes small as compared with the homolytic decomposition of covalent bonds. There are different metal ions, such as Mn(III), Mn(VII), Ce(IV), V(V), Co(III), Cr(VI) and Fe(III), which could be utilized mainly for this purpose. Alcohols, thiols, ketones, aldehydes, acids, amines and amides are used as reducing agents [88].

Mino and Kaizermann [89] were the first who applied ceric ions for the initiation of vinyl monomers polymerization. Nowdays, redox initiation systems based on cerium (IV) ions have been extensively used in aqueous polymerization [90–92] as well as in graft [12, 13, 97] or block [93–96] polymerization of vinyl monomers such as acrylates, acrylonitrile, and acrylamide. The reducing agents may be alcohols [90, 98], aldehydes [99], acids [91, 92], thiols [100], diketones [101], or polymers with these functional groups [93, 96]. Among them, 1,2-diols [94, 102, 103], in particular, mono- and polysaccharides [15, 104], are known to be very efficient in redox initiation systems. Therefore, ceric ions have been widely applied to grafting of acrylamide, acrylonitrile, acrylates and other vinyl monomers onto various carbohydrates: cellulose [12, 13], dextran [16], starch [15], sodium alginate [14] and so on. Cerium(IV) ions are usually involved in the the form of cerium(IV) ammonium nitrate (**CAN**), cerium(IV) ammonium sulfate, cerium(IV) sulfate and ceric perchlorate. In these double salts, CAN and ceric ammonium sulfate, the tetravalent cerium is situated in the anion [88]. The crystal structure, with cerium (IV) at the center of the anion complexed by six bidentate nitrate groups, shows that the correct name of $(NH_4)_2[Ce(NO_3)_6]$ is di-ammonium hexanitratocerate. Similarly, solid sulfate analogues $(NH_4)_4[Ce(SO_4)_4]\cdot 2H_2O$ and

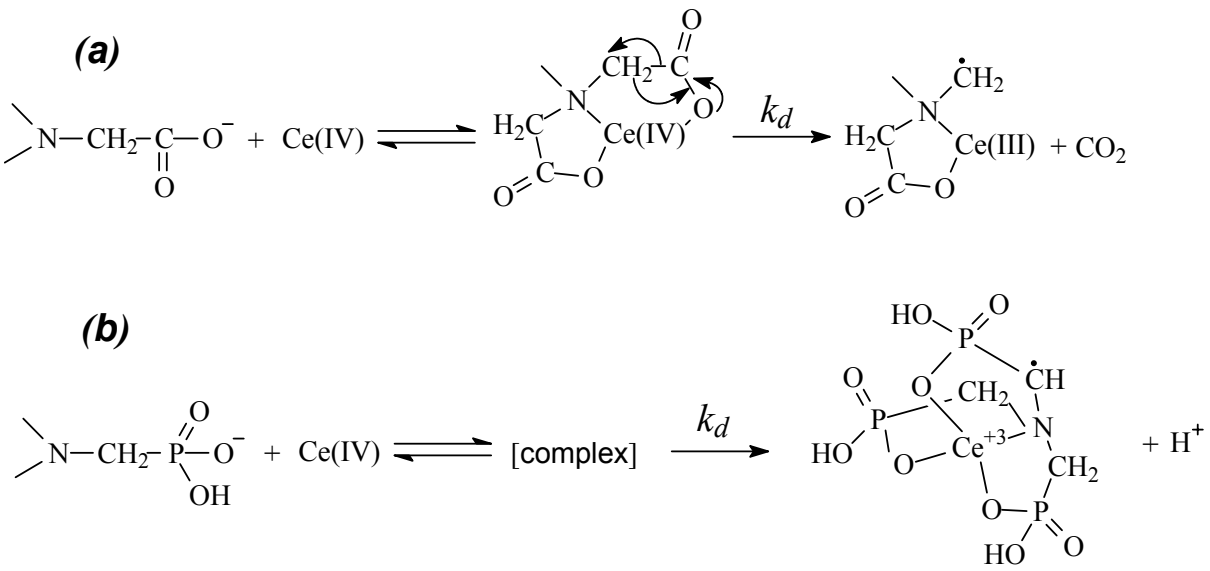


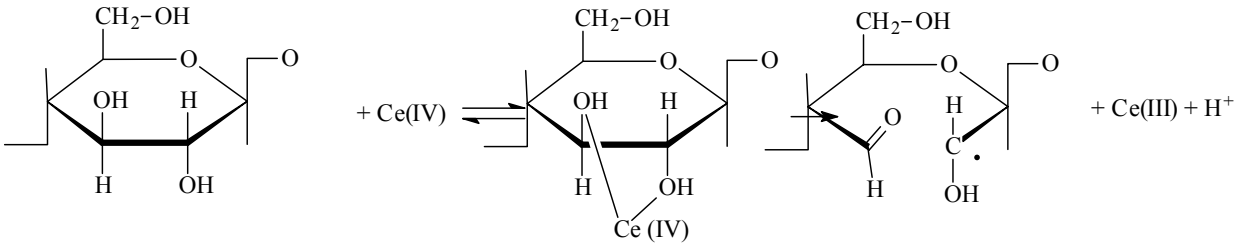
Fig. 9. Scheme of primary free radicals formation by interaction of (***a***) CAN – nitrilotriacetic acid and of (***b***) CAN – amino tri(methylene phosphonic acid) (**ATMP**).

$(NH_4)_2[Ce(SO_4)_3]$ are correctly – sulfatocerates. In solution, Ce(IV) is also present as a complex anion [105].

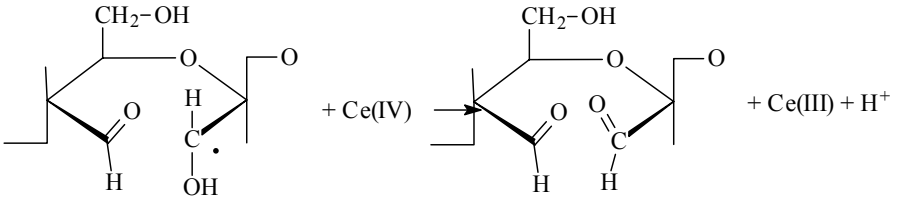
Mechanism of the primary free radical formation

An initiating radical is formed through the complex formation between the reducing agent and the tetravalent cerium salt. The chelating agent acts not only as a reducing agent, but also as a promotor for the initiation. The schemes of primary free radical formation by interaction of CAN with chelating agents nitrilotriacetic acid [92] and different derivatives of phosphonic acid [91] are presented in **Fig. 9**. The analysis of polymer end-groups by the infrared absorption technique has confirmed the proposed mechanism [106].

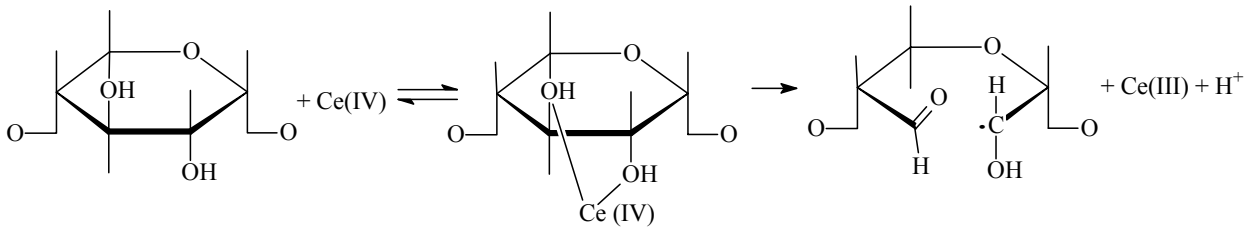
The tetravalent cerium salts are widely used for the grafting of different vinyl monomers onto cellulose and starch. For clearing the initiating mechanism of grafting, the reaction of Ce(IV) with cellulose, saccharides, polyatomic alcohols and model compounds was studied [12, 104, 107]. It was found that oxidation of polyatomic alcohols containing α-glycolic groups with Ce(IV) ions proceeds with the cleavage of C-C bond. The transformation of xylite and sorbite were found to proceed with C_2-C_3 or C_3-C_4 bonds spliting. Glucose oxidation Ce(IV) acted firstly onto hemiacetal group. As a result HCOOH was eliminated and arabinose was formed. α-methyl glucoside was oxidized to HCOOH and CO_2 Considering this data, the following initiating mechanism for the grafting onto cellulose was proposed:



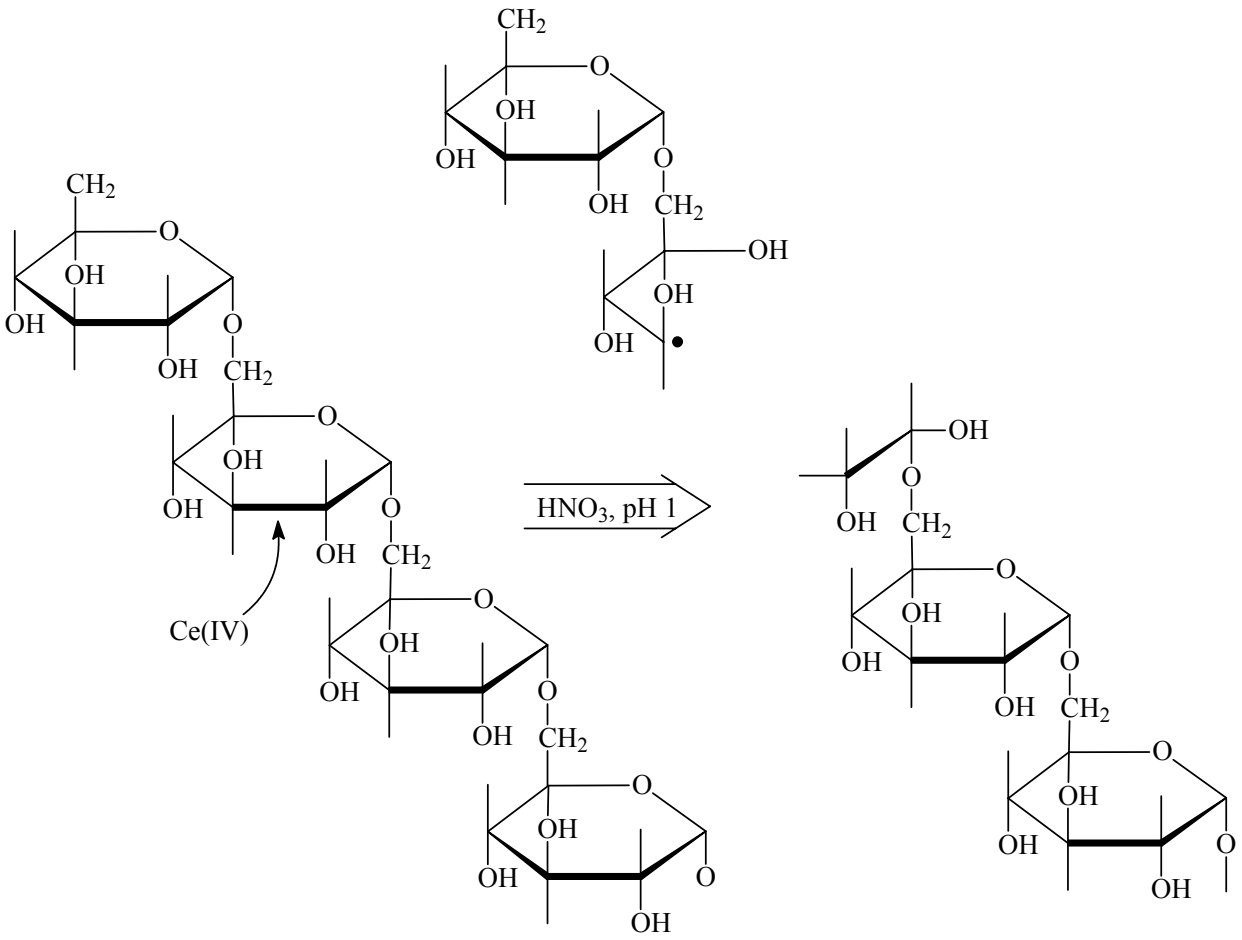
[chelate complex] [free-radical]



When other polysaccharides are treated by cerium (IV) the formation of primary radicals proceeds via similar mechanism [108]:



However, at extremely low pH (pH = 1) dextran chain is splitted by cerium (IV) into two parts. This mechanism of initiation was found when alkylcyanoacrylate grafting was studed [16, 109]:



In the study [97], a possibility of acrylamide polymerization with the initiation by ceric ions without any reducing agent was revealed. It was confirmed by IR- and NMR-spectroscopy that hydrated CAN formed a π-complex with acrylamide. Two mechanisms of the ceric-initiated polymerization of acrylmide were proposed. Initiation of homopolymerization without nitric acid and reducing agent follows a radical mechanism based upon Ce^{4+}-coordinated acrylamide. The mechanism of the ceric salt-initiated graft copolymerization of acrylamide onto cellulose (which reacted as redusing agent) can be explained in two ways: firstly, a free-radical mechanism involving Ce(IV)/Ce(III) redox system, and, secondly, a radical mechanism based on Ce^{4+}-coordinated acrylamide. Nevertheless, there are many other studies showing the impossibility of ceric salt initiation of acrylamide [91, 110, 111] and MMA [112] polymerization without the addition of the reducing agent. This conclusion was proved by the observation that the rate of ceric ion disappearance is independent of monomer concentration and is directly proportional to the concentrations of ceric ion and reducing agent [102, 110].

Kinetics of solution polymerization

There are numerous works investigating the polymerization kinetics of different vinyl monomers with the initiation by different redox systems based on ceric ions. For

example, in the case of the polymerization of acrylamide with the initiation by cerium(IV)–2-chloroethanol redox pair [110] and for the polymerization of acrylonitrile with the initiation by cerium(IV) ammonium sulfate–diol [102, 103] it was shown that the rate of polymerization, R_p, was directly proportional to the concentration of reducing agent and inversely proportional to the ceric ion concentration, but it shows the square dependence on the concentration of monomer. The latter dependence rules out the possibility of mutual termination of the growing radicals. However, mutual type of termination was observed in the case of cerium(IV) ammonium sulfate–malonic acid initiated polymerization of MMA and methylacrylate in aqueous sulfuric acid [113] and CAN–isobutyl alcohol initiated polymerization of MMA in aqueous nitric acid [98]. The polymerization of MMA in aqueous nitric acid with CAN–isopropyl alcohol as initiating system obeys power lows with exponents equal to 1/2 and 3/2 with respect to isopropyl alcohol and monomer concentrations, respectively, within the range ((3÷5)×10^{-3} mol/l) of Ce(IV). However, at lower Ce(IV) concentration (<1×10^{-3} mol/l), the monomer and Ce(IV) power exponents were changed to 1 and 1/2, respectively. The rate of the ceric ion disappearance was linearly proportional with respect to the concentration of Ce(IV) and isopropyl alcohol. One can conclude that the termination reaction can proceed either by the oxidative termination at high Ce(IV) concentration or by the bimolecular interaction of the polymeric radicals at low Ce(IV) concentration [14].

It was suggested, that for the ceric salts initiated vinyl polymerization primary free radicals are formed through complex fomation between ceric ion and reducing agent. Termination occurs by the interaction of propogating chain radicals and ceric ions, or mutual combination of growing chain radicals. The following scheme was generally proposed for the polymerization initiated by the redox system based on cerium(IV) ions [88].

Complex formation

$$\text{Ce (IV)} + \text{R} \rightarrow \text{[Ce (IV)–R]} \quad (1)$$

Production of primary radical

$$\text{[Ce (IV)–R]} \xrightarrow{k_d} \text{Ce (III)} + \text{R}\cdot \quad (2)$$

Initiation

$$\text{R}\cdot + \text{M} \xrightarrow{k_i} \text{RM}\cdot \quad (3)$$

Propagation

$$\text{RM}\cdot + n\text{M} \xrightarrow{k_p} \text{R(M)}_n\text{M}\cdot \quad (4)$$

Termination:

Termination by cerium(IV)

$$R(M)_nM\cdot + Ce\ (IV) \xrightarrow{k_{t_1}} M_n + Ce\ (III) + H^+; \quad (5)$$

Mutual termination

$$R(M)_nM\cdot + \cdot M(M)_nR \xrightarrow{k_{t_2}} R{-}M_n{-}M{-}M{-}M_n{-}R; \quad (6)$$

$$R(M)_nM\cdot + \cdot M(M)_nR \xrightarrow{k_{t_3}} R{-}M_n{-}MH + M{=}M_n{-}R \quad (7).$$

Influence of ceric ions, reducing agent and monomer concentrations on the yield and molecular mass of polymer

For acrylamide polymerization using CAN – 2-chloroethanol as a redox system, it was found that the molecular mass of polymer decreases by increasing the concentration of ceric ion and increases if the concentrations of monomer and 2-chloroethanol [110] increase. The following dependences were found for grafting of acrylonitrile onto polyoxyethylene with redox initiating system based on $Ce(NH_3)_2(SO_4)_3$ [93]. The yield and molar mass of copolymer and the content of polyacrylonitrile are increased simultaneously, when acrylonitrile concentration is rised at constant PEO and Ce(IV) amount. The next experiments were carried out at different amounts of PEO; keeping the concentration of acrylonitrile and ceric salt constant. As it was expected, the increase in PEO concentration results in larger conversion of acrylonitrile and higher yield of copolymer. Potentially, this is a consequence of an intensive formation of the initiating centers due to the increase in the concentration of OH-groups. The influence of Ce(IV) concentration on the yield and the composition of block-copolymer was studied. Maximal yield of block-copolymer was observed at ceric ions concentration corresponding to $1<\frac{[Ce(IV)]}{[PEO]}<2$. Taking into account that the average functionality of PEO relative OH-groups usually is equal to $1<f<2$, this result confirms the assumption of equivalent [Ce(IV)]/[PEO] ratio at the optimal conditions.

The same dependence of polymer yield on the diol and cerium (IV) concentrations was observed for polymerization of MMA initiated by CAN in combination with polytetrahydrofuran diol and polycaprolactone diol [94].

The influence of the redox system component (CAN – ATMP) concentration on the yield and molecular mass of polyacrylonitrile was studied in Ref. [91]. The non-monotonic dependences of the polymer yield and molecular mass on the reducing agent concentration as well as on ceric ions concentration were observed. This was explained by the possibility of degradative chain transfer by ATMP at rather high ATMP concentration with respect to ceric ions on one hand and by the oxidative chain termination by Ce(IV) at its high concentration on the other hand. These peculiarities

are promoted by a heterogeneous character of polymerization. The precipitation of polymer during polymerization decreases the contribution of mutual termination of growing macroradicals in the termination reactions and increases a contribution of termination at the expense of capture of small easily diffusing molecules such as ceric ion, primary radicals and ATMP.

Problem statement

It was shown previously that 1,2-diols, mono- and polysaccharides are very efficient reducing agents in redox initiation systems based on tetravalent cerium salts. However the application of ceric ions containing redox systems for inverse emulsion polymerization is not known at present. Therefore, it is of special interest to show the applicability of the redox system based on ceric ions in the miniemulsion polymerization of water-soluble vinyl monomers, including acrylamide. In that case, a sorbitol-containing surfactant could play a role of a reducing agent. For example, sorbitan monostearate (Span 60) is commercially available and relatively low-cost emulsifier for the stabilization of inverse emulsions and miniemulsions. On one hand, this system should possess the advantages of redox initiation systems. On the other hand, the primary free radicals should be localised at the surface of MPP. As a consequence, the system should possess some peculiarities, e.g. an enhanced colloidal stability of the emulsion droplets and latex particles.

Thus, the proposed initiating system seems to be perspective for the development of relatively inexpensive and simple method for the synthesis of hydrophilic polymers and polymer nanoparticles. Besides, the growing radical and resulting polymers become surface-active since an alkyl tail of the surfactant incorporates into polymer chain. This initiating method could be very promising for obtaining multiblock copolymers from water-soluble and oil-soluble comonomers.

3. RESULTS AND DISCUSSION

3.1. Colloidal Properties of a Reaction Medium

The first question, which arises by considering the emulsion polymerization, is the stability of dispersion system. It is especially important in the case of miniemulsion polymerization, where the nucleation and polymerization occur in each monomer droplet without changing their identity during the synthesis. Therefore it is necessary that the system keeps its stability both after the preparation of miniemulsion and during the polymerization.

The breaking of emulsion can occur due to molecular diffusion degradation (Ostwald ripening, τ_1 mechanism) or due to coalescence by collisions (τ_2 mechanism). For suppression the Ostwald ripening process, it is necessary to add into the system a small amount of a third component (osmotic pressure agent), which must be preferentially distributed in the dispersed phase. Stabilization of emulsions against coalescence can be obtained by an addition of the appropriate surfactants.

The HLB numbers by Griffin were widely used for a quantitative estimation of the emulsifier efficiency (**Tab. 1**). For non-ionic surfactants these numbers can be calculated as follows [114]:

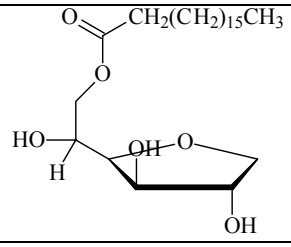
$$HLB_{(Griffin)} = 20\frac{M_H}{M}, \qquad (3.1.1)$$

where M is the molecular mass of the surfactant, and M_H is the molecular mass of its hydrophilic part.

In the case of inverse emulsion, non-ionic surfactants with HLB values in the range of 4–6 are mostly used. This type of surfactants stabilizes the emulsion by steric factors [52].

In the present work, a solution of acrylamide in 0.1 M aqueous solution of NaCl was used as a dispersed phase of miniemulsion, and a continuous phase consisted of a solution of emulsifier in cyclohexane. The industrial emulsifier sorbitane monostearate (Span 60) with low HLB was chosen as stabilizer. The content of sorbitane monostearte in commertial product from Aldrich is about 50%. The residue

Tab. 2. The colloidal properties of emulsifier Span 60 (T = 25°C)

Name	**Formula**	**HLB**	**CMC×10⁴, mol/l**	**Γ_m×10¹⁰, mol/cm²**	**a_s, Å²**
sorbitane monostearate **(Span 60)**		4.79	3.2*	44.8*	3.7

* the data are taken from Ref. [115].

consists mostly of sorbitane monooleate and other sorbitane esters. The calculated Griffin's HLB value according to eq. 3.1.1 is given in **Tab. 2**.

In the Ref. [115], CMC values for Span homologous series were determined on the boundary of 1% aqueous solution of acrylamide/Span in cyclohexane. In particular, CMC of 3.2×10^{-4} mol/l for Span 60 was obtained. It was also found that the CMC values increase with the growth of acrylamide concentration in the system, what was associated with the rise of emulsifier solubility in water phase even in the presence of a small amount of acrylamide. The surface excess concentration ($\Gamma_m\times10^{-10}$ mol/cm²) was determined for a system of 1% aqueous solution of acrylamide/Span in cyclohexane.

The surface area per surfactant molecule can be calculated as follows [114]:

$$a_s = \frac{10^{16}}{N_A \Gamma_m}, \qquad (3.1.2)$$

where N_A is the Avogadro's number (6.02×10^{23} g^{-1}mol^{-1}), and Γ_m is the surface excess concentration (mol/cm²). The result of calculation from data of work [115] is given in

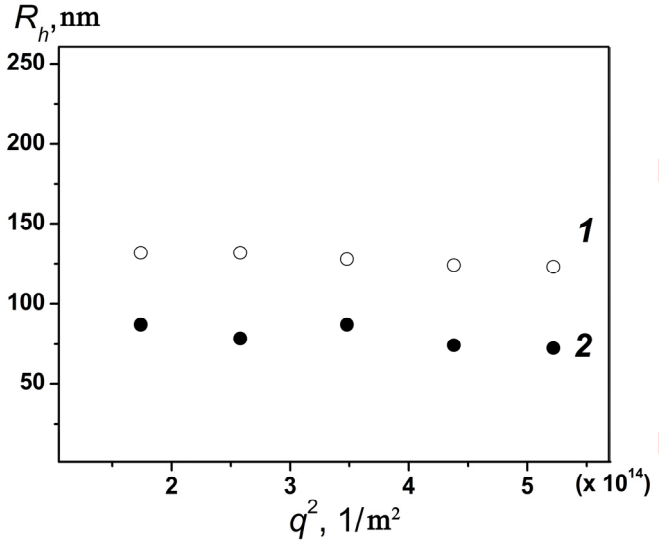


Fig. 10. Dependence of the hydrodynamic radius (R_h) of (***1***) droplets and (***2***) latexes on the angle of scattered light. Conditions of synthesis: W/O = 1/7, c_{AAm} = 7.0 mol/l, c_{LMA} = 1.1 ×10^{-2} mol/l, c_{AIBN} = 3.7×10^{-4} mol/l and c_{em} = 3.3 wt. % (in oil).

Tab. 2.

Evaluation of the size of miniemulsion droplets and latex particles under polymerizarion conditions used in this work from DLS data showed that the hydrodynamic radius (R_h) of the droplets was (120±10) nm and that of latex particles was (70±10) nm. As follows from **Fig. 10** the value of R_h does not practically depend on the angle of measurement. That specifies relative uniformity of the sizes of miniemulsion droplets and latex particles.

It was also demonstrated that the size of droplets is not affected by the emulsifier concentration in the selected range (from 1.7 to 3.3 wt. %). However, an increase in the amount of emulsifier improves the sedimentation stability of the emulsion and decreases the amount of coagulum in the course of polymerization.

The information about the size and shape of droplets allows us to calculate the area occupied by one emulsifier molecule on a droplet surface (a_s) using the following equations:

$$n_{drop} = \frac{V_{all}}{V_{drop}} = \frac{V_{all}}{\left(\frac{\pi}{6} d^3\right)}, \qquad (3.1.3)$$

where n_{drop} is the number of miniemulsion droplets in the system, V_{all} is the total volume of droplets, V_{drop} is the volume per one droplet, and d is the diameter of a droplet. Then, the value of a_s is simply calculated as:

$$a_s = \frac{S}{n_{em}} = \frac{n_{drop}\pi d^2}{n_{em}}, \qquad (3.1.4)$$

where S is the total area of droplets in the system, and n_{em} is the number of surfactant molecules.

The values of V_{all} equals to 4 ml and of d equals to 240 nm were taken for the calculation. Thus, the surface area, a_s, per Span 60 molecule was 9 Å^2 and 18 Å^2 for 3.3 wt. % and 1.7 wt. %, respectively. Comparing these values with the value of

Tab. 3. Interfacial tension σ_{12} at the water/oil interface

Aqueous phase	**Oil phase**	**σ_{12}, mN/m**
Water	Cyclohexane	46.6
0.1 M NaCl	Cyclohexane	40.7
0.1 M NaCl+acrylamide 10%	Cyclohexane	30.3
0.1 M NaCl	22.6% LMA in cyclohexane	27.0
0.1 M NaCl	1% Span 60 in cyclohexane	2.5
0.1 M NaCl	Miniemulsion (3.3% Span60)	14.7

a_s = 3.7 nm for the saturated adsorption layer of Span 60 (**Tab. 2**), one can conclude that the surface coverage of the miniemulsion droplets by surfactant molecules is incomplete. This conlusion is also independently supported from the measurement of the interfacial tension on the boundary of inverse emulsion/aqueous solution of NaCl. As can be seen in **Tab. 3**, the interfacial tension at the boundary between aqueous NaCl and inverse miniemulsion (14.7 mN/m) is much higher than that at the boundary between the same aqueous phase and the saturated emulsifier solution (2.5 mN/m). These data suggest that in the presence of emulsion droplets, the concentration of the surfactant in this system is smaller than CMC. Hence, surfactant micelles are absent in the continuous phase and interfacial layers on miniemulsion droplets did not reach saturation. The absence of free emulsifier micelles in the system argues for the benefit of the droplet nucleation.

Tab. 3 shows that the addition of acrylamide into the aqueous phase or LMA into the organic phase leads to a decrease in the interfacial tension. By considering the fact of the interfacial activity of acrylamide [53, 115, 116], it is therefore reasonable to assume that the local concentration of the monomers near the interface becomes larger, and, as a consequence, the probability of these monomers copolymerization increases.

3.2. Free-radical Polymerization and Copolymerization of Acrylamide Initiated by Azobisisobutyronitrile

As it was shown by Gromov *et al.* [57], the solubility of AIBN in the aqueous phase is improved when emulsions of aqueous solution of acrylamide/heptane and aqueous solution of acrylamide/toluene are used. The conclusion that the local concentration of AIBN grows near the interfacial boundaries was reported for the microemulsion polymerization of acrylamide and its copolymerization of MMA [116, 117]. Due to initiator concentration near interfacial boundaries, the copolymerizating of the monomers with different hydrophilicities becomes more probable.

3.2.1.Free-radical Polymerization of Acrylamide

In order to optimize the copolymerization conditions, the homopolymerization of acrylamide was studied. The influence of the amount of emulsifier (Span 60) and initiator on the rate of polymerization and the molecular mass of polyacrylamide was investigated. The following synthesis conditions were utilized: the concentration of acrylamide in the aqueous phase, c_{AAm}, was 7 mol/l, water-to-oil mass ratio, W/O, was equal to 1/6, and the temperarure was about 60°C. The relevant data from all

Tab. 4. Yield of polyacrylamide and its M_w in relation to the concentrations of initiator c_{AIBN} and emulsifier c_{em} in oil phase

Sample, №	$c_{AIBN}\times10^3$, mol/l	c_{em}, wt.%	Time of synthesis, t, h	Yield, wt. %	$M_w\times10^{-6}$	
					GPC[1]	SLS[2]
Span 60						
PAAm-1$_{AIBN}$	1.2	3.3	3	24	0.82	—
PAAm-2$_{AIBN}$	4.7	3.3	3	99	2.70	2.65*
PAAm-3$_{AIBN}$	1.2	1.7	3	35 (coagulum)	1.54	—
PAAm-4$_{AIBN}$	4.7	3.3	4	99	2.00	—
PAAm-5$_{AIBN}$	4.7	1.7	3	80 (latex)	2.92	3.00**
				15 (coagulum)	—	—

* Measured in water and ** formamide.
[1] GPC – gel permeation chromatografy
[2] SLS – static light scattering

syntheses are summarized in **Tab. 4**. The chemical structure of polymers was confirmed by ^{1}H NMR and IR – spectroscopy.

It was found that the increase of emulsifier concentratrion, c_{em}, from 1.7 to 3.3 wt. % has improved the aggregative stability of emulsion and allowed one to avoid coagulum formation during polymerization (**Tab. 4**, samples PAAm-2$_{AIBN}$ and PAAm-5$_{AIBN}$). The quantitative yield of polymer (up to 100%) with high molecular mass (M_w = (2÷3) ×10^6, M_w/M_n = 4÷9) was obtained using relatively high concentration of initiator (c_{AIBN}= 4.7×10^{-3} mol/l) (**Tab. 4**, samples PAAm-2$_{AIBN}$, PAAm-4$_{AIBN}$ and PAAm-5$_{AIBN}$). At the reduced concentration of the initiator (c_{AIBN} = 1.2×10^{-3} mol/l) the increase

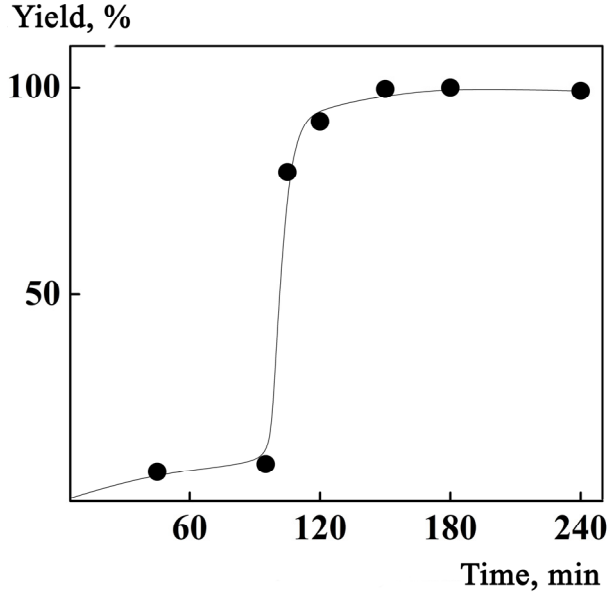


Fig. 11. Dependence of polymer yield on reaction time at homopolymerization of acrylamide (**Tab. 4**, sample PAAm-4$_{AIBN}$).

of the emulsifier amount negatively affected the yield (24 %) and molecular mass of polymers (M_w = 0.82×10^6) (**Tab. 4**, samples PAAm-1$_{AIBN}$ and PAAm-3$_{AIBN}$). The participation of emulsifier molecules or its impurities in the reactions of decontamination of primary radicals and in the reactions of polymer chain termination can be the reason of the simultaneous decrease in molecular mass and reaction rate at relatively high amount of Span 60. By summarizing the data, the optimal conditions for copolymerization would be: c_{AIBN} = 4.7×10-3 mol/l and c_{em} = 3.3 wt. %. As it is seen from **Fig.11** the quantitative yield of polymer (about 100%) is reached in 3-4 h at the chosen conditions.

It is known from literature that variations in molecular mass and rate of polymerization follow different patterns depending on the amount of emulsifier, the concentrations of monomer and initiator, and the nature and ratio of phases, when polymerization of acrylamide is carried out in inverse emulsion stabilized by Span 60 [61]. Our data on the effect of c_{AIBN} and c_{em} on the rate of polymerization and molecular mass are consistent with the study of the emulsion polymerization of acrylamide with the same initiator and emulsifier using heptane as a continuous phase [57]. In the cited paper, the reaction orders with respect to the emulsifier were negative, molecular mass decreased with an increase of c_{em}, and self-acceleration of polymerization took place after the initial slow stage. These trends were the most noticeable at high concentration of acrylamide in the aqueous phase (7.45 mol/l). The authors explained these features by the redistribution of the reaction mixture components between phases, in particular, by experimentally observed partial transition of AIBN from heptane to the aqueous phase. The latter effect manifests itself most considerably in the presence of a large amount of acrylamide.

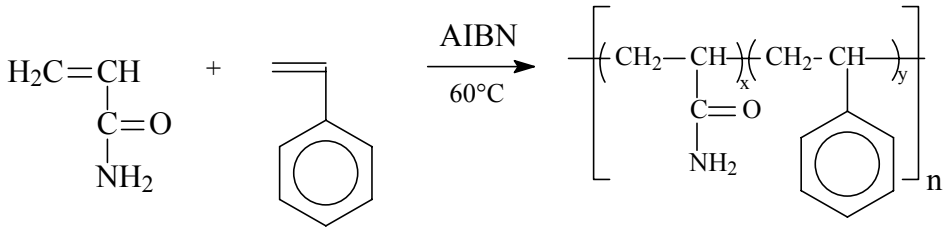
The polymerization conditions used in this study were as follows: high concentrations of acrylamide and emulsifier and the use of cyclohexane as an oil phase (as heptane, this compound possesses low dissolving ability with respect to AIBN). These conditions are nearly the same as those in [57]. Therefore, the above-described phenomena may also be explained by the redistribution of reaction mixture components between oil and aqueous phases, as well as at the interfacial layer. In particular, when high amount of emulsifier is used, it participates in a large proportion in termination of growing radicals.

If the amount of initiator is relatively small, the primary radicals form mostly in continuous phase and interfacial layer. A large proportion of these radicals may be entrapped and deactivated in the interfacial layer, which lowers a polymerization rate. At the same time, growing radicals located near this layer can also be terminated with emulsifier and its impurities. When the amount of AIBN gets large, relatively large

proportion of it can be dissolved in an aqueous phase reach of acrylamide. So, primary radicals, formed in disperced phase contribute to increasing in polymerization rate and decreasing in chain termination at the interfacial boundary.

3.2.2.Free-radical Copolymerization of Acrylamide with Styrene

As it was pointed out above, the formation of a large surface between the water and oil phases and the increase of the local concentration of monomers and AIBN near the interfacial boundary create favorable conditions for the occurrence of polymerization near the interface. Therefore, the copolymerization of monomers with strongly different hydrophilicities becomes more probable. As a model reaction, the copolymerization of acrylamide with styrene was taken:



The initial mixture was equimolar; the concentrations of components were 7 mol/l of acrylamide, 0.9 mol/l of styrene, 9.3×10^{-3} mol/l of AIBN, 1.7 wt. % of emulsifier; the ratio of W/O was 1/6; and the temperature was about 60°C. As one could see in **Fig. 12**, the yield of reaction products reached ~20 % in 3 h without further increase.

The sample became completely water-dilutable after washing with hot chloloroform in a Soxhlet extractor. It was confirmed by ^{1}H NMR-spectroscopy that the product of reaction was the copolymer of acrylamide with styrene. The molar ratio of

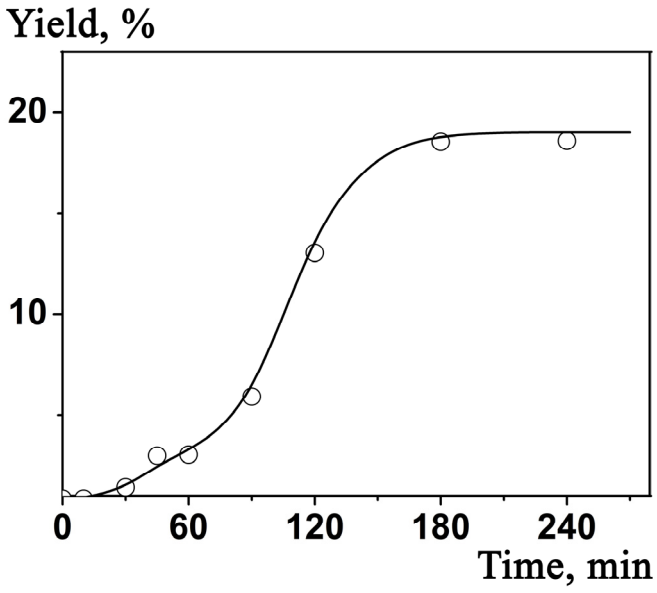


Fig. 12. Dependence of products yield on reaction time at copolymerization of acrylamide with styrene.

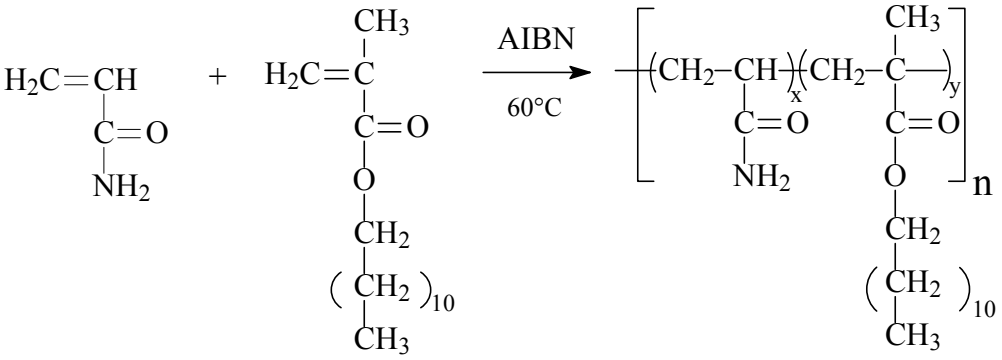
acrylamide units/styrene units (98/2) showed that only a small part of hydrophobic monomer was incorporated into the copolymer chain as microblocks or isolated monomer units. The obtained polydisperse copolymer (M_w=1.5×10^6, M_w/M_n=12) was separated into two fractions by GPC in analytical regime. As it was estimated by ^{1}H NMR-spectroscopy, the both high- (M_w=1.85×10^6, M_w/M_n=1.7), and low-molecular weight (M_w=0.17×10^6, M_w/M_n=3) fractions contained of about (1.2±0.1) mol. % styrene units. The associative properties of these fractions will be described in details in section 3.4. Homopolymer of acrylamide was not isolated. The total conversion of acrylamide has reached the value of 33%, while for styrene it was 1.4%.

The obtained results correlate with the results presented by Willert and Landfester [54] for the case of the surface-active initiator. In the cited work, molar ratio of acrylamide with respect to styrene was 1.5:1; the concentration of acrylamide was 7 mol/l, and the concentration of styrene was 0.9 mol/l; azo-di(poly(ethylene glycol) isobutyrate) was used as a surface-active initiator. The products of reaction were: polyacrylamide – 3 wt. %, polystyrene – 1 wt. %, copolymer containing 1.5 % of styrene units – 96 wt. %, at total conversion of acrylamide of 63 % and styrene of 9%.

Thus, this work, as well as the work [54] confirms the possibility of synthesis of amphiphilic copolymers based on acrylamide in inverse miniemulsions. Moreover the preferred formation of copolymer proves that AIBN concentrates on the interfacial boundary and works as the surface-active initiator under reaction conditions used in our experiment.

3.2.3.Free-radical Copolymerization of Acrylamide with Laurylmethacrylate

Series of HM polyacrylamides with different degree of modification was obtained on the basis of the above-described experimental data. LMA was used as a hydrophobic comonomer. Copolymerization was carried out at the acrylamide concentration in aqueous phase of 7 mol/l, the ratio of W/O of 1/6, c_{em} of 3.3 wt. % and the temperature of 60°C. The amount of the initiator was 1.2×10^{-3} and 4.7×10^{-3} mol/l. The comonomer ratio in aqueous and oil phases ([acrylamide]:[LMA]) was changed from 99:1 to 90:10; in addition, a ratio of 1:1 was taken. **Tab. 5** shows the results of copolymerization. The scheme of copolymerization is:



The analysis of obtained data (**Tab. 5**, GPC data) let one to make the following remarks. The yield of polymers was of about 25–50%, the molecular mass, M_w, of copolymers reached (0.7–1.2)×10^6 (M_w/M_n = 3÷5) at c_{AIBN} = 1.2×10^{-3} mol/l and the time of synthesis took 2 h. The high-molecular weight HM polyacrylamides (M_w = (2.2–3.2)×10^6, M_w/M_n = 3÷6, yield of 85–95%) were obtained at c_{AIBN} = 4.7×10^{-3} mol/l within 3-4 h. Unfortunately, the direct comparison of the rates of copolymerization is impossible to determine because of different duration of synthesis.

Tab. 5. Copolymerization of acrylamide and LMA in miniemulsions

Sample, №	**[acrylamide]: [LMA]**	***t*, h**	**Yield, wt. %**	**M_w×10^{-6} (GPC)**	**M_w×10^{-6} (SLS) in water/in formamide**
Span 60					
c_{AIBN} = 1.2 × 10^{-3}mol/l					
HMPAAm-1$_{AIBN}$	99:1	2	36	1.15	—/16.75
HMPAAm-2$_{AIBN}$	98:2	2	48	0.74	—/13.3
HMPAAm-3$_{AIBN}$	95:5	2	24	1.13	—/9.64
HMPAAm-4$_{AIBN}$	90:10	2	35	1.09	—
c_{AIBN} = 4.7 × 10^{-3}mol/l					
HMPAAm-5$_{AIBN}$	99:1	4	91	2.56	—
HMPAAm-6$_{AIBN}$	98:2	4	95	2.17	9.9/6.0
HMPAAm-7$_{AIBN}$	95:5	3	85	2.62	5.6/—
HMPAAm-8$_{AIBN}$	90:10	4	90	3.20	—
HMPAAm-9$_{AIBN}$*	50:50	4	47	0.50 (PLMA)	—
				3.30 (PAAm)	—
PLMA**	0:100	20	83	0.30	—

* Synthesis conditions: [acrylamide] = 7 mol/l, [LMA] = 0.7 mol/l, c_{AIBN} = 7.4×10^{-3} mol/l и c_{em} = 3.3 wt. %.

** Synthesis conditions: [LMA] = 0.7 mol/l, c_{AIBN} = 7.4×10^{-3} mol/l и c_{em} = 3.3 wt. %.

The self-acceleration of copolymerization was also observed after the initial slow stage (**Fig. 13**) similar to acrylamide homopolymerization.

The solubility of copolymerization products in water depends on the content of LMA in the reaction mixture: polymers would be water soluble if LMA content is less than 10%. When LMA content is higher than 10% the polymers become only partially soluble in water. Moreover, if the LMA content does not exceed 50%, their solutions are opalescent.

The fractional composition of acrylamide:LMA = 1:1 copolymerization product (**Tab. 5**, sample HMPAAm-9AIBN) was studied by means of selective extraction. The sample was successively extracted with water (to isolate polyacrylamide) and THF (to isolate PLMA). It turned out that, along with the copolymer (44 wt. %), which was soluble in none of the used solvents (water, THF, and formamide), homopolymers (8 wt. % polyacrylamide and 48 wt. % PLMA) were presented.

The chemical structure of homopolymers was investigated by ^{1}H NMR study and IR spectroscopy. The IR spectra of the copolymer exhibited a broad band peaking at 1631 cm^{-1}, corresponding to vibrations of Amide I and Amide II and the band due to the stretching vibrations of a C=O bond of an ester group (1730 cm^{-1}) (**Fig. 14**).

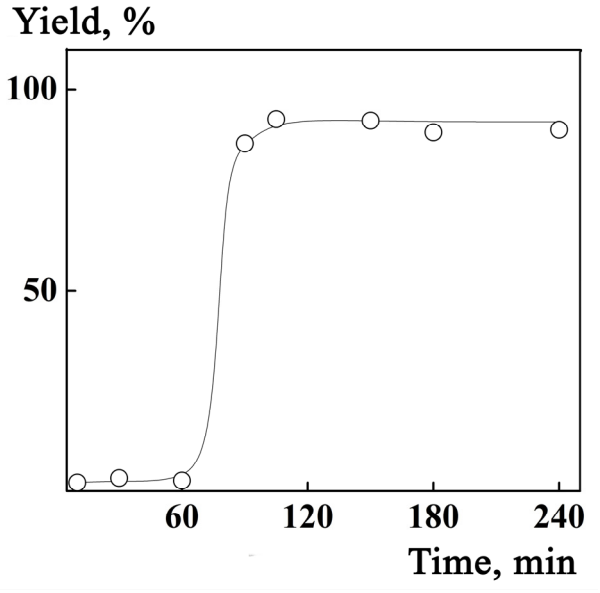


Fig. 13. Dependence of copolymer yield on reaction time at copolymerization of acrylamide with LMA at LMA concentration of 10 mol. % in the initial reaction mixture (**Tab. 5** sample HMPAAm-8$_{AIBN}$).

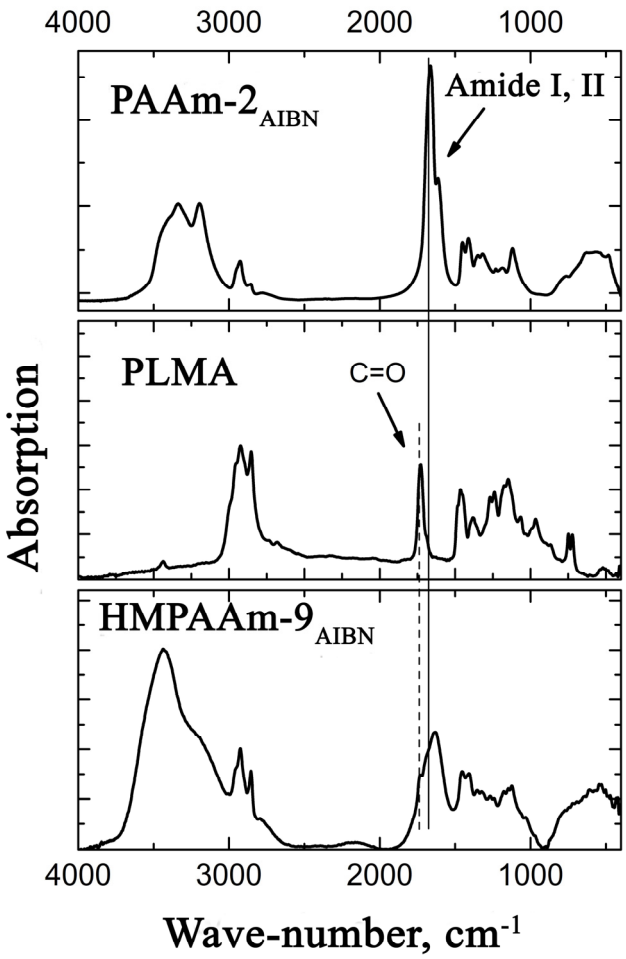


Fig. 14. The IR spectra of the samples PAAm-2$_{AIBN}$ **(Tab. 4),** PLMA and copolymer HMPAAm-9$_{AIBN}$ **(Tab. 5)**.

The content of acrylamide units in the copolymer, according to the elemental analysis data, was 98 mol. %, and the content of LMA units was 2 mol. % (C:N = 6.05). Thus, the total conversion of LMA was 31% at an almost 100% conversion of acrylamide. Similar to the above described copolymerization of acrylamide with styrene, the data on the compositional heterogeneity of copolymer HMPAAm-9_{AIBN} correlate with the results from Ref. [54], in which homopolymers polyacrylamide, polystyrene, and poly(methyl methacrylate) were isolated along with the copolymers.

The decreases in molecular masses and product yields, in the case of copolymerization, compared with homopolymerization of acrylamide arise from rapid formation of the polymeric radical carrying low-reacting styrene or LMA group on the end. The probability of a chain reaction therefore becomes small. Hence the rate of copolymerzation is sharply diminished due to decrease in kinetic chain length. The styrene radical is more low-reacting than LMA radical. It can be explained why in the case of the *acrylamide-styrene* copolymerization we observed the lower yield that for the *acrylamide-LMA* copolymerization.

To confirm that PLMA may be prepared in the course of miniemulsion copolymerization, the homopolymerization of LMA was carried out in cyclohexane in the presence of miniemulsion droplets containing an aqueous solution of NaCl (**Tab. 5**, sample PLMA). As one could see in **Fig. 15**, the yields of the polymers were 44 and 83% for 4 and 20 h, respectively. The amount of PLMA formed for 4 h and its molecular mass were found to be close to the corresponding parameters of copolymer

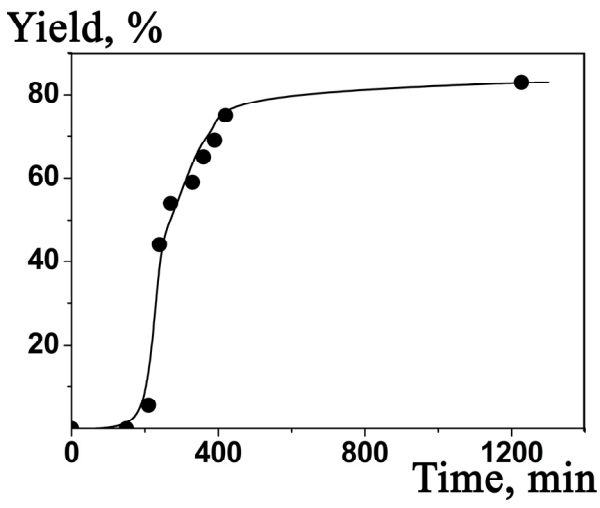


Fig. 15. Dependence of PLMA yield on reaction time at the presents of miniemulsion (**Tab. 5**, sample PLMA).

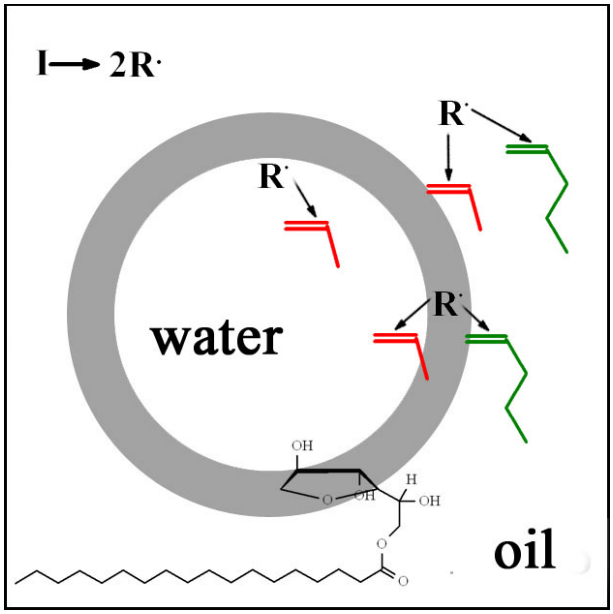


Fig. 16. Scheme of the miniemulsion copolymerization with initiation by AIBN at both phases and on the interfacial boundary. The hydrophilic monomer shows with red, and hydrophobic with green color.

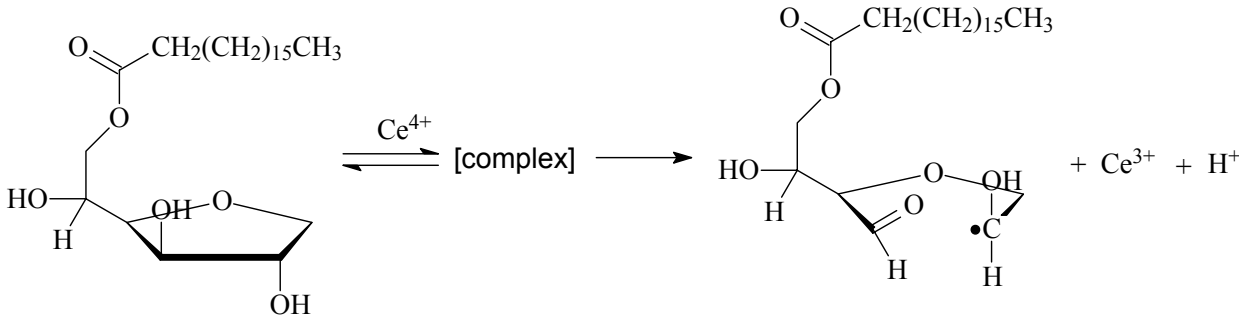
(HMPAAm-9_{AIBN}). Hence, it follows that the initiation of copolymerization may proceed in the continuous phase with participation of both acrylamide and LMA molecules. The chain propagation can also proceed with participation of LMA in this phase.

In **Fig. 16** the possible localization of initiation of copolymerization of acrylamide and hydrophobic monomer is schematically shown: in disperse phase with participation of acrylamide, in continuous phase with participation of acrylamide or hydrophobic comonomer, and at the interfacial boundary with participation of both monomers. The possibility of initiation and propagation of polymer chain in continuous phase results in increase of compositional heterogeneity of polymerization products due to the formation of PLMA.

It was shown earlier [39] that HM polyacrylamides synthesized via the micellar polymerization procedure lose solubility in water, if the content of LMA units is above 0.2–0.4 mol. %. Determination of such small content of hydrophobic units by means of direct spectral methods is practically impossible. Therefore, in this study, the amount of hydrophobic units incorporated into the polymer chain of soluble copolymers was estimated indirectly by studing their associative properties. Aqueous solutions of the copolymers were studied by fluorescence spectroscopy with pyrene as a probe, light scattering, and viscosimetry. The results of measurements are described below in section 3.4.

3.3. Free-radical Polymerization and Copolymerization of Vinyl Monomers Initiated by Surface-Activ Redox System based on Ce (IV) Salt

As was previously shown in the theoretical section, it is important to select a suitable initiator in order to obtain amphiphilic multiblock copolymers at miniemulsion condition. To provide the initiation at the interfacial boundary and propagation of polymer chain near interphase the initiator should be surface-active. It was also shown that free radicals capable to initiate polymerization of vinyl monomers formed when ceric ions act on diol fragment of mono- and polysaccharides. For the sake of experimental realization of the idea of heterophase copolymerization the new initiating redox system based on ceric ions and sorbitan monostearate (Span 60) is proposed in this work. By analogy with the initiation mechanism of grafting onto polysaccharides, the following mechanism of primary radical formation is supposed:



The use of the surface-activ component allows us to exclude any additional emulsion stabilizers. The components of the initiating system are brought into different phases; therefore, the formation of free radicals occurs exclusively at the interfacial boundary. Since an alkyl tail of a surfactant incorporates into polymer chain, the growing radical and rezulting polymers become surface-active.

3.3.1.Free-radical Polymerization of Acrylamide

Homopolymerization of acrylamide carried out by the given way of initiation leads to the incorporation of the surface-active initiator fragments, namely residual of stearic acid, in the growning polymeric chain. Thus, even in the absence of hydrophobic monomer, the proposed method allows us to receive the amphiphilic polymer.

To select the optimal conditions for synthesis of a high-molecular weight polymer with a high yield, the effect of following factors on the above-mentioned parameters was investigated: the amounts of emulsifier and initiator (CAN), the mass ratio of phases, and temperature. The way of the introduction of ceric salt into reaction media was also studied. The concentration of acrylamide was varied in the range from 3.5 to 7 mol/l. The time of synthesis was 4 h. The results are summerized in **Tab. 6**. It was found that c =1.7÷2.2 wt. % of Span 60 in the oil-phase was enough to form stable emulsions and latexes at room temperature at the water-to-oil ratio of 1/6. The double decrease in the surfactant amount resulted in insufficient sedimentation stability of miniemulsion and in the formation of about 30 % of coagulum (**Tab. 6**, sample PAAm-13_{CAN}). Moreover, even higher amount of coagulum (~80%) was produced when the polymerization temperature was increased up to 60°C at c_{em}=1.7 wt. % (**Tab. 6**, sample PAAm-6_{CAN}). The emulsion stabilization at increased temperature is reached by increasing the emulsiefer amount up to 3.3 wt. % (**Tab. 6**, sample PAAm-7_{CAN}). This argues that at high temperature the system becomes less stable to coalescence due to stronger Brownian motion of particles, an increased solubility of monomer in the opposite phase, and an increased solubility of Span 60 in the oil-phase.

The size of miniemulsion droplets and latex particles was measured by DLS. An example of the typical distribution over hydrodynamic radii is presented in **Fig. 17** (sample PAAm-$11_{CAN,}$ **Tab. 6**). The size of the miniemulsion droplets was measured just after sonication. R_h of latex particles was found to depend on the acrylamide concentration in the aqueous phase: from 50 – 55 nm at c_{AAm} = 50 % to 75 – 80 nm at c_{AAm} = 25 %, respectively. The increase of temperature up to 60°C did not alter the size of particles.

Tab. 6. The results of polymerization of acrylamide in inverse miniemulsions with initiation by system CAN - Span 60

Sample №	W/O	c_{em}, wt. %	$c_{CAN}\times10^3$, mol/l	Yield[1], %	$M_w\times10^{-6}$ (GPC)	M_w/M_n
c_{AAm} = 3.5 mol/l						
PAAm-1_{CAN}	1/6	2.2	35	100	1.2[2]	23[2]
PAAm-2_{CAN}	1/6	2.2	17	100	1.65	9.2
PAAm-3_{CAN}	1/6	2.2	11	100	1.8	4.1
PAAm-4_{CAN}	1/6	2.2	7	68	0.92	6
c_{AAm} = 4.4 mol/l						
PAAm-5_{CAN}	1/6	2.2	21	87	1.75	7.8
PAAm-6_{CAN}[3]	1/6	2.2	21	53[4]	1.66	2.6
PAAm-7_{CAN}[3]	1/6	3.3	21	100	0.73[5]	30[5]
c_{AAm} = 7.0 mol/l						
PAAm-8_{CAN}	1/6	1.7	35	53[6]	0.69	5.9
PAAm-9_{CAN}[7]	1/6	2.2	17	89	1.2[8]	9.5[8]
PAAm-10_{CAN}	1/6	2.2	17	97	1.61	5.3
PAAm-11_{CAN}	1/6	2.2	14	98	1.8	5
PAAm-12_{CAN}	1/3	1.7	14	86.5[9]	0.96	7
PAAm-13_{CAN}	1/6	0.85	14	85.5	0.86	7

[1] Determined gravimetrically
[2] Bimodal molecular weight distribution: low-molecular weight fraction – M_w=0.009×10⁶ and high-molecular weight fraction – M_w=1.6×10⁶, M_w/M_n=2.7
[3] Synthesis carried out at 60 °C
[4] Product composition: coagulum – 80%, latex – 20%
[5] Low-molecular weight fraction: M_w=0.025×10⁶, M_w/M_n=2.6. High-molecular weight fraction: M_w=1.2×10⁶, M_w/M_n=4.2
[6] Product composition: coagulum – 32%, latex – 68%
[7] CAN was added after sonication
[8] Low-molecular weight fraction: M_w=0.12×10⁶, M_w/M_n=2.7. High-molecular weight fraction: M_w=1.5×10⁶, M_w/M_n=2
[9] Product composition: coagulum – 30%, latex – 70%

The dependence of the yield and molecular mass of prepared polymers on the concentration of the redox system components grows through the maximum. While the amount of Span 60 was kept approximately constant to support the emulsion stability (c_{em}=1.7-2.2 wt.%, W/O=1/6, T=25°C), the concentration of oxidizer, c_{CAN}, was varied over a wide range. As one can see from **Fig. 18,** by changing c_{CAN} in the range (11÷21)×10^{-3} mol/l and by doubling the acrylamide concentration from 3.5 up to 7 mol/l, molecular mass, M_w, remained practically on the same level of 1.6÷1.8 ×10^6. The polymers were prepared with a quantitative yield (**Tab. 6**, samples PAAm-2$_{CAN}$, PAAm-3$_{CAN}$, PAAm-5$_{CAN}$, PAAm-10$_{CAN}$ and PAAm-11$_{CAN}$). The decrease in polymer yield (down to 50%) and molecular mass (0.7÷1.2×10^6) was observed by decreasing the ceric ions concentration down to 7×10^{-3} mol/l (**Tab. 6**, sample PAAm-4$_{CAN}$) and by increasing the ceric ions concentration up to 35×10^{-3} mol/l (**Tab. 6**, samples PAAm-1$_{CAN}$ and PAAm-8$_{CAN}$). Similar extremal dependence of polymer yield and molecular mass of polymer on Ce(IV) concentration of was observed earliar [91] when polymerization of acrylonitrile was initiated by the system amino tri(methylene phosphonic acid) (ATMP) and CAN. In the referenced work, the grow of polymer yield and molecular mass started at the concentration of Ce (IV) equal to 6×10^{-3} mol/l.

The decrease in surfactant amount (c_{em}=0.85 wt.%) resulted in the decrease of molecular mass of polymer (M_w=0.9×10^6, M_w/M_n=7) at c_{CAN} of 14×10^{-3} mol/l, c_{AAm} = 7 mol/l (**Tab. 6**, sample PAAm-13$_{CAN}$).

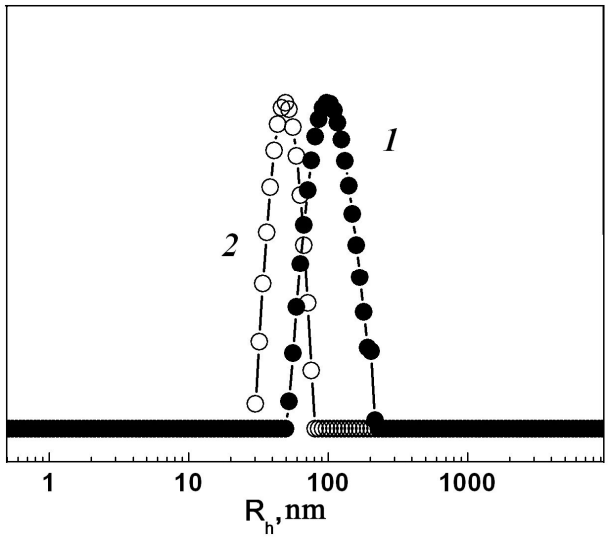


Fig. 17. Distributions of scattered light over hydrodynamic radii (R_h) of scattering particles for (***1***) miniemulsion and (***2***) latex. The observation angle is 90°. Sample PAAm-11$_{CAN}$ (**Tab. 6**).

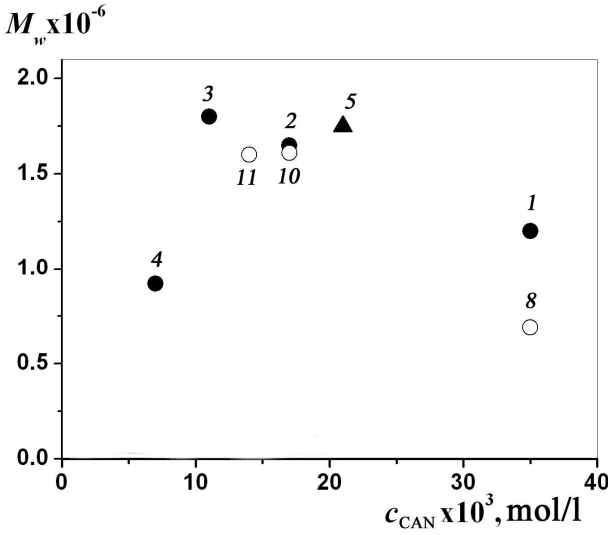


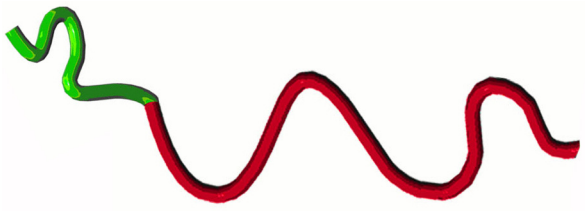
Fig. 18. Dependence of molecular mass on concentration of Ce(IV) in the system. Conditions of synthesis: W/O=1/6, c_{em}=1.7÷2.2 wt.%, T=25°C, (●) – c_{AAm} = 3.5 mol/l, (▲) – c_{AAm} = 4.4 mol/l and (○) – c_{AAm} = 7.0 mol/l. The figures are designated the numbers of samples from **Tab. 6**.

The increase in polymerization temperature reduces the polymer yield (down to 50 %, from which 80 % is coagulum), but the molecular mass remains practically constant (M_w=1.7×10⁶) (**Tab. 6**, sample PAAm-6$_{CAN}$). This could be explained by a decrease in interfacial surface at coagulation resulting in a decrease of the initiation rate. The increase in emulsifier amount in order to support the aggregative stability has resulted in increase in the yield and polydispersity and decrease in the molecular mass (M_w=0.7×10⁶, M_w/M_n=30) (**Tab. 6**, sample PAAm-7$_{CAN}$).

The decrease in oil phase volume up to W/O=1/3 at the constant concentration of initiator, emulsifier and acrylamide has resulted in decrease in the molecular mass (M_w=1×10⁶, M_w/M_n=7) (**Tab. 6**, sample PAAm-12$_{CAN}$).

Thus, the optimal conditions for obtaining the high-molecular weight polymers (1.6÷1.8×10⁶) with high yield are as follows: c_{CAN} = (11÷21)×10^{-3} mol/l, which conforms [CAN]:[Span 60] from ~1:26 up to 1:17, c_{em} = 1.7÷2.2 wt. %, W/O = 1:/6, T=25°C. The ratio [CAN]:[acrylamide] has to be in the range 1:200÷1:500.

The structure of the formed polymers generally depends on the type of the termination reaction of a material chain. Thus, the mutual termination of growing chain radicals by disproportionation (it is more preferable for acrylamide) as well as monomolecular termination on Ce(IV) and transfer to monomer result in formation of monochelic polymers. The monomolecular termination of a macroradical by the primary radical results in formation of telechelic polymers. It is difficult to estimate the contribution of each type of termination reactions because the conditions of the polymerization are heterogeneous. The formation of monochelic polymer is more probable. At the following scheme, the residual fragment of emulsifier is shown with green, polyacrylamide chain – with red.



The polydispersities of the prepared polymers are rather high (5 – 10). The error caused by band broadening was up to about 20% for high molecular mass polymers (estimated by the method of Hamielec and Ray [118]). The MMD broadening can be explained by the specific features of the heterophase polymerization under study: the initiation at the interfacial boundary and several possible termination reactions with different allocations (for example, termination by disproportionation inside the droplets, termination by ceric ions inside the droplets, and termination by radicals anchored at the interfacial boundary). One can also expect the incomplete

homogenization of miniemulsions (by fusion and fission processes) due to the fast mixing procedure prior the beginning of polymerization. By comparing the samples PAAm-9_{CAN} and PAAm-10_{CAN} (**Tab. 6**) one could notice that the method of injection of the initiating oxidizer has an impact on the polymer characteristics. The addition of a ceric salt solution in a prepared miniemulsion with subsequent additional emulsification results in lower molecular mass and broader MMD in contrast to polymers produced by emulsification of two phases, each containing the corresponding part of the redox initiator.

If we assume that the sample contains only one residue of Span 60, an average degree of polyacrylamide modification should be about 0.04 mol. % (typical M_n = 1.8×10^5). Determination of such a small content of hydrophobic units by means of direct spectral methods is practically impossible.

The formation of an amphiphilic polymer during the synthesis provides the high aggregativ stability of the latex. The cross-linked latex particles were easily dispersed in organic and aqueous media. They were prepared as follows. Acrylamide was copolymerized with 2 mol. % of BAAm under the synthesis conditions specified in **Tab. 7**. The prepared latexes were stable over a month. The particles size after dispersion was measured by DLS and transmission electron microscopy (**TEM**). The typical data is presented in **Tab. 7** and in **Fig. 19**. The dispersions in organic medium were prepared by dilution of latex with cyclohexane. The dispersions in aqueous medium were prepared by dilution of dryed latex in water. The characteristic sizes of latex particles are given in **Tab. 7**. The growth of the particle size by two times in aqueous medium can be attributed to the swelling of weakly crosslinked polyacrylamide in water. The mean particle size by TEM is about three times smaller than that by DLS

Tab. 7. Synthesis conditions and sizes of cross-linked latex based on acrylamide in inverse miniemulsion with initiation by system CAN – Span 60 (c_{em} = 1.7 – 2.2 wt.%, W/O =1/6)

Sample №	c_{AAm}, **mol/l**	$c_{CAN}\times10^2$, **mol/l**	R_h (±***RPW***[1]) **of latex, nm (DLS)**		***d* of latex, nm (TEM)**	
			cyclohexane	***water***	***cyclohexane***	***water***
PAAm-14_{CAN}	3.5	3.5	75 (±0.38)	115**(±0.41	40	—
PAAm-15_{CAN}	4.4	2.1	85 (±0.38)	200 (±0.41)	65	—
PAAm-16_{CAN}*	7.0	1.7	65 (±0.46)	196 (±0.61)	56	100
PAAm-17_{CAN}	7.0	1.7	60 (±0.33)	142 (±0.35)	31	77

* CAN was added in emulsion as a solution
** in 1% aqueous solution of SDS
[1] ***RPW*** – relative peak width

due to removal of a large amount (roughly ¾ by weight) of water from their interior and due to different way of averaging (*z*- average R_h and number-average *d*).

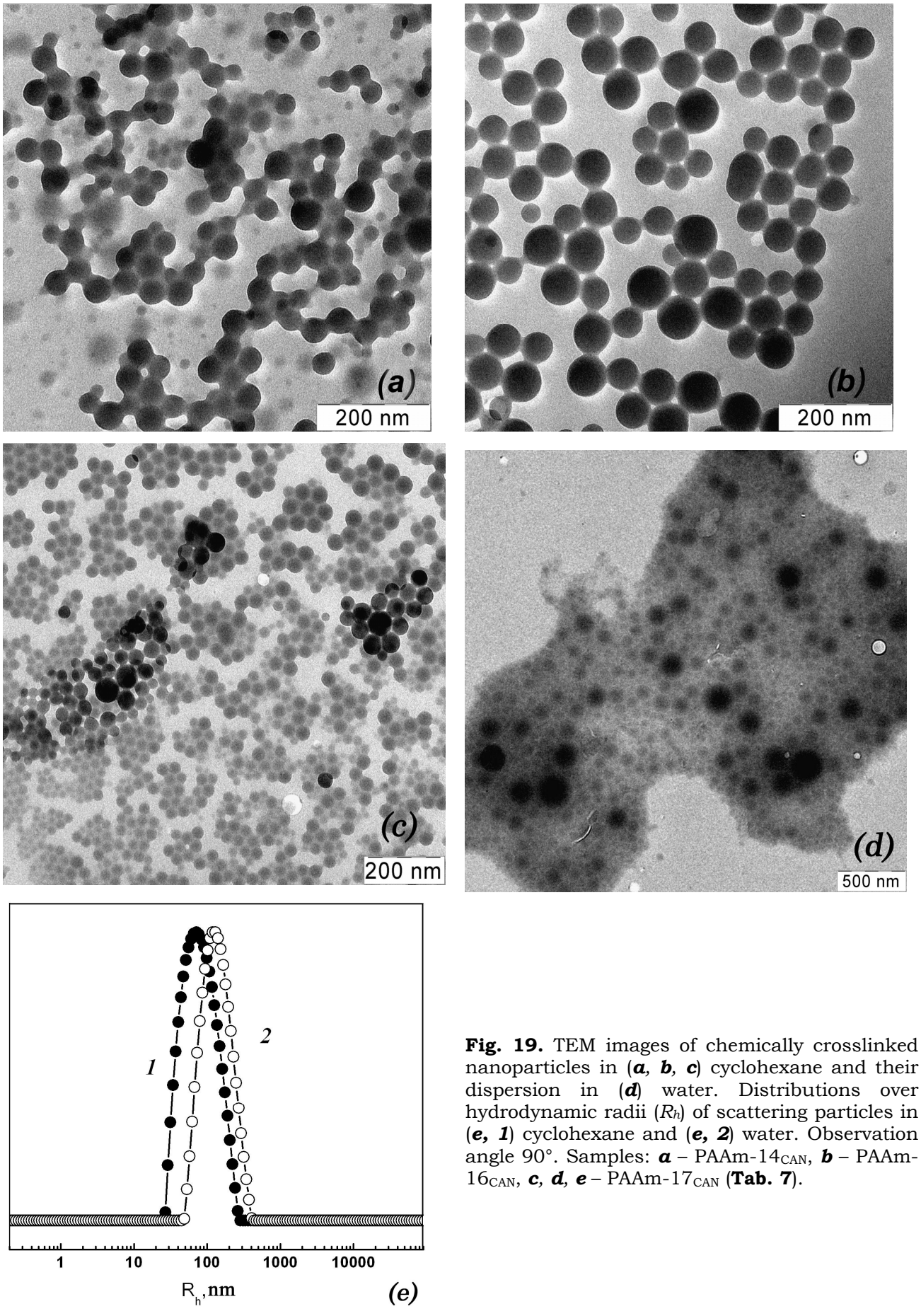


Fig. 19. TEM images of chemically crosslinked nanoparticles in (***a***, ***b***, ***c***) cyclohexane and their dispersion in (***d***) water. Distributions over hydrodynamic radii (R_h) of scattering particles in (***e, 1***) cyclohexane and (***e, 2***) water. Observation angle 90°. Samples: ***a*** – PAAm-14_{CAN}, ***b*** – PAAm-16_{CAN}, ***c***, ***d***, ***e*** – PAAm-17_{CAN} (**Tab. 7**).

3.3.2.Free-radical Polymerization of Acrylic Acid

The possibility to apply this initiation system to the synthesis of latex particles based on various water soluble vinyl monomers was shown on the example of acrylic acid. The synthesis conditions were as follows: concentration of acrylic acid – 1.6 mol/l, c_{CAN} = 1.6×10^{-2} mol/l, c_{em} = 2.2 wt. %, W/O = 1/6, T=60°C. BAAm (2 mol. % with respect to acrylic acid salt) was taken as a cross-linking agent. The polymer was obtained with the yield of 80 % within 24 h. The chemical structure of polymer was confirmed by IR – spectroscopy. The IR spectra of the polymer exhibited a band peaking at 1560 cm^{-1} corresponding to the stretching vibrations of COO^-.

The prepared latex was stable over at least a week. It was readily redispersed in cyclohexane (R_h = 180 nm, *RPW* = ±0.42) and water (R_h = 118 nm, *RPW* = ±0.37) (DLS data, **Fig. 20**).

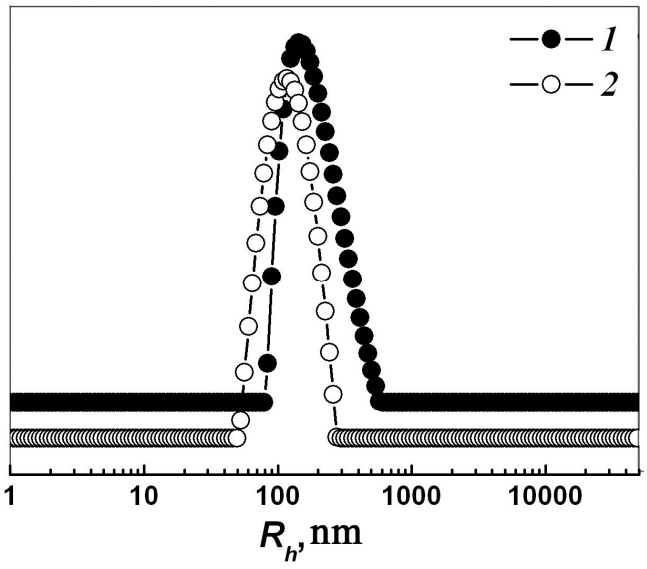


Fig. 20. Distributions of scattered light over hydrodynamic radii (R_h) of scattering particles of latex in (***1***) cyclohexane and (***2***) water. Observation angle 90°.

3.3.3.Free-radical Copolymerization of Acrylamide with Styrene

The usage of surface-active initiator provides the initiation at the interfacial boundary and propagation of polymer chain near the interphase. These features should favore the copolymerization of monomers of differing hydrophilicity distributed in different phases. The copolymerization reactions of acrylamide with styrene and LMA were taken as model reactions.

The initial mixture was equimolar; the concentrations of components were 4.4 mol/l for AAm, 0.56 mol/l for styrene, (1.7 ÷ 2.2) wt. % for emulsifier; the water-to-oil phase ratio was 1/6; and the polymerization time was about 24 h. The results are summerized in **Tab. 8**. The chemical structure of polymers was confirmed by ^{1}H NMR – spectroscopy. The degree of modification y was calculated according to equations given in the experimental part (Nuclear Magnetic Resonance). The latex particle size R_h

was about (100 ± 5) nm as revealed by DLS measurements.The influence of the following factors on copolymerization was investigated: the amount of initiator (CAN), the ratio of phases, and temperature. The yield and molecular mass of polymer were taken as an assessment.

The copolymers with low molecular mass (M_w ~ (0.2 – 0.3)×10^6) and low yield (5 – 10) % were received at ceric ion concentrations of (10÷20)×10^{-3} mol/l at room temperature (**Tab. 8**, samples HMPAAm-2_{CAN} and HMPAAm-3_{CAN}). The decrease in water-to-oil ratio to 1/3 resulted in copolymer with lower molecular mass (M_w = 0.03×10^6) (**Tab. 8**, sample HMPAAm-1_{CAN}).

The high-molecular weight products (M_w ~ (0.8 – 1.2)×10^6, yield ~ 40%) were obtained at high temperature (60°C) (**Tab. 8**, samples HMPAAm-4_{CAN} and HMPAAm-5_{CAN}). As it was pointed out above, the emulsion stability decreases when the temperature increases. Therefore, ~(10–20)% of coagulum was formed during the polymerization. The increase in ceric ion concentration from 12×10^{-3} to 42×10^{-3} mol/l resulted in decrease in molecular mass (~1.5) as expected for free-radical polymerization.

The modification degree of polyacrylamide was about 1 mol. % of styrene units. It shoud be noted that all samples were completely soluble in water and able to form opalescent solutions. This allows assuming that no homopolystyrene was formed in

Tab. 8. The results of copolymerization of acrylamide with styrene in inverse miniemulsions with CAN - Span initiation system, c_{em} = 1.7 – 2.2 wt. %, W/O = 1/6

Sample №	**c_{CAN}×10^3, mol/l**	**[CAN]: [monomers]**	**Yield, %**	**y, mol.%**	**M_w×10^{-6} (GPC)**	**M_w/M_n**
T = 25°C						
HMPAAm-1_{CAN}*	21	1:400	5	1.05	0.03	3
HMPAAm-2_{CAN}	21	1:400	7	1	0.30	4
HMPAAm-3_{CAN}	12	1:714	11 latex 94 coagulum 6	0.65	0.19	6
T = 60°C						
HMPAAm-4_{CAN}	42	1:200	40 latex 75 coagulum 25	0.57	0.79	26
HMPAAm-5_{CAN}	12	1:714	40 latex 82 coagulum 12	1.33	1.20	18

* Synthesis conditions: W/O = 1/3, c_{em} = 3.4 wt.%

the course of copolymerization.

To varify this conclusion, homopolymerization of styrene was carried out in cyclohexane in the presence of miniemulsion droplets containing an aqueous solution of NaCl. No polymer was obtained during 20 h at 60°C.

Thus, the received data for the model copolymerization reaction of acrylamide with styrene confirms the possibility of synthesis of HM copolymers based on acrylamide with initiation by Ce(IV) – Span 60 redox system. In this case, the initiation cannot occur in the continuous phase and hence hydrophobic polymer cannot be formed.

3.3.4.Free-radical Copolymerization of Acrylamide with Laurylmethacrylate

LMA was used as another hydrophobic comonomer. Equimolar monomer mixture was taken for copolymerization. The concentrations of components were as follows: 3.5 mol/l of acrylamide, 0.45 mol/l of LMA, 1.7 wt. % of emulsifier; 3.6×10^{-2} mol/l for CAN, and the ratio of water-to-oil phases was 1/6. The yield of reaction products reached of about 20 % in 4 h at room temperature.

The fractional composition of this product was estimated by selective extraction. It turned out that, along with the high yield (73 wt. %) of copolymer, which was soluble in none of the used solvents (water, THF, and formamide), some amount of homopolyacrylamide (27 wt.%, M_w = 6×10^4, M_w/M_n=2) was presented. The chemical structure of polyacrylamide was confirmed by IR spectroscopy. The absence of PLMA in THF extract was verified by ^{1}H NMR spectroscopy and GPC. The IR spectra for the copolymer exhibited a broad band peaking at 1631 cm^{-1}, corresponding to vibrations of Amide I and Amide II and the band due to the stretching vibrations of a C=O bond of an ester group (1730 cm^{-1}) (**Fig. 21**). The content of acrylamide units in the copolymer according to the elemental analysis data was 97 mol. % and the content of LMA units was 3 mol. % (C:N = 3). Thus, the total conversion of LMA reached 2% at the 80% conversion of acrylamide.

The cross-linked latex particles were easily dispersed in organic and aqueous media. They were prepared by addition of 2 mol. % of BAAm in the course of polymerization. The prepared latexes were stable over a month. Latex particles were readily redispersed in cyclohexane (R_h = 84 nm, *RPW* = ±0.37) and water (R_h = 108 nm, *RPW* = ±0.16) (DLS data, **Fig. 22**). According to TEM (**Fig. 23**), the particle size of initial latex was d = 67 nm.

The possibility of homopolymerization of LMA was verified by carriying out this reaction in cyclohexane in the presence of miniemulsion droplets containing an

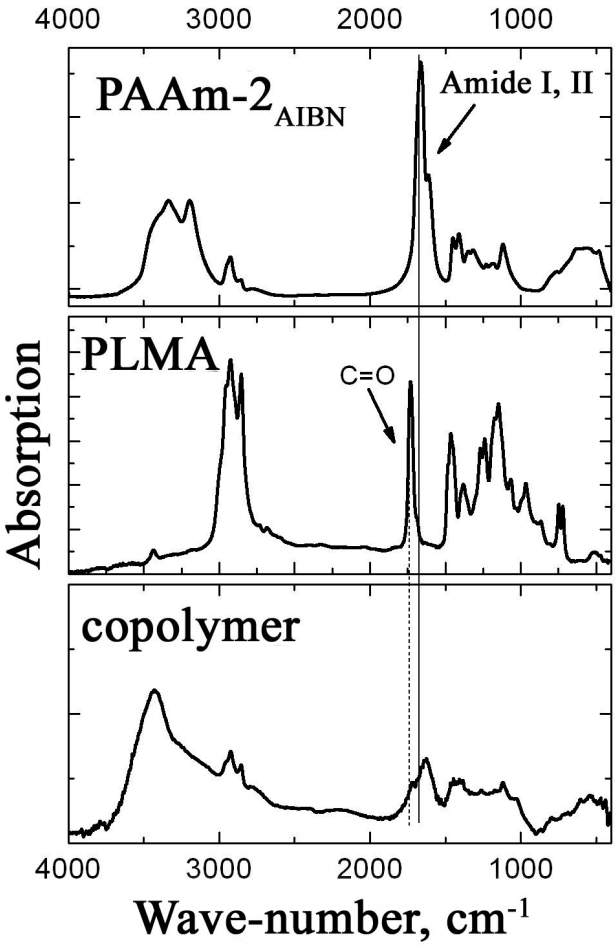
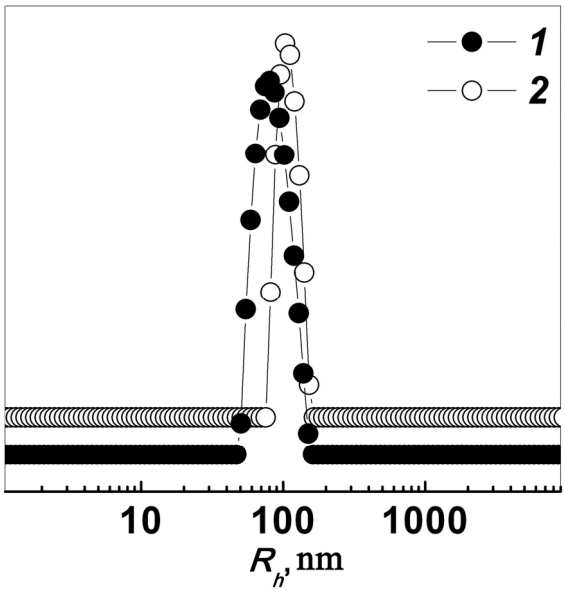


Fig. 21. The IR spectra of the samples PAAm-2_{AIBN} (Tab. 4), PLMA and copolymer *acrylamide–LMA* prepared with initiation by CAN – Span 60.



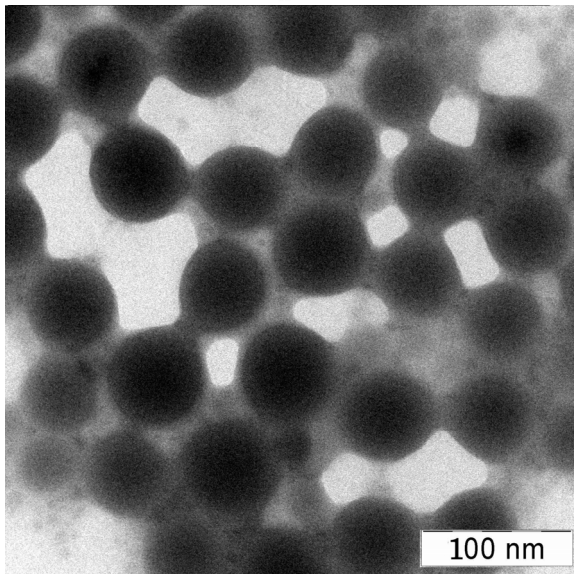


Fig. 22. Hydrodynamic radius (R_h) distributions of crosslinked latex particles based on copolymer *acrylamide–LMA* in (***1***) cyclohexane and (***2***) water. Observation angle 90°.
Fig. 23. TEM image of chemically crosslinked *acrylamide–LMA* copolymer nanoparticles in cyclohexane.

aqueous solution of NaCl. We were not able to obtain any polymer by carrying out the reaction for 20 h at 20°C.

The received results confirm the possibility of synthesis of HM copolymers based on acrylamide with initiation by Ce(IV) – Span 60 redox system. In this case the initiation takes place only at the interfacial boundary. The scheme is shown on **Fig. 24**. The finding excludes the probability of initiation and propagation of polymer chain in a continuous phase.

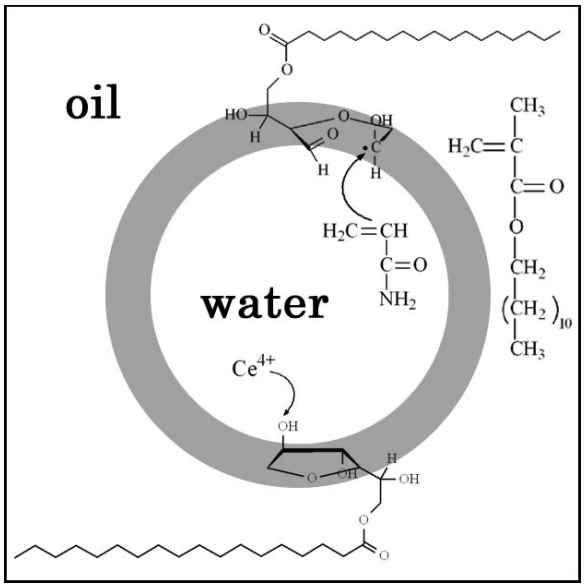


Fig. 24. Scheme of the miniemulsion copolymerization with initiation at the interfacial boundary by surface-active system based on Ce(IV).

3.4. Assotiative and Rheological Polymer Properties

As previously mentioned, the possible modification degree of water-soluble samples was about 0.2-0.4 mol. %. Determination of such small content of hydrophobic units by means of direct spectral methods is practically impossible. Therefore, in this study, the amount of hydrophobic units incorporated into the polymer chain of soluble copolymerization products was estimated indirectly by studing the associative properties of copolymers. Aqueous solutions of copolymers were studied by pyrene fluorescence spectroscopy, light scattering and viscosimetry.

Fluorescent Spectroscopy

It is known that the ratio of intensities of the first I_1 and third I_3 bands in the fluorescence spectrum of pyrene is extremely sensitive to the polarity of the probe microenvironment. Thus, the polarity parameter of pyrene in water is $I_1/I_3 \sim 2$. If hydrophobic micelles are formed, this parameter drops down to 1.2-1.1 [39].

It is known that polymers syntesized by the miniemulsion technique are polluted with emulsifier [47]. To purify, the polymer powders were washed with hot benzene. As one could see in **Fig. 25**, the curves of polarity parameter of pyrene shift after purification to higher concentrations both for copolymers *acrylamide-LMA* formed in the presence of AIBN (sample HMPAAm-6_{AIBN}, **Tab. 5**) and for polymers containing the residual Span 60 (sample PAAm-2_{CAN}, **Tab. 6**). This confirmes that the extraction removes the emulsifier, which is capable of forming mixed micelles.

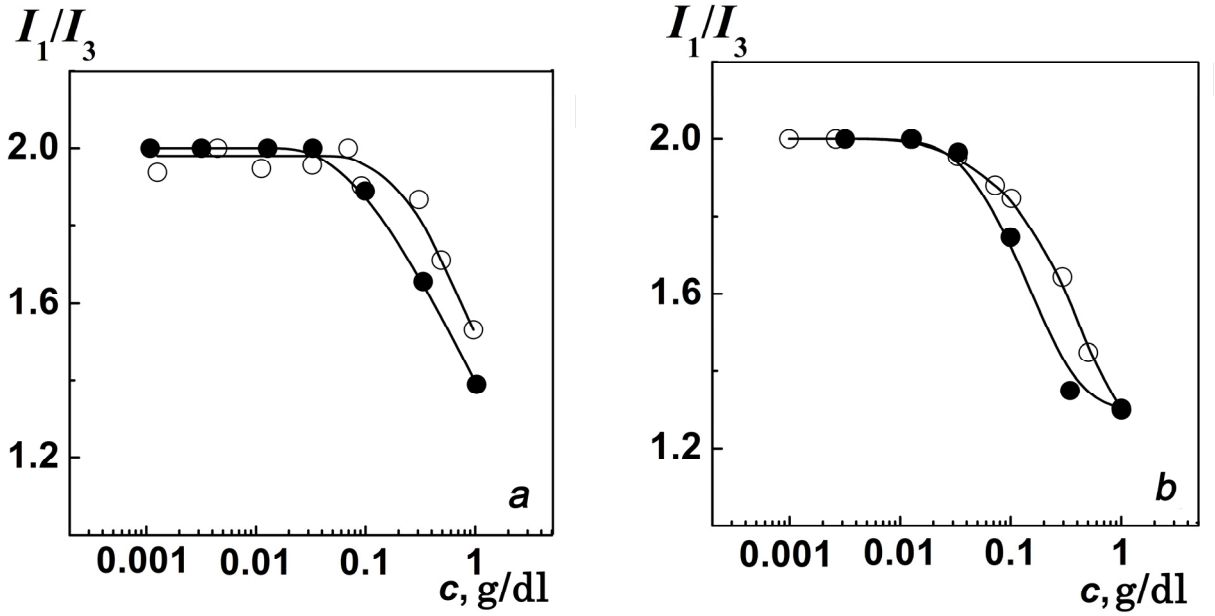


Fig. 25. Concentration dependences of pyrene polarity parameter I_1/I_3 in aqueous solutions of polymers (***a***) HMPAAm-6_{AIBN} and (***b***) PAAm-2_{CAN}. ● – initial polymer, ○ – purified polymer.

The beginning of the hydrophobic domain formation (i.e. CAC) can be determined as a point where a pyrene polarity parameter (I_1/I_3) *vs* polymer concentration graph turns down. **Fig. 26** plots the concentration dependences of the polarity parameter of pyrene for HM polyacrylamide prepared at LMA content in the initial reaction mixture equal to 2 and 5 mol. % (samples HMPAAm-6_{AIBN} and HMPAAm-7_{AIBN}, **Tab. 5**). Similar dependence is shown for HM polyacrylamide prepared with initiation by CAN – Span 60 redox system in **Fig. 27** (samples PAAm-2_{CAN}, PAAm-

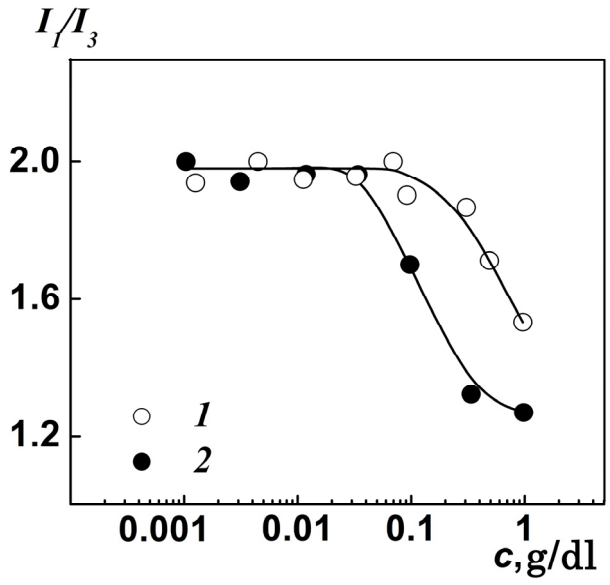


Fig. 26. Concentration dependences of pyrene polarity parameter I_1/I_3 in aqueous solutions of HM polyacrylamide with various content of LMA in the initial reaction mixture: (curve 1, sample HMPAAm-6_{AIBN}) 2 mol.% and (curve 2, sample HMPAAm-7_{AIBN}) 5 mol. %.

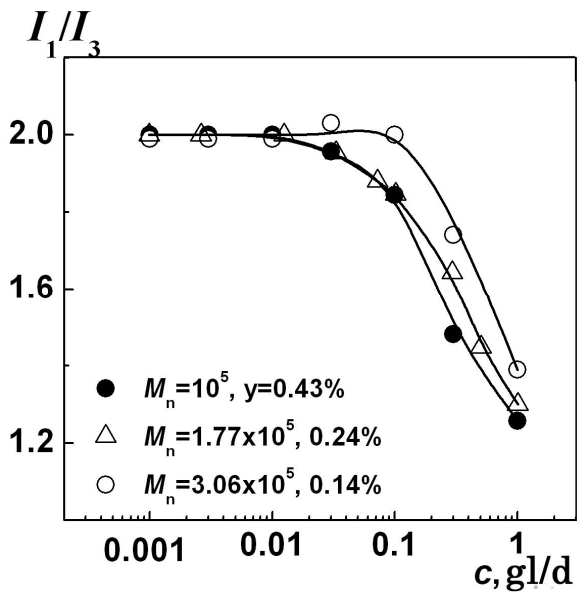


Fig. 27. Concentration dependences of pyrene polarity parameter I_1/I_3 in aqueous solutions of HM polyacrylamide: (○) PAAm-9_{CAN}, (▲) PAAm-2_{CAN} and (●) PAAm-10_{CAN}.

9_{CAN} and PAAm-10_{CAN}, **Tab. 6**). The fact that the polarity parameter of pyrene drops with the increase in polymer concentration indicates the formation of hydrophobic domains. This provides indirect confirmation of the incorporation of hydrophobic fragments into the polymer chains. In particular, this confermes the incorporation of LMA units into *acrylamide–LMA* copolymers prepared with AIBN as initiator, as well as the incorporation of Span 60 alkyl fragments as terminal groups into polyacrylamide prepared with CAN – Span 60 redox system.

For LMA copolymers, the curves shift to lower concentration with the increase in modification degree. Thus, the hydrophobic aggregation for HM polyacrylamide prepared at the content of LMA in the initial reaction mixture equal to 5 mol. % begins at polymer concentration of 0.03 g/dl. For this sample, the bend of the curve was more pronounced than that for the sample prepared at the content of LMA equal to 2 mol. % (**Fig. 26**). This confirms the higher content of hydrophobic domains in the system.

In the case of initiation with redox system based on ceric ions the monochelic polyacrylamides, capable to form star-like micelles in aqueous medium, were obtained. This property is assigned by HLB, which depends on the number-average molecular mass (M_n) of the sample. The lower modification degree y corresponds to sample with higher molecular weight. Therefore, the CAC and the curve of pyrene polarity parameter shift to higher concentration of polymer of higher M_n (**Fig. 27**). As it was discussed earlier, the "monochelic" is the more probable copolymer type formed during polymerization. The formation of telechelic copolymers is also possible in this case. Therefore, star-like micelles as well as flower micelles connected by telechelic bridges can both contribute in associative properties.

Static and Dynamic Light Scattering

The ability of HM polyacrylamides to form supramolecular aggregates in water was confirmed by SLS and DLS studies.

The copolymer *AAm–styrene* prepared with AIBN initiation was separated by GPC in analytical regime into two fractions: high- (M_w=1.85×10^6, M_w/M_n=1.7) and low-molecular weight (M_w=0.17×10^6, M_w/M_n=3). The aqueous solutions (c = 1 mg/ml) of these narrow fractions were studed by DLS (**Fig. 28**). The results argue to the presence of macromolecules (*1*) and aggregates (*2*) in both fractions (low-molecular weight fraction: R_{h1}≈20 nm (*RPW* = ±0.21), R_{h2}≈236 nm (*RPW* = ±0.27), high-molecular weight fraction: R_{h1}≈42 nm (*RPW* = ±0.33), R_{h2}≈433 nm (*RPW* = ±0.31)).

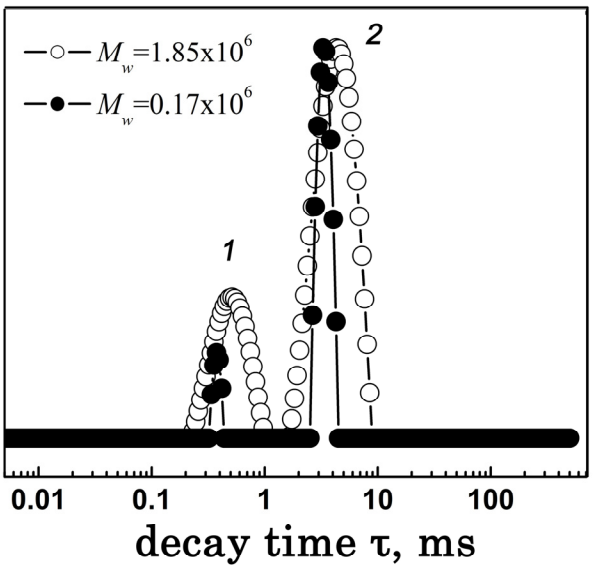


Fig. 28. Intensity normalized spectra of decay times for high (○) and low-molecular weight (●) fractions of copolymer *acrylamide–styrene*, prepared with AIBN. The observation angle is 90°. *c* = 1 mg/ml.

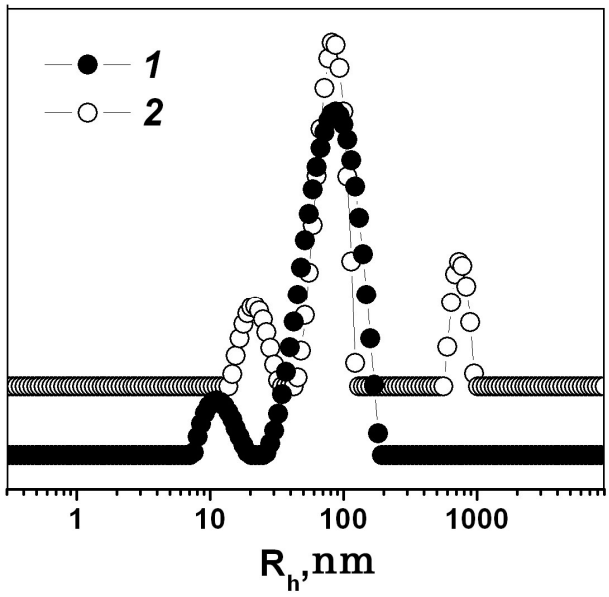


Fig. 29. Scattered light intensity distribution with respect to the apparent size of scattering particles in the aqueous solution of copolymers (***1***) HMPAAm-6$_{AIBN}$ and (***2***) HMPAAm-7$_{AIBN}$. The concentration is 0.5 mg/ml, and the observation angle is 60°.

Aqueous solutions of copolymers *acrylamide–LMA* prepared with AIBN initiation were studied by DLS and SLS. The distribution curves in dilute solutions of these polymers (**Fig. 29**) exhibit the peaks corresponding to macromolecules (curve 1: R_h≈12 nm, *RPW* = ±0.31) along with the peaks corresponding to supramolecular aggregates (curve 1: R_h≈80 nm, *RPW* = ±0.45). Moreover, in the sample prepared at the content of LMA in the reaction mixture equal to 5 mol. %, beside the aggregates (R_h≈80 нм) the large clusters (R_h≈740 nm, *RPW* = ±0.33) are present. The comparison of SLS data for polyacrylamide and *acrylamide–LM*A copolymers prepared using AIBN confirms the aggregation of copolymers in contrast to homopolymers. For example, the normal

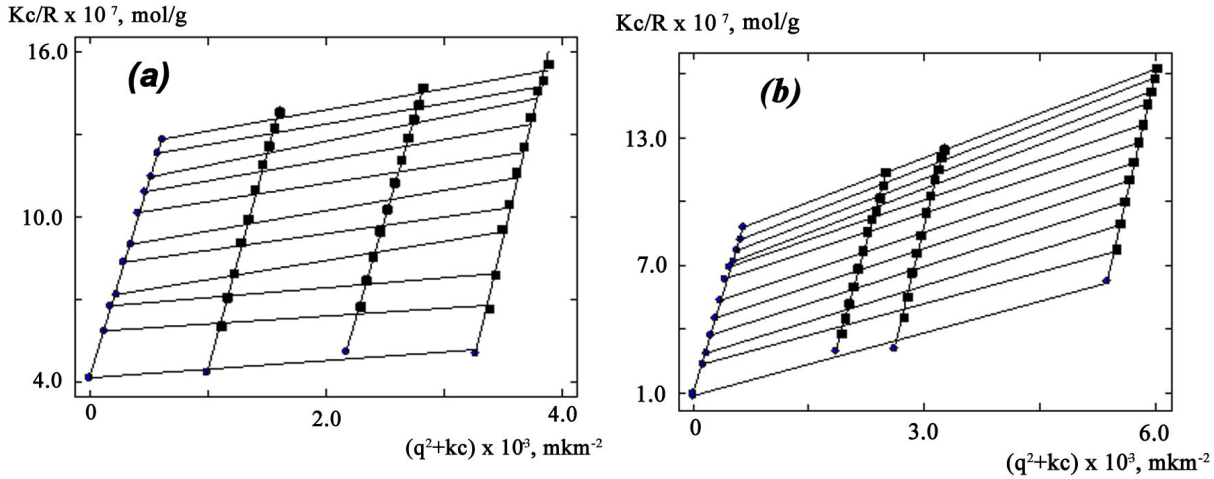


Fig. 30. Zimm plots for (**a**) PAAm-2$_{AIBN}$ and (**b**) HMPAAm-6$_{AIBN}$ in water.

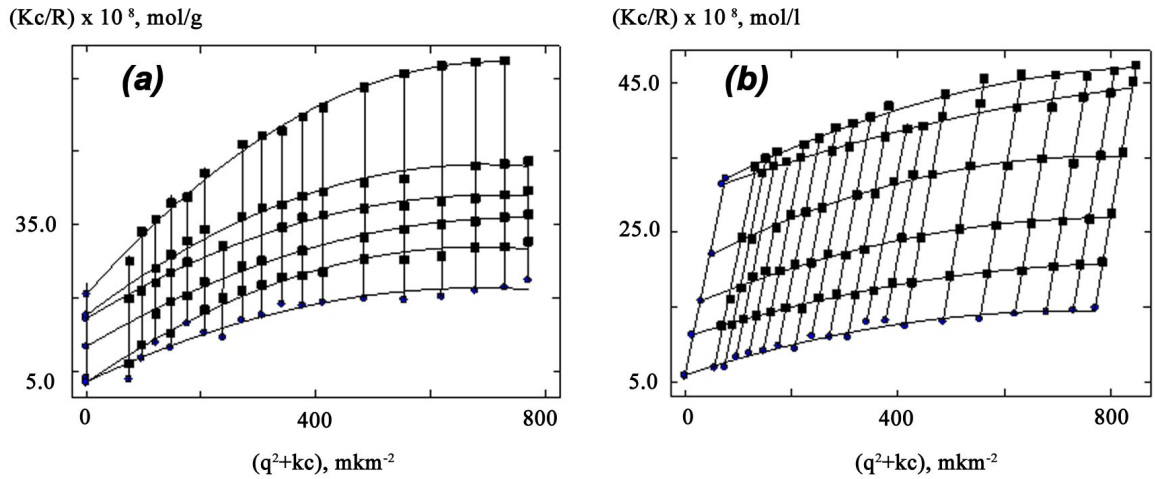


Fig. 31. Zimm plots for (**a**) HMPAAm-1_{AIBN} and (**b**) HMPAAm-2_{AIBN} in formamide.

Zimm plot was constructed (**Fig. 30*a***) for aqueous solutions of polyacrylamide (**Tab. 4**, sample PAAm-2_{AIBN}), and the value of M_w, as estimated from this plot, coincided with the value derived from GPC data. At the same time, the SLS study of strongly dilute aqueous solutions (c = 0.3–1 mg/ml) of the copolymers (**Tab. 5**, samples HMPAAm-6_{AIBN}, HMPAAm-7_{AIBN}) led to the overestimated values of M_w compared to the GPC data (**Tab. 5, Fig. 30*b***). The effective aggregation numbers calculated as M_w (SLS):M_w (GPC) turned out to be ~2.2–4.5.

As evidenced by the SLS measurements of these samples in formamide (curved Zimm plots (**Fig. 31**) and overestimated values of M_w for samples HMPAAm-1_{AIBN}, HMPAAm-2_{AIBN}, HMPAAm-3_{AIBN} and HMPAAm-6_{AIBN} in **Tab. 5**), the intermolecular aggregation proceeds in this solvent as well. As was shown in [119], formamide is the most suitable solvent for molecular mass measurements of acrylamide copolymers with the substituted acrylamide. However, our data shows that LMA based copolymers may demonstrate both aggregation and macroseparation in formamide. In particular, dilute solutions in formamide (c = 1 mg/ml) for copolymers HMPAAm-3_{AIBN} and HMPAAm-4_{AIBN} synthesized at the content of LMA in the reaction mixture equal to 5 and 10 mol. % turned out to be opalescent. These copolymers were also incompletely soluble in the mixture of 0.1 M $NaNO_3$–acetonitrile used for GPC studies (solubility values, as estimated from the areas under chromatograms, were 90 and 40%, respectively).

The ability of HM polyacrylamides prepared with redox system based on ceric ions to form supramolecular aggregates in water was confirmed by SLS and DLS studies. The copolymer was separated by GPC in analytical regime into two fractions: high- (M_w=1.5×10⁶, M_w/M_n=2) and low-molecular weight (M_w=0.12×10⁶, M_w/M_n=2.7). The aqueous solutions of these narrow-dispersed fractions were studed by DLS (**Fig.**

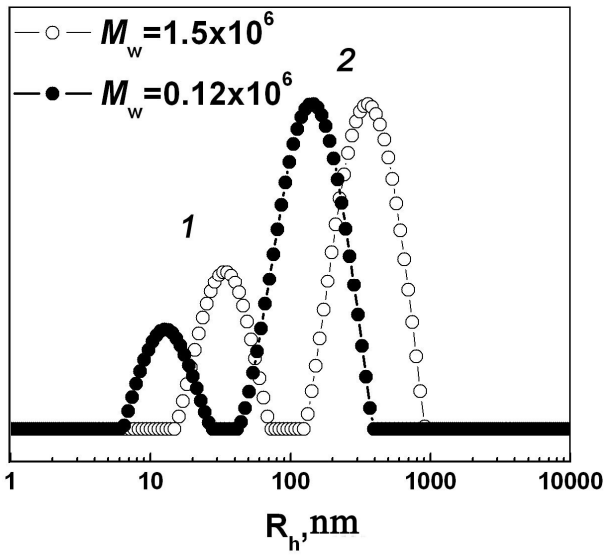


Fig. 32. Scattered light intensity distribution with respect to the apparent size of scattering particles for (○) high- and (●) low-molecular weight fractions of copolymer PAAm-9_{CAN}. The concentration is 1 mg/ml, and the observation angle is 90°.

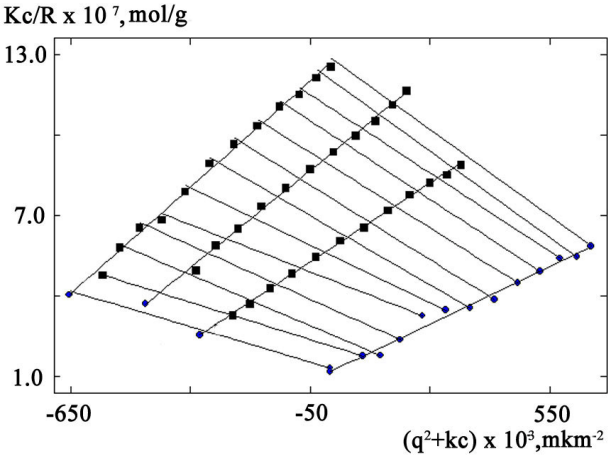


Fig. 33. Zimm plot for PAAm-2_{CAN} in water.

32). The results argue to presence of the macromolecules (*1*) and aggregates (*2*) in both fractions (low-molecular weight fraction: R_{h1}≈15 nm, R_{h2}≈150 nm, high-molecular weight fraction: R_{h1}≈35 nm, R_{h2}≈400 nm). Both, the size of macromolecules and aggregates are increased with the increase in molecular mass.

As evidenced by the SLS measurements of the sample PAAm-2_{CAN} in water (curved Zimm plots (**Fig. 33**) and overestimated values of M_w = 7.5×10^6), the intermolecular aggregation proceeds in this solvent.

Rheological Properties of Polymer Solutions

For copolymers *acrylamide–LMA* prepared by initiation with AIBN the viscosimetric measurements were carried out. **Fig. 34** shows the viscosity of aqueous solutions of polyacrylamide (**Tab. 4**, sample PAAm-2_{AIBN}) and HM polyacrylamide prepared at the content of LMA equal to 2 mol. % (**Tab. 5**, sample HMPAAm-6_{AIBN}) as a function of concentration. The sharper rise in the viscosity at transition to semidilute regime was observed in the case of copolymer solution. The test samples are characterized by close M_w values; therefore, the above differences may be explained solely by hydrophobic association.

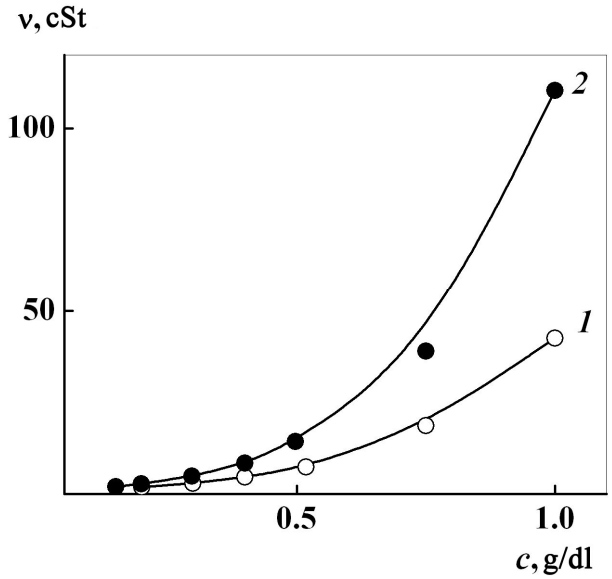


Fig. 34. Concentration dependence of the kinematic viscosity ν for the aqueous solution of (***1***) PAAm-2_{AIBN} and (***2***) HMPAAm-6_{AIBN}.

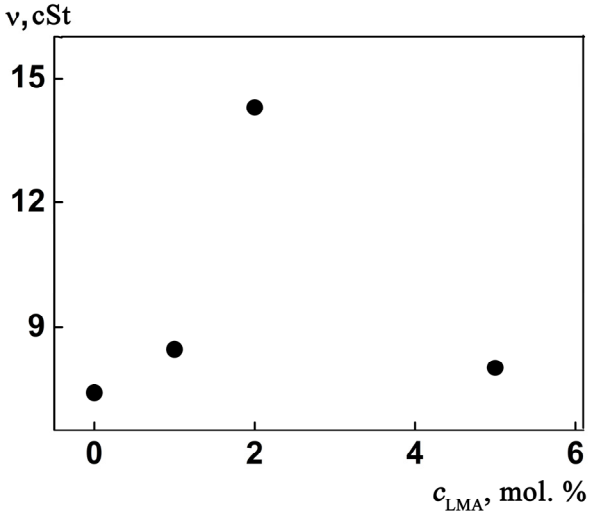


Fig. 35. The kinematic viscosity ν of 0.5% aqueous solution of HM polyacrylamide *vs* the content of LMA in the reaction mixture. The synthesis conditions are as follows: c_{AIBN} = 4.7×10^{-3} mol/l и c_{em} = 3.3 wt. % (in the oil phase) (**Tab. 4** and **Tab. 5**).

Fig. 35 plots the kinematic viscosity of 0.5% solutions of the copolymers versus the content of LMA in the reaction mixture. This dependence has an extreme behavior. By increasing the content of LMA to 2 mol. % the viscosity of the polymer solution grows appreciably. Further increase in the amount of LMA in the reaction mixture to 5 mol. % promotes the formation of opalescent solutions with lower viscosity owing to incomplete phase separation of the system.

The rheologocal properties of a 2% aqueous solution of polyacrylamide (**Tab. 4**, sample PAAm-2_{AIBN}) and HM polyacrylamide prepared at the content of LMA equal to 1 mol. % (**Tab. 5**, sample HMPAAm-5_{AIBN}) with similar molecular masses were studied at

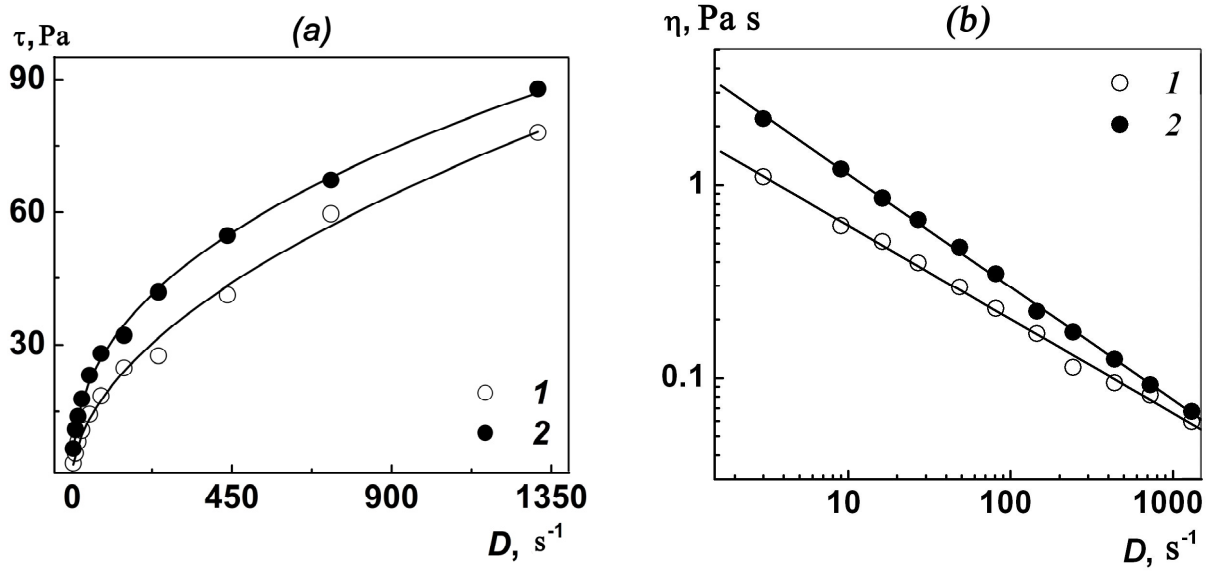


Fig. 36. Flow curves τ(*D*) (***a***) and dependende of effective viscosity η on shear rate *D* (***b***) of 2% aqueous solutions of (***1***) PAAm-2_{AIBN} and (***2***) copolymer PAAm-5_{AIBN}, T = 20°C.

continuous shear strain regime. The flow curves at 20°C are given in **Fig. 36**. Their shape denotes non-Newtonian character of flow.

All curves can be well fitted within the limits of the given range of measured values (with factors of correlation not below 0.99) with the Ostwald – de Waele equation [120]:

$$\tau = kD^n \quad , \qquad (3.4.1)$$

where τ is the shear stress; D is the rate of shear strain; n and k are the empirical parameters describing the flow.

The factor k, named as Ostwald – de Waele coefficient, is numerically equal to shear stress at the rate of shear strain equal to one. It characterizes the effective viscosity at the unity speed gradient. As one can see from **Fig. 37** the value of k is much higher and its drop is sharper with the rise of temperature for the modified sample than for polyacrylamide.

The flow index (the degree of flow anomaly) n shows a degree of a deviation from the Newtonian flow. Both studied systems are non-Newtonian and the values of n are less than unity. Moreover, in the case of copolymer, the deviation from the Newtonian flow is more pronounced as compared with homopolymer (the avarege value of flow index n_{av}=0.51 for PAAm-2$_{AIBN}$ and n_{av}=0.45 for HMPAAm-5$_{AIBN}$).

One of the major parameters of a polymer solution is the activation energy of viscous flow. It can serve as a criterion of strength of intermolecular interactions. This parameter was determined from the temperature dependence of viscosity (**Fig. 38**) in Arrenius coordinates. This can be described with the Arrenius - Frenkel - Airing

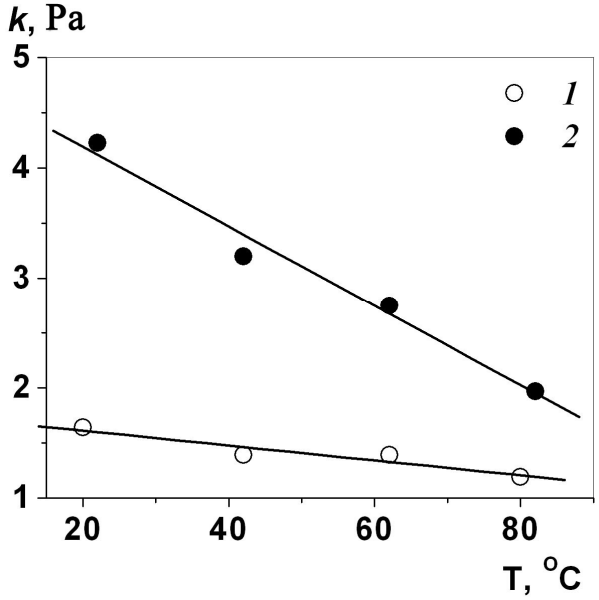


Fig. 37. The dependence of Ostwald – de Waele coefficient on temperature for (***1***) PAAm-2$_{AIBN}$ and (***2***) HMPAAm-5$_{AIBN}$.

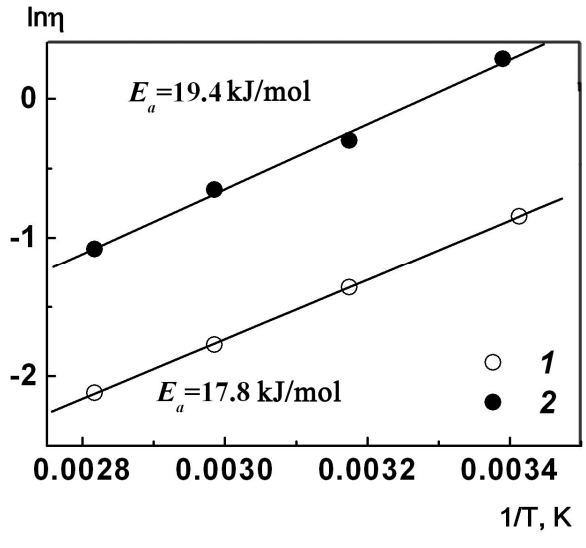


Fig. 38. The dependence of ln η on 1/T for 2% aqueous solutions of (***1***) PAAm-2$_{AIBN}$ and (***2***) copolymer PAAm-5$_{AIBN}$ for determination of E_a at τ = 20 Pa.

equation [121]:

$$\eta = B\exp(E_a/RT), \quad (3.4.2)$$

where E_a is the effective activation energy of viscous flow, and B is the empirical parameter with dimension of viscosity. The value of preexponential factor B depends on temperature as:

$$B = B'T^{3/2}. \quad (3.4.3)$$

However, taking into account the factor $T^{3/2}$, it gives only insignificant correction as compared with exponential factor.

The value of E_a was calculated by evaluating the slope ratio (**Fig. 38**). The copolymer solution is characterized by higher activation energy of the viscous flow (17.8 kJ/mol for PAAm-2_{AIBN}, 19.4 kJ/mol for HMPAAm-5_{AIBN}). It allows one to assume that in solutions of HM polyacrylamides the hydrophobic domains bring an additional contribution to formation of a transient polymer network besides topological entanglement which is characteristic for the unmodified samples.

A similar change in the solubility of polymers and a similar dependence of viscosity on the content of LMA units in the HM polyacrylamides were observed in the micellar copolymerization of acrylamide and LMA [5, 39].

The rheological characteristics of aqueous solutions of HM polyacrylamide synthesized by miniemulsion polymerization at LMA content of 2 mol. % in initial reaction mixture (sample HMPAAm-6_{AIBN}, **Tab. 5**) were compared with those of HM polyacrylamided synthesize by either micellar or solution polymerization. The last copolymers contained about 0.2 mol.% of LMA units distributed statistically in the

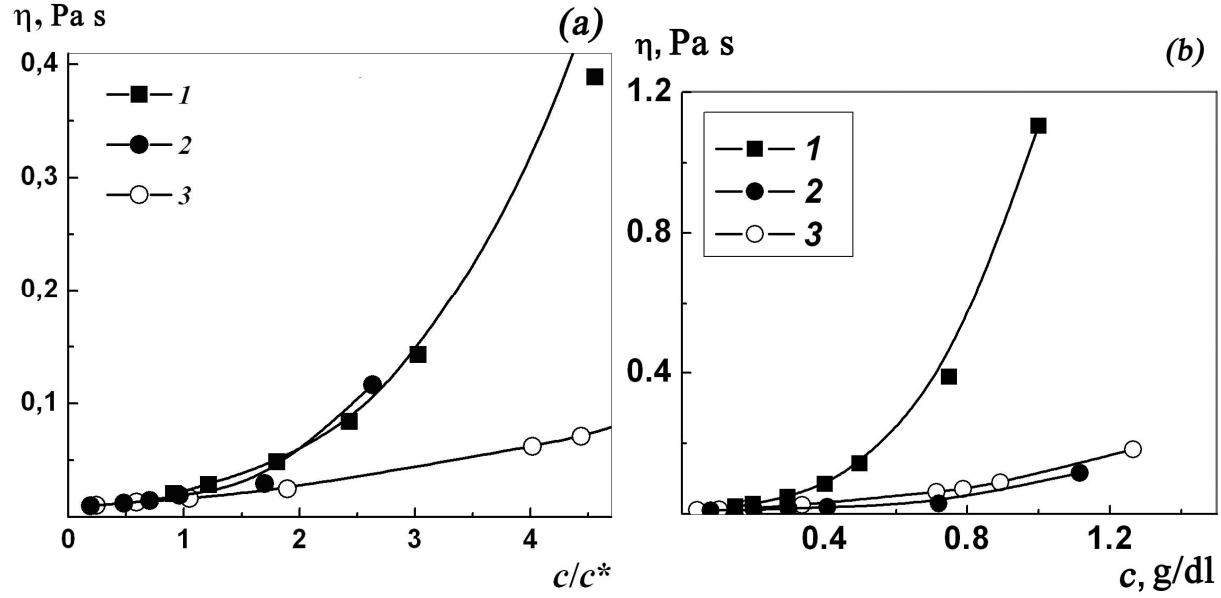


Fig. 39. The dependence of dynamic viscosity η on (***a***) reduced concentration c/c^* and (***b***) concentration c for aqueous solutions of copolymer *acrylamide-LMA* prepared by (***1***) miniemulsion technique (M_w = 2.17×10^6) and by (***2***) micellar polymerization (M_w = 0.62×10^6) and (***3***) homogeneous polymerization (M_w = 1.96×10^6).

case of solution polymerization or as microblocks in the case of micellar polymerization. The dependence of dynamic viscosity on reduced concentration c/c^* is represented in **Fig. 39*a***. Here, c^* was calculated for polyacrylamide with appropriate molecular mass from the following equations [122]:

$$c^* \approx 1/[\eta] \tag{3.4.4}$$

$$[\eta] = 10^{-4} M_w^{0.755} \tag{3.4.5}.$$

It is evident that the behaviour of a copolymer prepared via miniemulsion technique is similar to the behaviour of HM polyacrylamide with microblock structure. Statistical copolymer has lower value of viscosity in solution. At the same time, the absolute values of viscosity for miniemulsion sample are higher than that for microblock polymer prepared by micellar technique at the same concentration due to higher value of M_w (**Fig. 39*b***).

Thus, the reseived results confirm that HM polymers obtained by miniemulsion technique in which comonomers are distributed in different phases represent rheological characteristics similar to polymers obtained by micellar polymerization.

4. EXPERIMENTAL PART

4.1. Reagents and Materials

Acrylamide ("Aldrich") was recrystallized twice from chloroform. Lauryl methacrylate ("Aldrich") and styrene ("Aldrich") were distilled under reduced pressure prior to use (T_b = 165°C, 5 Torr and T_b = 40°C, 5 Torr, respectively). Ceric ammonium nitrate ("Sigma-Aldrich"), N,N′-methylenebis(acrylamide) ("Amresco") and sorbitan monostearate (Span 60, "Aldrich") were used as received. Azobisisobutyronitrile ("Aldrich") was recrystallized from methanol. Cyclohexane ("Merck") was distilled prior to use. Aqueous solution of NaCl (0.1 M) was utilized as osmotic agent in all miniemulsion preparations in order to prevent Oswald ripening of the droplets. Syntheses and analyses were performed with demineralised water of Milli-Q grade.

4.2. Synthetic Methods

Polymerization reactions were carried out in a three-necked flask (100 ml) equipped with backflow condenser, argon inlet and magnetic stirrer. For synthesises at high temperature, the flask was placed in oil-bath. Initial reaction mixtures were miniemulsified by ultrasonication with a sonifier (W450 Digital, Branson, Danbury, CT) at 90% amplitude (tip ½") for 120 - 150 s. To avoid polymerization, mixtures were cooled with an ice-bath during sonication.

4.2.1.Polymerization and Copolymerization of Acrylamide Initiated by Azobisisobutyronitrile

The copolymerization of acrylamide and LMA (molar ratio [acrylamide]:[LMA] = 98:2) initiated by AIBN was performed in the following way. Acrylamide (2 g, 2.8×10^{-2} mol) was dissolved in 0.1 M aqueous solution of NaCl (2 g) and then added to a solution of emulsifier (0.8 g) in cyclohexane (30 ml). Then the mixture was stirred and degassed with argon for 40 min. LMA (0.14 g, 5.6×10^{-4} mol) was added, and the resulting mixture was stirred for another 20 min under the argon flow. Miniemulsion, obtained by ultrasonication at low temperature for 150 s, was purged with argon for 1 h. To initiate the polymerization, the temperature was raised to 60°C, and AIBN

solution (1.4×10^{-4} mol) in toluene (0.66 ml) was added. The synthesis leaved for 4 h under continous stirring with the rate of 300 rpm.

The resulting polymer was precipitated into the excess acetone, then washed with hot acetone for 24 h in a Soxhlet extractor, and, finally, dried in vacuum at 40 ºC to a constant weight.

Polymerization of acrylamide was performed in the same way, but without an addition of LMA.

4.2.2.Polymerization and Copolymerization of Vinyl Monomers Initiated by Surface-Active Redox System based on Ce (IV) Salt

Polymerization of acrylamide initiated by surface-active redox system based on Ce(IV) was performed in the following way. The aqueous phase, consisting of a solution of acrylamide (2 g, 2.8×10^{-2} mol) in 0.1 M of NaCl (1.5 g) and the oil phase, consisting of a solution of Span 60 (0.5236 g, 1.2×10^{-2} mol) in cyclohexane (30 ml), were separately degassed with argon during 15 min. After a solution of CAN (7.0×10^{-5} mol) in 0.1 M aqueous solution of NaCl (0.5 ml) was added to aqueous phase, both aqueous and oil phases were placed in the flask. While sonication continued for 120 s, a gradual change in the dispersion color from canary to primrose was observed as a result of the conversion of Ce (IV) into Ce (III). The polymerization was performed at room temperature for 4 h at the stirring rate of 300 rpm. The reaction mixture was purged with argon throughout the synthesis.

Copolymers of acrylamide with hydrophobic comonomers were obtained by introducing an equimolecular amount of LMA or styrene into the oil phase. In the case of copolymerization with styrene, the synthesis temperature was kept at 60°C.

The resulting polymers were precipitated as described in the previous chapter section.

4.2.3.Synthesis of Cross-linked Polyacrylic Acid Initiated by Surface-Active Redox System based on Ce (IV) Salt

Acrylic acid (0.4597 g, 6.4×10^{-3} mol) was neutralized with a solution of NaOH (0.2552 g, 6.4×10^{-3} mol) in 0.1 M aqueous solution of NaCl (3 ml). The solution of acrylic acid salt (0.6 g, 6.4×10^{-3} mol) and BAAm (0.02 g, 1.3×10^{-5} mol) in 0.1 M of NaCl (3 ml) was used as an aqueous phase. The oil phase was consisted of a solution of Span 60 (0.5236 g, 1.2×10^{-2} mol) in cyclohexane (30 ml). Aqueous and oil phases were separately degassed with argon over 15 min. After the addition of CAN (6.4×10^{-5} mol in 0.5 ml of 0.1 M NaCl) into aqeous phase both phases were placed in the flask. Miniemulsion was obtained by ultrasonication of the mixture for 120 s at low

temperature. Polymerization was performed at 60°C for 24 h at the stirring rate of 300 rpm under purging with argon throughout the synthesis.

The resulting polymer was precipitated into the excess acetone, washed with hot acetone for 24 h in a Soxhlet extractor, and dried in vacuum at 40 ºC to a constant weight.

4.2.4.Synthesis of Cross-linked Polymeric Latex

In order to obtain cross-linked polymeric latexes, the procedure of polymerization or copolymerization was modified by the introduction of BAAm (2 mol.% with respect to acrylamide) into the aqueous phase.

4.2.5.Polymerization of Lauryl methacrylate

Aqueous phase, consisting of 0.1 M aqueous solution of NaCl (4 g), was added to a solution of emulsifier (0.8 g) and LMA (4.16 g, 2.8×10^{-2} mol) in cyclohexane (30 ml). Then the mixture was stirred and degassed with argon for 1 h at 40°C. Miniemulsion obtained by sonication was purged with argon for 1 h. To initiate the polymerization, the temperature was raised to 60°C and AIBN (2.8×10^{-4} mol) in toluene solution (1.3 ml) was added. Polymerization was performed at 60°C for 4 – 20 h at the stirring rate of 300 rpm.

The resulting polymers were precipitated into the excess methanol. The precipitate was allowed to stand for about 10 min, followed by swirling the contents of the flasks to coagulate the polymers and collecting the solids. The polymer was redissolved in THF and again precipitated in methanol. Then it was dried in a vacuum oven at 40°C for several days to reach constant weight. Conversions were calculated by gravimetry.

4.2.6.Polymer Purification from Emulsifier

To purify polymers from emulsifier, first, the polymer powders were washed with hot acetone for 24 h in a Soxhlet extractor. Then 2% of aqueous solution of polymer was vigorously stirred with the twofold excess of benzene at 40°C for 3 h. This procedure was repeated two times. Then the upper layer was decanted and the sample was freeze dried. The next drying was carried out in a vacuum oven at 40 °C for several days to reach constant weight.

4.2.7.Polymer Purification from Ceric Salts

To purify polymers from ceric salts, 2% aqueous polymer solution (~50 ml) was dialyzed against demineralised water (2 l) for a day repetedly four times. The

membranes were purchased from “Spectrum” (Spectra/Por MWCO 12-14.000). The total amount of cerium in dry samples was 0.05 wt. %. The content of cerium in polymer was reduced to 0.005 % after dialysis. The solution was freeze dried to obtain polymers. The next drying was carried out in a vacuum oven at 40 °C for several days to reach constant weight.

4.3. Methods of Polymer Characterization

4.3.1.Static and Dynamic Light Scattering

Static light scattering (**SLS**) measures the scattered light intensity as a function of scattering angle and solution concentration. This method allows to determine absolute molar masses in the range from 10^4 to 10^7 Dalton and a radius of gyration, $\left\langle R_g^2 \right\rangle^{1/2}$, and to characterize thermodynamic quality of solutions.

Data from SLS experiments are usually presented in a form of Zimm plot, which is based on the following equation [123]:

$$\frac{Kc}{R_\theta} = \frac{1}{M_w}\left(1 + \frac{1}{3}\left\langle R_g^2 \right\rangle q^2\right) + 2A_2 c, \tag{4.3.1}$$

where, c is the concentration, M_w is the mass-average molecular mass, R_θ is the reduced Raleigh ratio, and q is the scattering wave vector. The later parameter is calculated in the following way:

$$q = \frac{4\pi n \sin\left(\frac{\theta}{2}\right)}{\lambda}, \tag{4.3.2}$$

where λ is the wavelength of the incident light, and θ is the scattering angle. The R_θ is calculated by:

$$R_\theta = R_c(90^\circ)\cdot(\sin\theta)\cdot\left(I_\theta \big/ I_c\right), \tag{4.3.3}$$

where $R_c(90^\circ)$ is the absolute scattering intensity of standard (toluene), I_θ is the experimental scattering intensity of solution at the angle θ, I_C is the corrected experimental intensity of standard at 90°. The constant K for vertically polarized light is defined as:

$$K = \frac{4\pi^2 n_0^2}{\lambda_0^4 N_A}\left(\frac{dn}{dc}\right)^2, \tag{4.3.4}$$

where n is the index of refraction of solution, n_0 is the index of refraction of solvent, n_{tol} is the index of refraction of standard, λ_0 is the wavelength of the incident light, N_A is the Avogadro's number, and $\frac{dn}{dc}$ is the refractive index increment.

By taking the value of $\frac{Kc}{R_\theta}$ vs. q^2+kc, where k is an arbitrary plotting constant chosen purely for convenience in viewing the results, Zimm plot is then presented in a grid-like manner with two sets of parallel lines. One set consists of angular measurements at each concentration, and another set consists of concentration measurements at each angle. Extrapolating the concentration to zero for each angle yields a straight line in q^2. The slope divided by the intercept of this line yields R_g. The intercept of both extrapolated lines (i.e. the double extrapolation to zero angle and zero concentration) yields the mass-average molecular mass of the polymer in solution (**Fig. 40**).

Dynamic light scattering (**DLS**) is the experimental method, where measured fluctuations of the intensity of scattered light are used to determine size, shape and interaction between particles in solution. In dilute solutions of macromolecules or colloidal particles DLS is related to diffusion motion [124].

In DLS experiments, the time autocorrelation function of the scattered light intensity $G_2(t)=<I(0)I(t)>$ is measured with the self-beating method within the range of delay times from nanoseconds to minutes. These intensity fluctuations are related to fluctuations of the corresponding electric field. And therefore the time autocorrelation function of the scattered light intensity, $G_2(t)$, has to be converted into the correlation

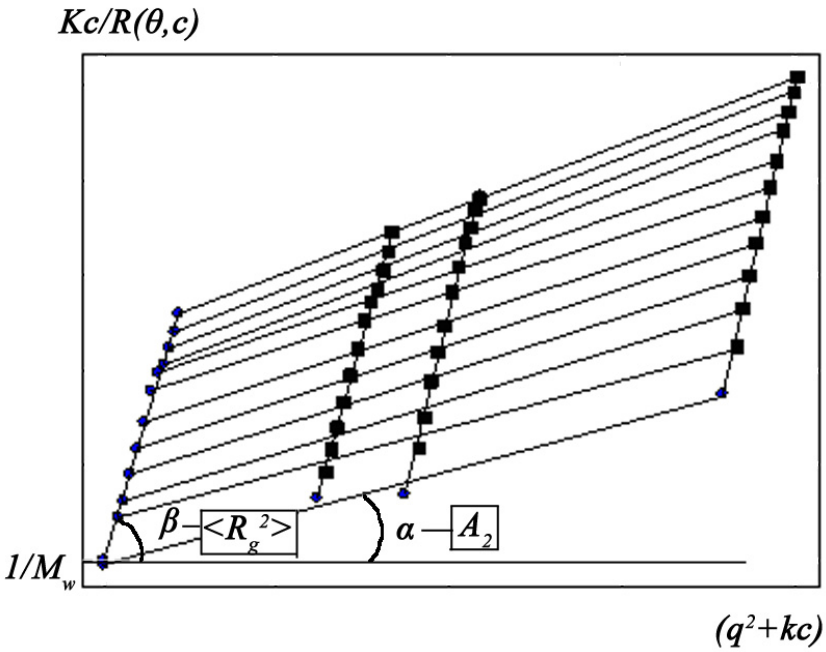


Fig. 40. Schematic static Zimm plot.

function $g_1(t)$ of the scattered electric field. This is done by applying the Siegert's relationship:

$$g_2(t) = 1 + \beta \left| g_1(t) \right|^2 , \tag{4.3.5}$$

or

$$\left| g_1(t) \right| = \beta^{-\frac{1}{2}} \sqrt{\frac{G_2(t)}{G_2(\infty)} - 1} , \tag{4.3.6}$$

where $g_2(t) = G_2(t)/G_2(\infty)$, $G_2(\infty)$ is the experimentally determined baseline, β is the coherence factor determined by the geometry of the detection.

In dilute solutions of monodisperse particles, field correlation function is related with the translational diffusion as follows:

$$| g_1(t) | = \exp(-t/\tau) = \exp(-\Gamma t) = \exp(-Dq^2 t) , \tag{4.3.7}$$

$$D = \lim_{q \to 0} (\Gamma / q^2) , \tag{4.3.8}$$

where τ is the decay time, $\Gamma = 1/\tau$ is the decay rate, and D is the diffusion coefficient. If there is a large number of independent decay processes in the system, then $g_1(t)$ is a massed sum of individual contributions. In continuous form, one can write:

$$g_1(t) = \int_0^\infty A(\tau) \exp(-t/\tau) d\tau , \tag{4.3.9}$$

where $A(\tau)$ is a distribution of scattered light over decay times.

In present work, CONTIN program ("ALV") was used for evaluation of the distribution function $A(\tau)$ by applying the inverse Laplace transform method. For every relaxation maximum found in the spectra of the decay times, the average decay time, $\bar{\tau}$, the efficient diffusion coefficient, D, and the hydrodynamic radius, R_h, were calculated using the following relations:

$$\ln(\bar{\tau}) = \frac{\sum_i A_i \ln(\tau_i)}{\sum_i A_i} \tag{4.3.10}$$

$$D = \frac{1}{q^2 \bar{\tau}} , \tag{4.3.11}$$

$$R_h = \frac{k_b T}{6\pi\eta D} = \frac{k_b T}{6\pi\eta} q^2 \bar{\tau} , \tag{4.3.12),}$$

where η is the solvent viscosity, k_B is the Boltzmann constant, and T is the absolute temperature. In the case of particles much smaller in size than the wavelength of the incident radiation ($qR<<1$), the values of D and R_h are independent of q and the angle of observation. The expression 4.3.12 is valid only in the case of an ensemble of

monodisperse spheres if qR~1. In other cases, the true values of D and R_h can be obtained by extrapolation the parameters q and c to zeros.

Relative peak width (***RPW***) was calculated as following:

$$RPW = \sqrt{\left[\frac{\sum_i (\ln(\tau_i))^2 A_i}{\sum_i A_i} - (\ln(\bar{\tau}))^2\right]} \qquad (4.3.13)$$

The size of emulsion droplets and latex particles were measured on "Malvern Particle Sizer" ("Zetasizer Nanoseries, Malvern Instrument") or "ALV DLS/SLS-5022F" ("ALV GmbH") instrument at 25°C under the scattering angle of 150°. The M_w of polyacrylamide samples, the apparent molecular masses of hydrophobically modified polyacrylamides, and the hydrodynamic radii of macromolecules and aggregates were measured on the "ALV DLS/SLS-5022F" ("ALV GmbH") instrument at 25°C in the range of scattering angles of 30°–140°. A JDS Uniphase helium/neon laser operating at 633 nm with 22 mW was used as the light source. Refractive index increment dn/dc of 0.170 was determined for polyacrylamide and HM polyacrylamides in water [39] and dn/dc of 0.108 – in formamide [119]. The polymer solution for analysis was dedusted with filtration throw Durapore ("Millipore") or Spartan ("Schleicher&Schuell") membranes with the porous size of 0.45 μm.

4.3.2.Gel Permeation Chromatography (GPC)

The molecular mass of polyacrylamide and hydrophobically modified polyacrylamides were estimated by GPC on a Waters chromatograph equipped with a M2410 refractometer and Ultrahydrogel 2000 and 1000 columns. The flow velocity used in our experiments was 1 ml/min, and the temperature was equal to 30°C. Eluent was prepared by mixing 0.1 M $NaNO_3$ and acetonitrile with the ratio of 7:3. The use of this eluent along with Ultrahydrogel columns ensured the complete washing of the hydrophobically modified polymers out of the column and the absence of the inverse-phase retention [39]. The salt was added to suppress electrostatic interaction between charged polymer groups (which could appear as a result of hydrolysis of amide group) with the charge on the sorbent surface.

Calibration was performed by utilizing the polyacrylamide samples with known (from light scattering data) molecular masses of M_w = (0.5–3)×10^6 and standard PEO samples (Polymer Standards Service-USA Inc, M_p = (0.3–5.8)×10^5).

The average molecular mass and molecular mass distribution were calculated using relations [125]:

$$\overline{M_n} = \frac{\int_0^\infty W(M)dM}{\int_0^\infty W(M)\frac{1}{M}dM} \quad (4.3.14)$$

$$\overline{M_w} = \frac{\int_0^\infty W(M)MdM}{\int_0^\infty W(M)dM} \quad (4.3.15)$$

$$\overline{M_z} = \frac{\int_0^\infty W(M)M^2dM}{\int_0^\infty W(M)MdM} \quad (4.3.16),$$

The molecular mass, *M,* was evaluated from the calibration equation:

$$\lg M = \sum_{i=0}^{n} C_i V_e^i , \quad (4.3.17)$$

where V_e –is the retention volume for *i*-fraction, and C_i is the calibration coefficient.

The molecular mass of polylaurylmethacrylate was determined by GPC in THF. The measurement conditions were as follows: “Shodex RI-71” refractometer, “Waters” μ-Styragel 10^3, 10^4 columns, and a Polymer Standard Service column PSS 10^5 calibrated relative to polystyrene standards. The transition to the universal calibration was performed via the Kuhn–Mark–Houwink equation with the use of the following constants: K = 1.5×10^{-4} and a = 0.70 for polystyrene and K = 6.55×10^{-5} and a = 0.70 for PLMA, respectively [127].

The fractionation was carried out in analytical GPC regime by multiple eluting sample and fractions collecting. The first fraction was taken according to rising branche of a chromatogram and the second – according to descending branche of a chromatogram. After evaporation and freeze-drying, these fractions (1 – 2 mg) were dissolved in the mixture of 0.1 M $NaNO_3$ and acetonitrile (7:3) for GPC analysis, and in water or D_2O (copolymer of acrylamide and styrene) for DLS and NMR.

4.3.3.Fluorescent Spectroscopy

Fluorescence spectroscopy of pyrene, which is known to be very sensitive to the polarity of its microenvironment, is widely used to study the intramicellar interactions, polymer - emulsifier interactions, aggregation of emulsifier and macromolecules, etc [126]. Furthermore, the pyrene chromophore has a high extinction value and a high

quantum yield of fluorescence. Its fluorescence spectrum shows a fine structure with five predominant peaks (**Fig. 41**). The so-called emission peak I_3 (λ=383) shows minimal intensity variation with polarity, whereas peak I_1 (λ=371) shows significant intensity enhancement in polar solvents. The smaller the polarity of the probe microenvironment, the smaller the ratio I_1/I_3 of pyrene is. The 0-0 transition from the lowest excited electronic state, giving rise to the I_1 peak, is symmetry-forbidden. Its intensity can be increased by distortion of the π-electron cloud in polar media, while the I_3 peak is not forbidden and is solvent-insensitive. In water, I_1/I_3 = 2, whereas in apolar solvent it has a value well below unity, e.g. in cyclohexane, I_1/I_3 = 0.6 [128]. Pyrene, as a hydrophobic compound, is poorly soluble in water (up to 7×10^{-7} M). Therefore, the probe resides predominantly within the hydrophobic microdomain pseudophase when applied to the micellar systems. Hereby, the polarity of the microenvironment in which the probe is located is decreased and the I_1/I_3 ratio decreases to unity.

In aqueous solutions, emulsifiers are known to self-aggregate into micelles at a well-defined critical micellar concentration (**CMC**). CMC can be determined as a point of inflection on the dependence curve of I_1/I_3 on emulsifier concentration. Likewise, polymer micelle-like aggregates start to form along the polymer chain at a critical aggregation concentration (**CAC**). I_1/I_3 gradually changes in a wide region of polymer concentration due to macromolecules heterogeneity. Therefore CAC is convenient to determine as a concentration at which the ratio I_1/I_3 begins to fall on the curve I_1/I_3 = f(*c*).

In the present work, steady-state fluorescence spectra were recorded on a

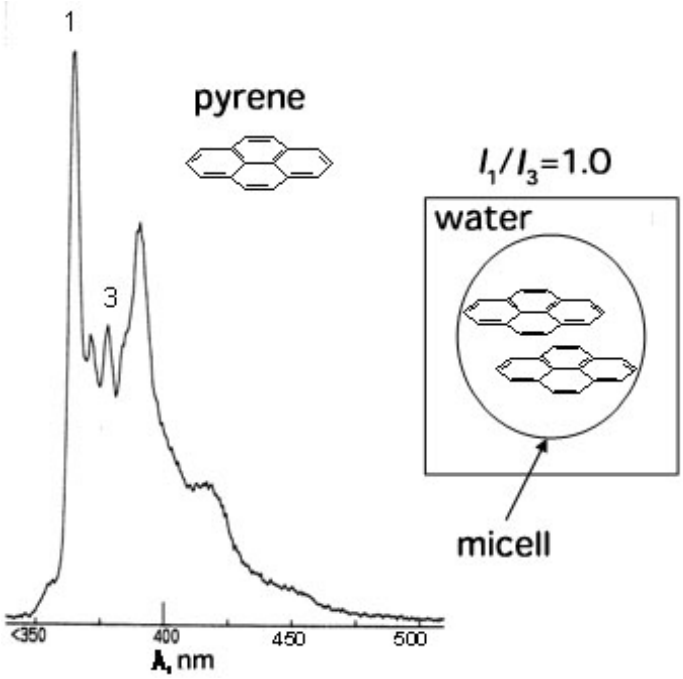


Fig. 41. Fluorescence spectrum of pyrene in water. Using pyrene properties to study hydrophobic interaction.

Hitachi MPF-3 fluorescence spectrophotometer using pyrene as a fluorescent probe. Pyrene, obtained from "Fluka", was recrystallized three times from absolute ethanol. Excitation of pyrene was done at 338 nm. Sample solutions were prepared by dissolving a known amount of polymer in the deionized water. Solutions were stirred at room temperature for at least three days. Then 0.012 ml of pyrene stock solution in ethanol (2×10^{-4} mol/l) was added into the flask with polymer solution (3 ml). This solutions were stand in dark for a day prior to measurements. The intensity ratio of pyrene fluorescence was determined as the ratio of I_{371}/I_{383} from the emission spectrum [39].

4.3.4.Other Physicochemical Metods

Infra-Red Spectroscopy (IR)

IR-spectroscopy measurements were performed on a "Bruker" "IRFS-113v" FTIR spectrophotometer equipped with a DTGS detector using samples prepared as KBr pellets. The spectra were recorded in the range of 1000–4000 cm^{-1} with the resolution of 2 cm^{-1}. For polyacrylamide, the characteristic bands on the IR spectra corresponding to vibrations of alkene CH (ν = 2800 - 2950 cm^{-1}), amine NH (ν = 3400 cm^{-1}), Amide I (ν = 1660 $см^{-1}$), and Amide II (ν = 1610 $см^{-1}$) were observed. In the case of polylaurylmethacrylate, the bands corresponding to vibrations of alkene CH (ν = 2800 – 2950cm^{-1}) and to the stretching vibrations of C=O bonds of the ester group (1730 cm^{-1}) were monitored.

Nuclear Magnetic Resonance (NMR)

Proton nuclear magnetic resonance (^{1}H NMR) spectra were recorded on a Bruker AVANCE spectrometer at 400 MHz. In order to perform measurements, polyacrylamide and HM polyacrylamide were dissolved in deuterated water; PLMA was dissolved in deuterated chloroform using TMS as internal standard. For the backbone protons of polyacrylamide and HM polyacrylamide the chemical shift of (-CH_2-) was 1.7 ppm, the chemical shift of (-CH-) was 2.3 ppm. For PLMA the most characteristic shifts were 3.9 ppm (-O-C$\underline{H}_2$-), 1.6 ppm (-O-CH_2-C$\underline{H}_2$-), 1.3 ppm (-(C$\underline{H}_2$)$_9$-), and 0.9 (-CH_3) for side chain.

In the case of benzene ring protons of copolymer acrylamide-styrene the chemical shift was 7.2-7.4 ppm. The content of styrene units in copolymer was calculated from the NMR data (**Fig.42**) using the following equations:

$$\frac{I_c}{I_a + I_b} = \frac{5y}{(2x+2y)+(x+y)}, \qquad (4.3.18)$$

$$x+y=1; \qquad (4.3.19)$$

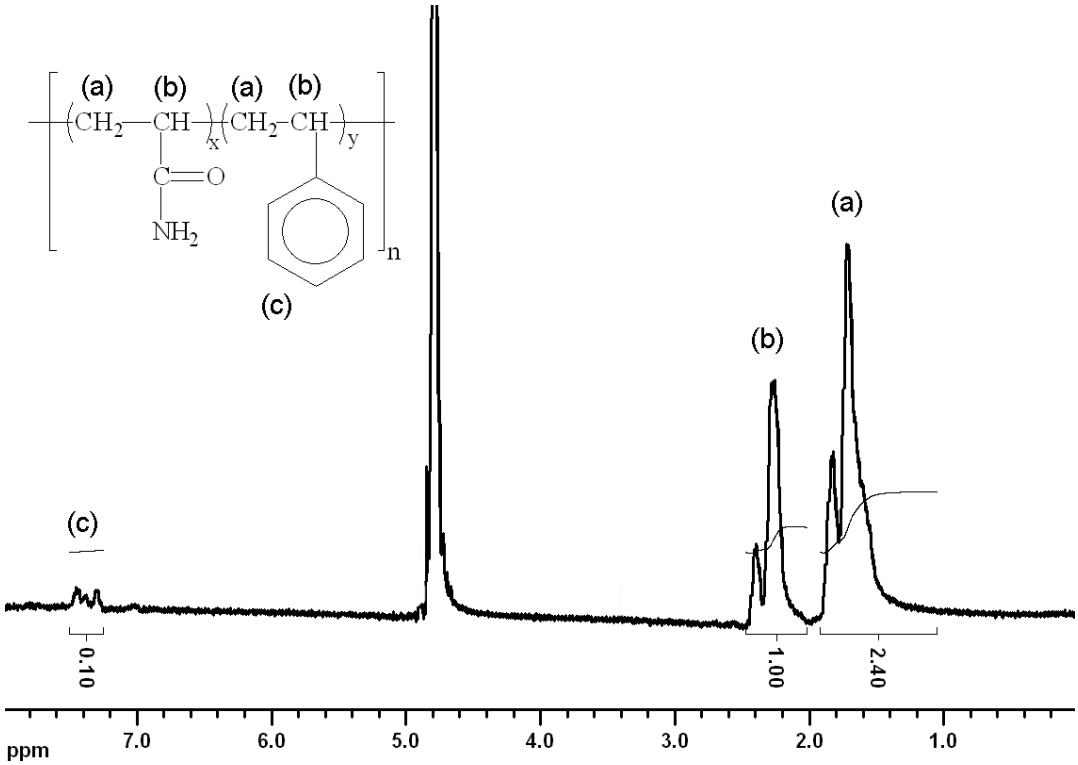


Fig. 42. ^{1}H NMR spectrum of copolymer *acrylamide-styrene* in deuterated water.

where *x, y* are the mole fractions of acrylamide and styrene units, respectively, I_a, I_b, I_c are the integrated areas of protons in CH_2, CH and C_6H_5 groups, respectively.

Elemental Analysis

The elemental analysis of the polymers was performed in the laboratory of microanalysis of the Nesmeyanov Institute of Organoelement Compounds, Russian Academy of Sciences. The C:N ratio in the sample HMPAAM-9_{AIBN}, was calculated using the following equation:

$$C\%/N\% = \frac{3\cdot 12(1-y)+16\cdot 12y}{14(1-y)}, \qquad (4.3.20)$$

where *y* is the mole fraction of LMA units. The content of LMA in the copolymer can be calculated from the equation:

$$y = \frac{14\,C\%/N\% - 36}{156 + 14\,C\%/N\%}. \qquad (4.3.21)$$

Viscosimetry

The viscosity of dilute solutions was measured using an Ostwald viscometer at 25°C. The volume of sample was equal to 5 ml.

Rheology

The rheological characteristics of semidilute solutions were examined on a Rheotest 2 rotary viscometer under continuous shear strain regime in a thermostated

measuring unit “Coaxial cylinders”. Temperature was varied from 20 to 80°C. Shear rates were varied in the range from 1.5 to 1300 s^{-1}.

Tensiometry

Surface and interfacial tension measurements were carried out at 25°C using a tensiometer “DCAT 21” from Dataphysics, employing the Du Nouy ring method. The radius of the Pt-Ir ring was 9.4425 mm and the wire radius was 0.185 mm. In the surface tension experiments each measurement was repeated 10 times and the average value was taken as a result. The interfacial tension experiments were carried out three times on freshly prepared bilayers each time and the average value was taken afterwords.

Transmission Electron Microscopy (TEM)

Electron microscopy was performed with a LEO912 AB OMEGA electron microscope. The polymer suspension after synthesis was diluted with cyclohexane and then applied to a 400 mesh formvar-coated copper grid and left to dry. For study of aqueous polymer dispersions, the dry cross-linked polymer powder was let to saturate in water for a day. Then the dispersion was diluted with water and ultrasonicated for 15 min. After that, the polymer dispersion was applied to a 400 mesh collodion-coated copper grid and left to dry. No further contrasting was applied.

CONCLUSION

In this thesis, two important aspects have been considered: the development and characterization of the miniemulsion technique for the synthesis of hydrophobically modified polyacrylamides, and investigation of their associative and rheological properties.

The synthesis of HM polyacrylamides in inverse miniemulsion was initialy optimized by free-radical polymerization of acrylamide initiated by AIBN. The possibility of copolymerization of monomers with different hydrophilicities was shown then on the *acrylamide – styrene* and *acrylamide – lauryl methacrylate* model pairs. The water-soluble copolymer containing 1-2 mol. % styrene unites was formed.

Then a series of high-molecular weight (M_w = 1.6-2.7×10^6) water-soluble HM polyacrylamides with hydrophobic LMA units were obtained with high yield. The associative and rheological properties of their aqueous solutions were studied by means of pyrene fluorescence spectroscopy, light scattering and viscosimetry. It was shown that solutions of these polymers possess the increased viscosity in comparison with solutions of corresponding polyacrylamides. The dependence of associative properties of HM polyacrylamides on hydrophobe content in reaction mixture was also studied. The water-soluble copolymers with LMA content of up to 5 mol. % demonstrated the associative behavior in aqueous solutions. Further increase in the amount of LMA in the reaction mixture promotes the formation of opalescent solutions with lower viscosity owing to incomplete phase separation of the system. The rheological characteristics of miniemulsion HM polyacrylamides were compared to that of HM polyacrylamides synthesized by micellar and solution polymerization. It was shown that HM-polymers synthesized by miniemulsion and micellar technique have similar thickening properties. In other words, the behavior of miniemulsion copolymer is similar to the behavior of HM polyacrylamide with microblock structure.

In this study, the new surface-active initiating system based on tetravalent cerium salt and emulsion stabilizer for polymerization of vinyl monomers in inverse miniemulsions has been proposed for the first time. It was found that polymerization of acrylamide proceeded under these conditions with the formation of water-soluble

monochelic HM polyacrylamides containing the residual of stearic acid as hydrophobic end-group. The influence of reagent ratio (acrylamide, Ce(IV) and Span 60) and the temperature on the molecular mass, yield of polymers and aggregative stability of the system was studied. The results allowed us to find the optimal conditions for the synthesis of high-molecular weight (M_w up to 2.0×10^6) HM polyacrylamides with high yield. The proposed method provides higher aggregative stability of resulted latexes as compared with conventional method with AIBN as initiatior. The associative properties of prepared polymer were studied by pyrene fluorescence spectroscopy, dynamic and static light scattering. It was shown that these polymers were able to form polymolecular micelles in water.

Also we showed the possibility of copolymerization of acrylamide with hydrophobic monomers – styrene and LMA. The designed surface-active redox system initiates polymerization on the interfacial boundary but does not initiate polymerization in oil phase that provides the absence of hydrophobic homopolymer in the reaction products.

Finally, chemically cross-linked nanoparticles based on polyacrylamide and polyacrylic acid were synthesied in inverse miniemulsions with the developed initiating system. The resulting nanoparticles (R_h = 50-70 nm) were easily redispersable in hydrophobic, so as in hydrophilic medium.

Thus, in this work the miniemulsion successfully applied technique for the synthesis of HM polyacrylamides with good thickening properties. From an economic point of view this method is more profitable than micellar polymerization. Polymerization in inverse miniemulsion allows one to increase the monomer concentration in reaction medium at rather low amount of emulsifier. We also have designed the new initiating system based on the tetravalent cerium salt and emulsion stabilizer. On one hand, this system possesses the advantages of redox initiation systems, on the other hand, initiating occurs on the interfacial boundary due to surface-active character of this redox pair. The proposed initiating system seems to be perspective for the elaboration of a relatively inexpensive and simple method for synthesis of hydrophilic polymers, HM-polymers and polymer nanoparticles. Since cross-linked nanoparticles are easily re-dispersible and form stable colloidal solutions, further interesting work could be related to functionalyzing of these nanoparticles for the creation of biosensors and diagnostic systems.

ZUSAMMENFASSUNG

Eine der neuen Entwicklungstendenzen in der Polymerforschung ist die Suche nach neuen synthetischen Verfahren für das Design von Polymerwerkstoffen mit besonderen Eigenschaften. Die Modifikation von bekannten Polymeren, denen neue qualitative Eigenschaften verliehen werden, ist das Hauptthema dieser Dissertation. Hydrophobisch modifizierte (HM) wasserlösliche Polymere auf Acrylamidbasis gehören zu den wichtigsten assoziierenden amphiphilen Polymeren. Die Zugabe einer kleinen Menge eines Hydrophobes Einheiten in die hydrophile Polymerkette ergibt Systeme mit einzigartigen rheologischen Eigenschaften. Aufgrund hydrophobischer Interaktionen können sich diese Polymere in wässrigen Lösungen mit einer Struktur von hydrophobischen Mikrodomänen verbinden. Daraus ergibt sich beim überschreiten einer gewissen Polymerkonzentration eine stark erhöhte Viskosität. Diese Systeme sind sehr vielversprechend als wässrige Verdickungsmittel in verschiedenen Bereichen der Industrie.

Heutzutage ist die mizellare Polymerisation die am häufigsten angewandte synthetische Methode zur Herstellung von HM Polyacrylamiden (HM PAAm). Der Nachteil dieser Methode ist die begrenzte Anfangskonzentration der reagierenden Mischung beschränkt durch den Einsatz des Gelbildungsprozesses während der Polymersation. Dies kann durch eine inverse Emulsion verhindert werden, wobei die Konzentration der Monomere in der Reaktion erhöht wird. Eine der erfolgversprechendsten Emulsionspolymersationen ist die Miniemulsionspolymersation. Im Vergleich zu Mikroemulsionen zeichnet sich die Miniemulsionspolymersation durch einen effizienteren Einsatz des Emulgators aus, und im Gegensatz zur konventionellen Emulsionpolymerisation ergeben sich stabilere und homogenere Latexes. Dabei besteht die Idee darin, dass die Polymerisation in jedem Tropfen abläuft. Diese Tropfen sich durch Hinzfügen eines Emulgators gegen Koaleszenz und durch Hinzufügen eines osmotischen Druckagenten gegen den Ostwald Reifemgsprozess stabilisiert. Dieses Verfahren ermöglicht die Bildung einer deutlichen Grenze zwischen der Wasser- und Ölphase, was wiederum günstige Bedingungen für die Polymerisation an der Grenzfläche schafft. Zusätzlich steigt die

Wahrscheinlichkeit der Copolymerisation der Monomere mit stark differenzierten Hydrophiliestufen durch die Wahl des adäquaten Initiators und die Einleitung der Polymerisation neben dieser Grenzfläche.

In dieser Arbeit wird das Verfahren der freien radikalischen Copolymerisation in einer inversen Emulsion auf die Synthese der HM Polyacrylamide übertragen. Er wurde der Einfluß unterschiedlicher Faktoren wie Temperatur, Reaktionszeit, Konzentration der Monomere, des Emulgators und des Initiators, und das Phasenverhältnis auf die aggregierte Bestädigkeit von Emulsionen und Latexes sowie auf den Ertrag und die molekulare Masse der resultierenden Polymere untersucht. Es wurde gezeigt, dass HM Polyacrylamide mit guten Verdickungsfähigkeiten erzeugt werden können.

Als erstes wurde um die Synthesebedingungen zu optimieren eine radikalische Miniemulsionspolymerisation der Acrylamide durchgeführt, eingeleitet durch den öllöslichen Initiator Azobisisobutyronitrile (AIBN). Danach wurde die Möglichkeit der Copolymerisation von Comonomeren mit verschiedenen hydrophilen Eigenschaften am Beispiel der Paare der Acrylamide/Styrol und Acrylamide/Lauryl Methacrylate (LMA) gezeigt. Das Ergebnis dieser Untersuchung war die Erzeugung eines wasserlöslichen mit hohem Molekulargewicht HM Polyacrylamids mit hydrophoben LMA Einheiten durch das inverse Eulsionsverfahren. Es wurden die assoziativen und rheologischen Eigenschaften der wässrigen Lösungen untersucht. Es konnte bewiesen werden, dass Lösungen solcher Polymere eine erhöhte Viskosität im Vergleich zu den Lösungen der entsprechenden nicht modifizierten Polyacrylamide aufweisen. Außerdem wurde das rheologische Verhalten der HM Polyacrylamide, die durch die Miniemulsionspolymersation erhalten wurden, mit denen, die mit Hilfe einer mizellaren Polymerisation und einer Lösungs Polymerisation erhalten wurden verglichen. Daraus resultierte, dass HM-Polymere die durch Miniemulsions- und Mizellarverfahren erhaltenen wurden, ähnliche Verdickungseigenschaften haben.

Gemeinsam mit dem bekannten Initiator AIBN wurde in dieser Studie ein neues oberflächenaktiv orientiertes System mit Hilfe des vierwertigem Cers erforscht. Bekannt ist, dass die unter Behandlung der 1,2-diol Substanzen mit Cer-Ionen geformten freien Radikale in der Impfung von Acrylamid, Acrylnitril, Acrylate und anderen Vinyl-Monomere auf Cellulose, Natriumalginat, Stärke und Dextran verwendet werden. Einer der handelsüblichen Emulgatoren für inverse Emulsionen ist Sorbitanmonostearat (Span 60), das 1,2-diol Fragmente enthält. Deshalb war es interessant, das Cer(IV) – Span 60 redox System für Miniemulsionspolymerisation von wasserlöslichen Vinylmonomeren, insbesondere Acrylamid, zu verwenden. Die vorgeschlagene Polymerisationsmethode ergab eine erhöhte Stabilität der Wasser-in-Öl

Emulsionen und Latexes bei einer geringeren Menge Emulgator im Vergleich zur Verwendung des konventionellen öllöslichen AIBN Initiators.

Wasserlösliche HM Polyacrylamide mit einem Rest Stearinsäure als hydrophobe End-Gruppe wurden mit einem Cerium Ammoniumnitrat (CAN) – Span 60 redox System synthetisiert. Diese Polymere sind in der Lage in wässrigen Lösungen zu assoziieren. Dann wurde das Acrylamid mit den hydrophoben Monomeren – Styrol und LMA copolymerisiert. Es wurde bewiesen, dass dieses oberflächenaktiven Redoxsysteme die Polymerisation an der Phasengreuze im Gegensatz zum öllöslichen Initiatoren übertragen. Gleichzeitig kommt es nicht zu einer Polymerisation in der Ölphase, was durch das Fehlen des hydrophoben Homopolymer in den Reaktionsprodukten bewiesen wurde.

Abschließend wurde die Möglichkeit der Synthese von chemisch vernetzten Nanopartikeln aufgrund von Polyacrylamide und Polyacrylsäure durch das Miniemulsionsverfahren mit CAN – Span 60 als Inintiator gezeigt. Resultierende Nanopartikel wurden mit Leichtigkeit im hydrophobischen und gleichermaßen im hydrophilischen Medium aufgelöst. In der Praxis können diese Nanopartikel, nach einer adäquaten Veränderung als Biosensoren sowie als Diagnostiksysteme angewendet werden.

REFERENCES

1. Water-soluble polymers. Synthesis, solution properties, and application. ACS Symposium Series / Ed. by S.W. Shalaby, C.L. McCormick, G.B. Butler. Washington, DC: American Chemical Society, 1991, v. 467, p. 523

2. Polymers in aqueous media. Performance through association. Advances in Chemistry / Ed. by J.E. Glass. Washington, DC: American Chemical Society, 1989, v. 223, p. 576

3. Finch C.A. Industrial Water-Soluble Polymers. Cambridge, UK: The Royal Society of Chemistry, 1996, p. 136

4. Candau F., Selb J. Hydrophobically-modified polyacrylamides prepared by micellar polymerization // Adv. Colloid Interface Sci., 1999, v. 79, pp. 149-172.

5. Rogovina L.Z., Vasil'ev V.G., Churochkina N.A., Pryakhina T.A. and Khokhlov A.R. Effect of the conditions of synthesis on the structure of hydrophobically modified polyacrylamides and rheology of their solutions and gels // Vysokomol. Soedin., Ser. A, 2004, v. 46, p. 644 [Polymer. Science, Ser. A, 2004, v. 46, pp. 385-394].

6. McCormick C.L., Nonaka T., Johnson C.B. Water-soluble copolymers: 27. Synthesis and aqueous solution behaviour of associative acrylamide/N-alkylacrylamide copolymers // Polymer 1988, v. 29, pp. 731-739.

7. Odian G. Principles of Polymerization. 3rd ed. John Wiley and Sons Inc. 1991, p. 768.

8. Landfester K. Miniemulsion for nanoparticle synthesis // Top. Curr. Chem., 2003, v. 227, pp. 75-123.

9. Asua J.M. Miniemulsion polymerization // Prog. Polym. Sci., 2002, v. 27, pp. 1283-1346.

10. Candau F. Microemulsion Polymerization. In: Encyclopedia of Polymer Science and Engineering / Ed. by H.F Mark, N.M.B. Kales, C.G. Overberger, G. Menges. 2nd ed. John Wiley and Sons Inc., 1987, v. 9, pp. 718–724.

11. Masa J.A., De Arbina L.L., Asua J.M. A comparison between miniemulsion and conventional emulsion terpolymerization of styrene, 2-ethylhexyl acrylate and methacrylic acid // J. Appl. Polym. Sci., 1993, v. 48, pp. 205-213.

12. Livshits R.M., Alachev V.P., Prokofeva M.V. and Rogovin Z.A. Vysokomol, Soed 1964, v. 6, pp. 655-658.

13. Galioglu O., Soydan A.B., Akar A., Sarac A.S. Block/graft copolymer synthesis via ceric salt // Die Ang. Makromol. Chem., 1994, v. 214, pp. 19-28.

14. Shah S.B., Patel C.P., Trivedi H.C. Ceric-induced grafting of ethyl-acrylate onto sodium alginate // Ang. Makromol. Chem., 1994, v. 214, pp. 75-89.

15. Reyes Z., Rist C. E., Russell C.R. Grafting vinyl monomers to starch by ceric ion. I. Acrylonitrile and acrylamide // J. Polym. Sci., Part A-1: Polym. Chem., 1966, v. 4, pp. 1031-1043.

16. Bertholon I., Lesieur S., Labarre D., Besnard M., Vauthier C. Characterization of Dextran-Poly(isobutylcyanoacrylate) Copolymers Obtained by Redox Radical and Anionic Emulsion Polymerization // Macromolecules, 2006, v. 39, pp. 3559-3567.

17. Kauzmann, W. Some Factors in the Interpretation of Protein Denaturation. In: Advances in Protein Chemistry / Ed. by C. B. Anfinsen, K. Bailey, M. L. Anson and J. T. Edsall. New York: Academic Press, 1959, v. 14, pp. 1-63.

18. Karunasena A., Brown R.G., Glass J.E. Hydrophobically Modified Ethoxylated Urethane Architecture. In: Advances in Chemistry / Ed. by J. E. Glass. Washington, DC: American Chemical Society, 1989, v. 223, pp. 496-542.

19. Maechling-Strasser C., François J., Clouet F., Tripette C. Hydrophobically end-capped poly(ethylene oxide) urethanes: 1. Characterization and experimental study of their association in aqueous solution // Polymer, 1992, v. 33, pp. 627-636.

20. Beaudoin E., Borisov O., Lapp A., Billon L., Hiorns R. C.; François J. Neutron Scattering of Hydrophobically Modified Poly(ethylene oxide) in Aqueous Solutions // Macromolecules, 2002, v. 35, pp. 7436-7447.

21. Kujawa P., Segui F., Shaban S., Diab C., Okada Y., Tanaka F., Winnik F. M. Impact of End-Group Association and Main-Chain Hydration on the Thermosensitive Properties of Hydrophobically Modified Telechelic Poly(N-isopropylacrylamides) in Water // Macromolecules, 2006, v. 39, pp. 341-348.

22. Sau A.S., Landoll L.M. Synthesis and Solution properties of hydrophobically modified (hydroxyethyl)cellulose. In: Advances in Chemistry / Ed. by J.E. Glass. Washington, DC: American Chemical Society, 1989, v. 223, pp. 343-364.

23. Peer W.J. Polymerization of hydrophobically modified polyacrylamide. Effects of surfactants and comonomers. In: Advances in Chemistry / Ed. by J.E. Glass. Washington, DC: American Chemical Society, 1989, v. 223, pp. 381-397.

24. Shah K.R. Hydrophilic-Hydrophobic Domain polymer systems. In: ACS Symposium Series / Ed. by S.W. Shalaby, C.L. McCormick, G.B. Butler. Washington, DC: American Chemical Society, 1991, v. 467, pp. 468-483.

25. Evani S. Water-dispersible hydrophobic thickening agent // Pat. 4432881 USA, 1984.

26. Zaroslov Y.D., Philippova O.E., Blagodatskikh I.V., Khokhlov A.R. Gelable liquid and method for selectively inhibiting the gelation of a gelable liquid // Pat. 7151078 USA, 2006.

27. Jones T.G.J., Tustin G.J. Hydrophobically Modified polymers for water control // Pat. 6803348 USA, 2004.

28. Feng Y., Billon L., Grassl B., Khoukh A., François J. Hydrophobically associating polyacrylamides and their partially hydrolyzed derivatives prepared by post-modification. 1. Synthesis and characterization // Polymer, 2002, v. 43, pp. 2055-2064.

29. Hill A., Candau F., Selb J. Properties of hydrophobically associating polyacrylamides: influence of the method of synthesis // Macromolecules, 1993, v. 26, pp. 4521-4532.

30. Stanley, jr. F.W. Water-in-oil emulsions of hydrophobe association polymers // Pat. 4524175 USA, 1985.

31. A.Yu. Grosberg, A.R. Khokhlov. Statistical Physics of Macromolecules, Moscow, Nauka, 1989; English translation: American Insitute of Physics, NY, 1994.

32. Evans D.F., Wennerstrom H. The colloidal domain. Where physics, chemistry, biology, and technology meet. New York: Wiley-VCH, 1994, p. 515.

33. A. R. Khokhlov and S. I. Kuchanov, Lectures on Physical Chemistry of Polymers (Mir, Moscow, 2000, p. 192) [in Russian]

34. Joseph C. Salamone Polymeric Materials Encyclopedia. CRC Press 1996, v. 8.

35. Shinoda, K. “Iceberg” Formation and Solubility // J. Chem. Phys., 1977, v. 81, pp. 1300-1302.

36. Middleton J.C., Cummins D.F., McCormick C.L. Rheological properties of hydrophobically modified acrylamide-based polyelectrolytes. In: ACS Symposium Series / Ed. by S.W. Shalaby, C.L. McCormick, G.B. Butler. Washington, DC: American Chemical Society, 1991, v. 467, pp. 338-348.

37. Tanford C., The hydrophobic effect: formation of micelles and biological membranes. 2nd ed. New York etc.: Wiley, 1980, IX, p. 233.

38. Bock J., Siano D. B., Valint jr. P. L., Pace S. J. Structure and properties of Hydrophobically Associating Polymers. In: Advances in Chemistry / Ed. by J. E. Glass. Washington, DC: American Chemical Society, 1989, v. 223, pp. 411-424.

39. Blagodatskikh I.V., Vasil’eva O.V., Ivanova E.M., Bykov S.V., Churochkina N.A., Pryakhina T.A., Smirnov V.A., Philippova O.E., Khokhlov A.R. New approach to the

molecular characterization of hydrophobically modified polyacrylamide // Polymer, 2004, v. 45, pp. 5897–5904.

40. Volpert E., Selb J., Candau F. Influence of the Hydrophobe Structure on Composition, Microstructure, and Rheology in Associating Polyacrylamides Prepared by Micellar Copolymerization // Macromolecules, 1996, v. 29, pp. 1452-1463.

41. Semenov A.N., Joanny J.-F., Khokhlov A.R. Associating polymers: Equilibrium and linear viscoelasticity // Macromolecules, 1995, v. 28, pp. 1066-1075.

42. Blagodatskikh, I.; Vasil'eva, O.; Pryakhina, T.; Churochkina, N.; Barahanova, A.; Vasil'ev, V.; Rogovina, L.; Smirnov, A.; Filippova, O.; Khokhlov, A. Molecular-mass characteristics and association behavior of weakly charged hydrophobically modified poly(acrylamides) // Polymer Science Series A, 2007, v. 49, pp. 763-772.

43. Ezzell S.A., McCormick C.L. Synthesis and solution characterization of pyrene-labeled polyacrylamides. In: ACS Symposium Series / Ed. by S.W. Shalaby, C.L. McCormick, G.B. Butler. Washington, DC: American Chemical Society, 1991, v. 467, pp.130-150.

44. Nilsson S., Thuresson K., Hansson P., Lindman B. Mixed Solutions of Surfactant and Hydrophobically Modified Polymer. Controlling Viscosity with Micellar Size // J. Phys. Chem. B, 1998, v. 102, pp. 7099-7105.

45. Evani S. Water-dispersible hydrophobic thickening agent // Pat. 4432881 USA, 1984.

46. Thuresson K., Lindman B. Effect of Hydrophobic Modification of a Nonionic Cellulose Derivative on the Interaction with Surfactants. Phase Behavior and Association // J. Phys. Chem. B., 1997, v. 101, pp. 6460-6468.

47. Bovey F.A., Kolthoff I.M., Medalia A.I., Meehan E.J. Emulsion polymerization. New York: Interscience, 1965, p. 445.

48. Gilbert R.G. Emulsion polymerization: A mechanistic approach. London: Academic Press, 1995, p. 362.

49. Sudol E.D., El-Aasser M.S. Miniemulsion polymerization. In: Emulsion polymerization and emulsion polymers / Ed. by P.A. Lovell, M.S. El-Aasser. Chichester, Weinheim: J. Wiley, 1997, pp. 700-722.

50. El-Aasser M.S., Sudol E.D. Features of emulsion polymerization. In Emulsion polymerization and emulsion polymers / Ed. by P.A. Lovell, M.S. El-Aasser. Chichester, Weinheim: J. Wiley, 1997, pp. 37-58.

51. Vanderhoff J.W., Bradford E.B., Tarkowski H.L., Schaffer J.B., Wiley R.M. Inverse emulsion polymerization. In: Advances in Chemistry. Washington, DC: American Chemical Society, 1962, v. 34, pp. 32-51.

52. Candau F. Inverse emulsion and microemulsion polymerization. In: Emulsion polymerization and emulsion polymers / Ed. by P.A. Lovell, M.S. El-Aasser. Chichester, Weinheim: Wiley &Sons Ltd, 1997, pp. 723-741.

53. Candau F., Leong Y.S., Pouyet G., Candau S. Inverse microemulsion polymerization of acrylamide: Characterization of the water-in-oil microemulsions and the final microlatexes // J. Colloid Interface Sci. 1984, v. 101, pp. 167-183.

54. Willert M., Landfester K. Amphiphilic Copolymers from Miniemulsified Systems // Macromolecular Chemistry and Physics 2002, v. 203, pp. 825-836.

55. Hernandez-Barajas J., Hunkeler D.J. Inverse-emulsion polymerization of acrylamide using block copolymeric surfactants: mechanism, kinetics and modeling // Polymer 1997, v. 38, pp. 437 – 447.

56. Capek I. The inverse mini-emulsion polymerization of acrylamide // Designed Monomers and Polymers 2003, v. 6, pp. 399–409.

57. V. F. Gromov, T. O. Osmanov, I. V. Glazkova, I. A. Gritiskova and E. N. Teleshov Emulsion polymerization of acrylamide // Polymer Science U.S.S.R., 1988, v. 30, pp. 1210-1215.

58. Adamson A.W., Gast A.P. Physical chemistry of surfaces. 6th ed. New York: Wiley, 1997. 784 p.

59. Vaskova V., Juranicova V., Barton J. Polymerization in inverse microemulsions. 1. Homopolymerizations of water- and oil-soluble monomers in inverse microemulsions // Makromol. Chem. 1990, v. 191, pp. 717-723.

60. Baade W., Reichert K.-H. Kinetics of the dispersion polymerization of acrylamide // Eur. Polym. J. 1984, v. 20, pp. 505-512.

61. Sochilina K.O.; Gromov V.F. Polymerization of water-soluble vinyl monomers in inverse emulsions Polymer science. Series B, 1995, v. 37, pp. 367-376.

62. Ugelstad J., El-Aasser M.S., Vanderhoff J.W. Emulsion polymerization: Initiation of polymerization in monomer droplets // J. Polym. Sci. Polym. Lett. 1973, v. 11, pp. 503-513.

63. Chou Y.J., El-Aasser M.S., Vanderhoff J.W. Mechanism of emulsification of styrene using hexadecyltrimethylammonium bromide-cetyl alcohol mixtures // Dispers. Sci. Technol. 1980, v. 1, pp. 129-150.

64. Choi Y.T., El-Aasser M.S., Sudol E.D., Vanderhoff J.W. Polymerization of styrene miniemulsions // J. Polym. Sci. Polym. Chem. Ed. 1985, v. 23, pp. 2973-2987.

65. Tang P.L., Sudol E.D., Adams M., El-Aasser M.S., Asua J.M. Seeded emulsion polymerization of n-butyl acrylate utilizing miniemulsions // J. Appl. Polym. Sci. 1991, v. 42, pp. 2019-2028.

66. Fontenot K., Schork F.J. Batch polymerization of methyl methacrylate in mini/macroemulsions // J. Appl. Polym. Sci. 1991, v. 49, pp. 633-655.

67. Landfester K., Willert M., Antonietti M. Preparation of Polymer Particles in Nonaqueous Direct and Inverse Miniemulsions // Macromolecules 2000, v. 33, pp. 2370-2376.

68. Rodriguez V.S., El-Aasser M.S., Asua J.M., Silibi C.A. Miniemulsion copolymerization of styrene-methyl methacrylate // J. Polym. Sci. Polym. Chem. Ed. 1989, v. 27, pp. 3659-3671.

69. Huang H., Zhang H., Li J., Cheng S.,Hu F., Tan B. Miniemulsion copolymerization of styrene and butyl acrylate initiated by redox system at lower temperature-preparation and polymerization of miniemulsion // J. Appl. Polym. Sci. 1998, v. 68, pp. 2029-2039.

70. Wu X.Q., Schork F.J. Batch and Semibatch Mini/Macroemulsion Copolymerization of Vinyl Acetate and Comonomers // Ind. Eng. Chem. Res. 2000, v. 39, pp. 2855-2865.

71. Rajatapiti P., Dimonie V.L., El-Aasser M.S. In-Situ Synthesis of PBA-graft-PMMA Copolymers to Be Used as Compatibilizing Agents in PBA/PMMA Composite Latex Particles via the Macromonomer Method // J. Macromol. Sci. Pure Appl. Chem. A. 1995, v. 32, pp. 1445–1460.

72. Gooch J.W., Dong H., Schork F.J. Waterborne oil-modified polyurethane coatings via hybrid miniemulsion polymerization // J. Appl. Polym. Sci. 2000, v. 76, pp. 105-114.

73. Putlitz B.Z., Landfester K., Fischer H., Antonietti M. The Generation of Armored Latexes and Hollow Inorganic Shells Made of Clay Sheets by Templating Cationic Miniemulsions and Latexes // Adv. Mater. 2001, v. 13, pp. 500-503.

74. Tiarks F., Landfester K., Antonietti M. Encapsulation of Carbon Black by Miniemulsion Polymerization // Macromol. Chem. Phys. 2001, v. 202, pp. 51–60.

75. Erdem B., Sudol E.D., Dimonie V.L., El-Aasser M.S. Encapsulation of inorganic particles via miniemulsion polymerization. I. Dispersion of titanium dioxide particles in organic media using OLOA 370 as stabilizer // J. Polym. Sci. Polym. Chem. Ed. 2000, v. 38, pp. 4419-4430.

76. Crespy D., Landfester K. Anionic Polymerization of ε-Caprolactam in Miniemulsion: Synthesis and Characterization of Polyamide-6 Nanoparticles // Macromolecules 2005, v. 38, pp. 6882-6887.

77. Landfester K., Tiarks F., Hentze H-P., Antonietti M. Polyaddition in miniemulsions: A new route to polymer dispersions // Macromol. Chem. Phys. 2000, v. 201, pp. 1-5.

78. Tiarks F., Landfester K., Antonietti M. One-step preparation of polyurethane dispersions by miniemulsion polyaddition // J. Polym. Sci. Polym. Chem. Ed. 2001, v. 39, pp. 2520-2524.

79. Marie E., Landfester K., Antonietti M. Synthesis of Chitosan-Stabilized Polymer Dispersions, Capsules, and Chitosan Grafting Products via Miniemulsion // Biomacromolecules 2002, v. 3, pp. 475-481.

80. Landfester K. Polyreactions in miniemulsion // Macromol. Rapid.Commun. 2001, v. 22, pp. 896-936.

81. Landfester K. Recent Developments in Miniemulsions - Formation and Stability Mechanisms // Macromol. Symp. 2000, v. 150, pp. 171–178.

82. Mason T.J. Industrial sonochemistry: potential and practicality // Ultrasonics 1992, v. 30, pp. 192-196.

83. Lauterborn W., Ohl C-D. Cavitation bubble dynamics // Ultrasonics Sonochemistry 1997, v. 4, pp. 65-75.

84. Landfester K., Bechthold N., Forster S., Antonietti M. Evidence for the preservation of the particle identity in miniemulsion polymerization // Macromol. Rapid Commun. 1999, v. 20, pp. 81–84.

85. Bechthold N., Landfester K. Kinetics of Miniemulsion Polymerization As Revealed by Calorimetry // Macromolecules 2000, v. 33, pp. 4682-4689.

86. Ham G.E. Copolymerization. New York: Interscience Publ., 1964. 939 p.

87. Kuchanov S.I., Khokhlov A.R. Theory of Interphase Free-Radical Copolymerization at the Oil-Water Boundary// Macromolecules 2005, v. 38, pp. 2937-2947.

88. Sarac A.S. Redox polymerization // Prog. Polym. Sci. 1999, v. 24, pp. 1149-1204.

89. Mino G., Kaizerman S. A new method for the preparation of graft copolymers. Polymerization initiated by ceric ion redox systems // J. Polym. Sci. 1958, v. 31, pp. 242-243.

90. Mino G., Kaizermann S., Rassmussen B. The polymerization of acrylamide initiated by ceric nitrate-3-chloro-1-propanol redox systems // J. Polym. Sci. 1959, v. 38, pp. 393-401.

91. Oz N., Akar A. Aminomethylene phosphonic acid–ceric ion redox systems for aqueous polymerization of vinyl monomers // Europ. Polym. J. 2000, v. 36, pp. 193-199.

92. Hsu W.-C., Chen C.-Y., Kuo J.-F., Wu E.M. Aqueous polymerization of acrylamide initiated by cerium(IV)-nitrilotriacetic acid redox initiator // Polymer 1994, v. 35, pp. 849-856.

93. Novitskaya M.A., Konkin A.A. Vysokomol Soed 1965, v. 7, pp. 1719-1725. [in Russian]

94. Arslan H., Hazer B. Ceric ion initiation of methyl methacrylate using polytetrahydrofuran diol and polycaprolactone diol // Europ. Polym. J. 1999, v. 35, pp. 1451-1455.

95. Nagarajan S., Sudhakar S., Srinivasan K.S.V. Poly(ethy1ene glycol) block copolymers by redox process: kinetics, synthesis and characterization // Pure and Appl. Chem. 1998, v. 70, pp. 1245-1248.

96. Tauer K., Khrenov V. Polymer Dispersions as intermediate state during the synthesis of specialty polymers // Macromol. Symp. 2002, v. 179, pp. 27-52.

97. Takahashi T., Hori Y., Sato I. Coordinated radical polymerization and redox polymerization of acrylamide by ceric ammonium nitrate // J. Polymer Sci., Part A-1: Polym. Chem. 1968, v. 6, pp. 2091-2102.

98. Fernandez M.D., Pelayo A., Otero T.F., Guzman G.M. Polymerization of methyl methacrylate initiated by the redox system Ce(IV)/isobutyl alcohol // J. Polym. Sci., Polym. Lett. 1985, v. 23, pp. 79-83.

99. Ahmed K.R., Natarajan L.V., Anvaruddin Q. Studies on aqueous polymerization of acrylonitrile. Cerium(IV)/acetaldehyde redox system // Macromol. Chem. 1978, v. 179, pp. 1193-1197.

100. Ozeroglu C., Ozduganci C. Low Temperature Initiation by 3-Mercaptopropionic Acid-Ce(IV) or -KMnO4 Redox System for Polymerization of Acrylamide Monomer // Polym.-Plast. Technol. Eng. 2006, v. 45, pp. 549-554.

101. Qiu K.-Y., Zhao J.-B., Dong J.-H. Radical polymerization and graft polymerization with ceric ion and 3-phenylmethyl-2,4-pentanedione system // Polym. Bull. 1994, v. 32, pp. 581-588.

102. Mohanty N., Pradhan B., Mohanta M.C. Vinyl polymerization of acrylonitrile by the cerium(IV)-propane-1,2-diol system // Eur. Polym. J. 1979, v. 15, pp. 743-746.

103. Mohanty N., Pradhan B., Mohanta M.C. Kinetics of Vinyl Polymerization. 1. Ceric Ion Induced Polymerization of Acrylonitrile in the Presence of Butane-1,4-diol // J. Macromol. Sci. Part A: Pure and Appl. Chem. 1983, v. 19, pp. 283-297.

104. Pottenger C.R., Johnson D.C. Mechanism of cerium (IV) oxidation of glucose and cellulose // J. Polym. Sci., Part A-1: Polym. Chem. 1970, v. 8, pp. 301-318.

105. Cerium. A guide to its role in chemical technology. USA: Molycorp. Inc. Mountain Pass, 1995. 42 p.

106. Sarac A.S., Ustamehmetoglu B., Erbil C. Potentiometric determination of the molecular mass of polymers // Polym. Bull. 1994, v. 32, pp. 91-95.

107. Kurlyankina V.I., Sarana N.V. and Kozmina O.P. // Russian Journal of Organic Chemistry 1970, v. 41, pp. 1315-1320. [in Russian]

108. Mishra A., Srinivasan R., Gupta R. P. psyllium-g-polyacrilonitrile:synthesis and characterization // Colloid Polym. Sci. 2003, v. 281, pp. 187-189.

109. Chauvierre C., Labarre D., Couvreur P., Vauthier C. Radical Emulsion Polymerization of Alkylcyanoacrylates Initiated by the Redox System Dextran-Cerium(IV) under Acidic Aqueous Conditions // Macromolecules 2003, v. 36, pp. 6018-6027.

110. Gupta K.C., Behari K. Cerium (IV)-2-chloroethanol redox-pair initiated polymerization of acrylamide in aqueous medium // J. Polym. Sci. 1986, v. 24, pp. 767-775.

111. Erbil C., Ustamehmetoglu B., Uzelli G., Sarac A.S. Conductometric determination of the end group ionization in acrylamide and acrylonitrile polymers initiated by carboxylic acids // Eur. Polym. J. 1994, v. 30, pp. 149-152.

112. Nagarajan S., Sreeja Kumari S.S., Srinivasan K.S.V. Kinetic and mechanistic studies on the block copolymerization of methyl methacrylate initiated by Ce^{4+}-poly (ethylene glycol) redox system // J. Appl. Polym. Sci. 1997, v. 63, pp. 565-571.

113. Subramanian S.V., Santappa M. Vinyl polymerization initiated by ceric ion reducing agent systems in sulfuric acid medium // J. Polym. Sci., Part A-1: Polym. Chem. 1968, v. 6, pp. 493-504.

114. Rosen M.J. Surfactants and interfacial phenomena. New York: Wiley, 1978. 304 p.

115. Yakovleva I.M., Simakova G.A., Gritskova I.A., Teleshev E. N., Gromov V.F. and Kobyakova K.O. Stability of water-in-oil emulsions of acrylamide // Colloid Journal 1991, v. 53, pp. 798-803.

116. Candau F., Leong Y.S., Fitch R.M. Kinetic study of the polymerization of acrylamide in inverse microemulsion // J. Polym. Sci., Polym. Chem. Ed. 1985, v. 23, pp. 193-214.

117. Vaskova V., Hlouskova Z., Barton J., Juranicova V. Polymerization in inverse microemulsions. 4. Locus of initiation by ammonium peroxodisulfate and 2,2'-azoisobutyronitrile // Makromol. Chem. 1992, v. 193, pp. 627-637.

118. Hamielec A.E., Ray W.H. An analytical solution to Tung's axial dispersion equation // J. Appl. Polym. Sci. 1969, v. 13, pp. 1319-1321.

119. Biggs S., Hill A., Candau F. Copolymerization of acrylamide and a hydrophobic monomer in an aqueous micellar medium: effect of the surfactant on the copolymer microstructure // J. Phys. Chem. 1992, v. 96, pp. 1505-1511.

120. Fried J.R. Polymer science and technology. 2nd ed. Upper Saddle River, NJ: Prentice Hall PTR, 2007. 582 p.

121. Bratukhin A. G., Bogolyubov V. S. Composite Manufacturing Technology. Chapman and Hall, 1994. 448 p.

122. Kulicke W.-M., Kniewske R., Klein J. Preparation, characterization, solution properties and rheological behaviour of polyacrylamide // Prog. Polym. Sci. 1982, v. 8, pp. 373-468.

123. Evans J. M. Manipulation of light scattering data. In Light Scattering From Polymer Solutions. / Ed. by M.B. Huglin. London and New York: Academic Press, 1972, pp. 89-162.

124. Dynamic light scattering: the method and some applications / ed. by W. Brown. Oxford Clarendon Press, 1993. 735 p.

125. Gel permeation chromatography. Ed. by K.H. Altgelt. New York: Dekker, 1971. 646 p.

126. Kale L.T., O'Driscoll K.F. Rheokinetics of polymerization of N-laurylmethacrylate // Polym. Eng. Sci. 1982. V. 22. № 7. P. 402-409.

127. Capek I. Fate of excited probes in micellar systems // Advances in Colloid and Interface Science, 2002, v. 97, pp. 91-149.

128. Yorstos Y.C., Youngmin C., Zhengming U., Shah P.C. Analysis and Interpretation of Water/Oil Ratio in Waterfloods // SPE Journal 1999, v. 4, pp. 413-424.

ERKLÄRUNG

Diese Dissertation wurde im Zeitraum von Januar 2005 bis Dezember 2007 im Institut Polymer Science der Universität Ulm erstellt.

Hiermit erkläre ich, daß ich diese Arbeit selbständig und nur mit den angegebenen Hilfsmitteln angefertigt habe. Alle Stellen, die dem Wortlaut oder dem Sinn gemäß anderen Arbeiten entnommen wurden, sind durch Angabe der Quellen kenntlich gemacht.

Ulm, den 26.05.2008

Elena Kobitskaya

CURRICULUM VITAE

PERSONAL DATA



Name:	Dipl. Chem. **Elena M. Kobitskaya (Ivanova)**
Citizenship:	Russian
Date and place of birth:	April 30, 1981, Chernigov (USSR)
Marital status:	married

Business address: Department of Polymer Science
University of Ulm
Albert Einstein Allee 11, Ulm 89069, Germany
Phone: +49(731)50-31391
Fax: +49(731)50-31399

Home address: Trollinger Weg, 24, 89075, Ulm, Germany

Mobile phone: +49(176)655-48186

e-mail: elena.kobitskaya@gmail.com

PROFESSIONAL SKILLS

Languages:	English, Russian (native)
Scientific skills:	Polymerization in homo- and heterophases Synthesis of (co)polymers with amphiphilic properties Synthesis of polymer particles in the size range 50-500 nm by emulsion and miniemulsion techniques Dynamic and Static Light Scattering, Gel Permeation Chromatography, Tensiometry (Du Nouy Ring, Wilhelmy Plate and Pendant Drop methods), Viscosimetry, UV-vis, Fluorescence Spectroscopy, Rheometry

EDUCATION and RESEARCH EXPERIENCE

2004-present **Moscow, Russia / Ulm, Germany**

- Laboratory of Physical Chemistry of Polymers, Nesmeyanov Institute of Organoelement Compounds, RAS, and Department of Polymer Science, University of Ulm
  "Synthesis of Hydrophobically Modified Poly(acrylamide) in Inverse Miniemulsions"

PhD student

2001 **Moscow, Russia**

- Group of Organoelement Functional Polymers, Nesmeyanov Institute of Organoelement Compounds, RAS
- Laboratory assistant

1998-2004 **Moscow, Russia**

- Department of Chemical Technology of Polymers, Mendeleev University of Chemical Technology, Moscow
  "Influence of the Modifier's Structure on Aggregation in Water Solutions of Hydrophobically-Modified Poly(vinyl alcohol)"
- Qualification of Engineer with the specialization of "Chemical Technology of High-Molecular Compounds" (equiv. to M. Sc.)

LIST of PUBLICATIONS

1. Ivanova E.M., Blagodatskikh I.V., Vasil'eva O.V, Barabanova A.I., Khokhlov A.R. *Synthesis of Hydrophobically Modified Poly(acrylamide) in Inverse Miniemulsions* // Polymer Science, Ser. A. 2008, v. 50, pp. 9–17.
2. Blagodatskikh I., Tikhonov V., Ivanova E., Landfester K., Khokhlov A. *New Approach to The Synthesis of Polyacrylamide in Miniemulsified Systems* // Macromol. Rapid Commun. 2006, v. 27, pp. 1900-1905.
3. Blagodatskikh I.V., Vasil'eva O.V., Ivanova E.M., Bykov S.V., Churochkina N.A., Pryakhina T.A., Smirnov V.A., Philippova O.E., Khokhlov A.R. *New approach to the molecular characterization of hydrophobically modified polyacrylamide* // Polymer 2004, v. 45, pp. 5897–5904.
4. Gololobov Yu. G., Petrovskii P.V., Ivanova E.M., Linchenko O.A., Schmutzler R., Ernst L., Jones P.G., Karaçar A., Freytag M., Okucu S. *C→N migrations of the ethoxycarbonyl group in reactions of ortho-substituted aryl isocyanates with the 1,3-zwitterion derived from triisopropylphosphine and ethil-2-cyanoacrylate* // Russian Chemical Bulletin, international edition, 2003, v. 52, pp. 427-436.
5. Gololobov Yu. G., Ivanova E.M., Petrovskii P.V. *Unusual reaction of hexaethylphosphorous triamide with mercuric chloride leading to the formation of metallic mercury //* Russian Chemical Bulletin, international edition, 2002, v. 51, p. 191.

LIST of CONFERENCES

1. **Conference "Trends in nanoscience", February 24-28, 2007, Kloster Irsee, Germany**

E. Ivanova, O. Vasil'eva, I. Blagodatskikh, V. Tikhonov, A. Khokhlov, K. Landfester

"Redox Initiation System Based on Ceric Ions and Sorbitol-Containing Surfactant for Miniemulsion Polymerization of Acrylamide" (poster). Book of abstracts, p. 22

2. **The 4th All-Russian Kargin conference "Polymers Science to 21 century", January 29 – February 2, 2007**

   E.M. Ivanova, I.V. Blagodatskikh, V.E. Tikhonov, O.V. Vasil'eva, A.R. Khokhlov, K. Landfester

   "Synthesis of Hydrophobically Modified Polyacrylamide in Inverse Miniemulsions with Surface-active Initiating System" (poster). Book of abstracts, p. 135 [in russian]

3. **Second SFB 569 Young Researcher Meeting, Kleinwalsertal – Austria, July 26-28, 2006**

   E. Ivanova

   "*Synthesis of Hydrophobically Modified Polyacrylamide in Inverse Miniemulsions*" (talk)

4. **XIII All-Russian conference "Structure and dynamics of molecular systems", June 25 – July 1, 2006, Yoshkar-Ola – Ufa – Kazan – Moscow**

   E.M. Ivanova, I.V. Blagodatskikh, O.V. Vasil'eva, A.I. Barabanova, A.R. Khokhlov, K. Landfester

   "*Copolymerization of Acrylamide and Lauryl methacrylate in Inverse Miniemulsions*" (poster) // Book of abstracts, p. 102. [in russian]

5. **Conference "Trends in nanoscience. Structure and functions", October 08-13, 2005, Kloster Irsee, Germany**

   E.M. Ivanova, I.V. Blagodatskikh, A.I. Barabanova, O.V. Vasil'eva, N.A. Churochkina, T.A. Pryahina, A.R. Khokhlov, K. Landfester

   "*Synthesis of Hydrophobically Modified Polyacrylamide via Mini- and Microemulsion Polymerization*" (poster) // Book of abstracts, p. 62.

6. **XII All-Russian conference "Structure and dynamics of molecular systems", June 27 – July 2, 2005, Yoshkar-Ola – Ufa – Kazan – Moscow**

   S.V. Bykov, I.V. Blagodatskikh, O.V. Vasil'eva, E.M. Ivanova, A.R. Khokhlov

   "*Study of Association in Dilute Solutions of Hydrophobically Modified Poly(vinyl alcohol)*" (poster) // Book of abstracts, p. 32. [in russian]

7. **International conference dedicated to 50th anniversary of A.N. Nesmeyanov Institute of Organoelement Compounds, RAS "Modern trends in organoelement and polymer chemistry", May 30 –June 4, 2004, Moscow, Russia**

   I.V. Blagodatskikh, O.V. Vasil'eva, N.A. Churochkina, T.A. Pryahina, E.M. Ivanova, S.V. Bykov, A.R. Khokhlov

   "*The Synthesis and Properties of Hydrophobically Modified Poly(acrylamide)s*" (poster) // Book of abstracts, p. 98.

8. **The 3rd All-Russian Kargin conference "Polymers -2004", January 27 – February 1, 2004, Moscow, MSU.**

   S.V. Bykov, I.V. Blagodatskikh, O.V. Vasil'eva, E.M. Ivanova, A.R. Khokhlov

   "*Study of Modified Poly(vinyl alcohol) Association in Aqueous Solutions*" (poster) // Book of abstracts, p. 225. [in russian]

9. **The 3rd All-Russian Kargin conference "Polymers -2004", January 27 – February 1, 2004, Moscow, MSU.**

   I.V. Blagodatskikh, O.V. Vasil'eva, S.V. Bykov, E.M. Ivanova, V.A. Smirnov, O.E. Philippova, A.R. Khokhlov

   "*New Approach to the Analysis of Molecular Heterogeneity of Associative Acrylamide Copolymers"* (poster) // Book of abstracts, p. 214. [in russian]

10. **Conference of students and PhD-students, May 28 – 30, 2003, Tver, Russia.**

    Ivanova E. M.

    "*Changing of Molecular Heterogeneity during Micellar Copolymerization of Acrylamide with Hydrophobic and Charged Comonomers*" (poster) // Book of abstracts, p. 26. [in russian]

ACKNOWLEDGEMENTS

I would like to thank everybody who helped me not only with writing this thesis, but with acquiring scientific knowledge and skills.

My primary thanks to my supervisors Prof. A.R. Khokhlov and Dr. I.V. Blagodatskikh, for their support, guidance and discussion of my work. I also thank Prof. K. Landfester for the possibility to use the experimental equipment from her group and for her correcting and refereeing my dissertation. I am indebted to Dr. V.E. Tikhonov for the discussion of my work.

My work would not be possible without the help of my colleagues in the Polymer Sciense group. I am very appreciating the wonderful atmosphere in the lab created by Dr. I.I. Potemkin, Prof. P.G. Khalatur and C. Sfetcu-Ion (Secretary). My special thanks to Dr. A. I. Barabanova and O.V. Vasil'eva for fruitful discussion of experimental results. I would like to thank Dr. V.A. Smirnov for fluorescent spectroscopy measurement and Dr. S.S. Abramchuk for TEM measurements. I wish to acknowledge Olga Guskova and all other students and researches in the lab for their cooperation.

My special thanks to Roman Valiulin and Christopher André Foster for proof-reading this manuscript.

I greatefully acknowledge financial support by the Sonderforschungsbereich 569 ("Hierarchische Strukturbildung und Funktion Organisch-Anorganischer Nanosysteme").

Finnaly, I would like to thank especially my mother, whithout whose contribution this work would not appear. And I want to express my love to my husband, who shared with me all joyful and difficult moments in the last few mounths.